

Author's response

The following document contains the answers to the referees' comments. All comments were very pertinent and helpful, we do appreciate their efforts very much and want to express here our gratitude for their work.

We start with the answers to each comment and the modifications that we have done to the manuscript to address them. The document includes in bold text the original comments, followed if necessary by a quote from the paper in regular text to provide context to the answers. The actual answers are presented in blue.

The answers to referee #1 start on page 1, to referee #2 (Brad Lipovsky) on page 16 and to referee #3 on page 25. After page 31 follows an annotated version of the manuscript, which includes highlighted text for all deletions and additions, as well as text boxes pointing to changes in the figures and the main ones in the text.

In addition to the specific changes described below, multiple minor modifications have been done with the following objectives:

- Consistency with British spellings
- Consistent use of the words disconnected and isolated
- Consistent use of the words subset and cluster
- Consistent use of hyphenation in compound words.

Answers to referee #1

General Comments

1. **My primary concern with the paper is the somewhat abbreviated model interpretation and incomplete comparison with previous work. What is there is very interesting, but the rich model record could be compared a bit more thoroughly to the borehole record (here and elsewhere). There is also no consideration for which model parameters this enhanced model might be sensitive to (though I think a detailed sensitivity study is well beyond the scope of this paper). I did appreciate the model technical detail discussion in the SI, and it would be nice to see those topics mentioned in the main text to encourage readers to look into the SI. My biggest concern in this area is what feels like an incomplete comparison to previous work. The authors acknowledge previous investigations of the disconnected (or weakly connected) system, and their model is an elegant extension of previous, simpler attempts to model it (Hoffman et al., 2016). However, the interpretation in this paper is that the subglacial drainage system becomes increasingly fragmented and disconnected as the summer progresses, while previous studies suggest summer brings *increased* connectivity (Gordon et al., 1998; Hoffman et al., 2016; Iken and Truffer, 1997; Murray and Clarke, 1995). This difference in interpretation should be discussed, and, if possible, reconciled.**

R. We have now emphasized in the modeling section (the new version of section 5.2 is provided together with this document) that the model aims to put forward a possible modification of current models (and thereby spur model development by the wider glacier hydrology community), and does not pretend to be capable of reproducing the observations beyond their

generic features. We have added additional material that compares the effect of the model modifications we have made – specifically the addition of a percolation threshold – with results from model runs without those modifications. We show that pressure fields predicted by the model without a percolation threshold are much smoother and show typically diffusive behaviour such as diurnal pressure variations decreasing smoothly in amplitude away from channels (as described in Hubbard et al, 1995), acquiring significant phase lags in the process. We agree that models that try to capture switches in connectivity need to be developed further. That said, we feel that it is worthwhile to suggest at least a direction for development at the same time as making the point that existing models require a connection / disconnection switch. As above, we have amended the modelling section to make this point clearer by including a simulation in which the percolation cut-off is omitted from the model. This also serves both, to underline the point about why the model modification is important, and as a basic “sensitivity test” to illustrate what the most important (and only truly new) model parameter does.

Regarding the comment that “previous studies suggest summer brings **increased** connectivity”, we believe our description is compatible with the views presented by those authors given their meaning of “increased connectivity”. The subtleties of the discussion require us to carefully distinguish the difference between two possible meanings of “increased connectivity”:

1. **Increase in efficiency of the connected system:** Due to its transition to an efficient channelized system (leading for example to shorter tracer transit times)
2. **Increase in the spatial extent of the connected system:** Enlarging the area affected by pressure variations in the connected system.

Firstly, connectivity increases dramatically at the spring event, and secondly, the development of the channelized system makes the system more efficient (while not necessarily occupying a larger part of the bed).

Some comments particular to each cited author:

- **Murray and Clarke, 1995:** Recognizes the existence and relevance of unconnected domains of the bed, and the heterogeneity and dynamism of such domains. However, with the limited timespan of their borehole records, they do not put forward any description regarding the evolution of such systems throughout the season. Therefore, there are no inconsistencies with our description.
- **Iken and Truffer, 1997:** They also highlight the importance of unconnected reaches of the bed and propose that an increase of their extent is responsible for the seasonal and multi-year slowdown of Findelengletscher glacier. Our interpretation is very consistent with theirs, as it can be illustrated by the following statement “We interpret the decrease in velocity and water pressure during the melt season as being caused by the formation of R channels at the expense of parts of the linked-cavity system.”.
- **Gordon et al., 1998:** Their description of the evolution of the subglacial system is completely consistent with our interpretation., where a poorly connected set of boreholes undergo a transition as the season progress. This leads to some boreholes becoming part of an efficient drainage system, others to become completely isolated and others exhibiting a transitional behavior. The relative lack of boreholes that became isolated can be attributed to the fact that the study does not include the late-season shut-down of the drainage system (Stage 2 to 3 transition), and perhaps also because the study area

was focused in the region where a major channel was predicted to exist during the melt season.

- **Hoffman et al., 2016:** Our interpretation is also consistent with these authors. However, the interpretation of Hoffman et al. (2016) as showing “increased connectivity” over summer is not the same notion of connectivity we are using here. They attribute the late summer slow down to a pressure drop in a weakly connected system, something that is consistent with our data.

In our interpretation, the alternative hypothesis they present for late summer slow down (discarded due to model results) seems equally likely, that is: attributing the slowdown to an increase in the size of the isolated domains of the bed. The model used by Hoffman et al (2016) does not dynamically change the portions of the bed that are connected or disconnected; instead, slow diffusion allows the low-frequency components of the pressure signal to be transmitted to the “weakly connected” (as opposed to completely disconnected) parts of the bed. This is in fact acknowledged in our study as well (Fig. 7), and a potential feature of the model we propose through the parameter k_{leak} .

2. **It would be nice to see a bit more acknowledgement of the possibility of borehole behavior being governed by the presence of subglacial till. This is discussed briefly in a few places, but the paper would benefit from additional consideration of it, or a stronger justification for a dominantly hard bed interpretation. For example, on p. 27 there is discussion about localized diffusive systems with limited flow, and it seems like till would fit the bill.**

R. This is a good observation. We have now considered it by adding the the following:

The paragraph in page 2, 5-8 has been changed to the following (the relevant text added is underlined):

“The extent to which water pressure is raised by increased water supply depends on the following three factors: the permeability of till underlying the glacier, the configuration of conduits, both at the bed and in the ice, and the storage capacity of the drainage system, which can act to buffer the effect of additional water supply.”

In the discussion (section 4.2) after the line 7 of page 27 the following paragraph will be added: “Hubbard et al. (1995), suggest that the bed substrate at their study site is composed of glacial till of varying grain size distributions, acknowledging that “a network of small channels” on a hard bed could also account for their observations. However, in terms of hydrology, till and a distributed drainage system at the ice-bed interface share many characteristics: we expect both to give rise to a diffusive model for water pressure if water storage in the distributed system is an increasing function of water pressure. The primary difference is in how the permeability of that system evolves. In the ‘hard-bed’ view, the permeability evolves over time in response to changes in effective pressure, whereas for a granular till, porosity and therefore permeability are simply functions of effective pressure and therefore respond instantly to changes in it (Flowers, 2015). The main inconsistency of appealing to drainage through continuous till layer as the main pathway for water flow is that we would expect to see more standard diffusive behaviour, and certainly no sharp switches between connected and disconnected portions of the bed. In addition, till with a sufficient coarse-grained fraction of cobbles and boulders would probably be capable of supporting the formation of cavities in the lee of those larger grains. In short, if till

is capable of creating cavities, or is interspersed with bedrock bumps or somehow capable of supporting switching events by other means, then our interpretation would not be affected by assuming a hard or granular bed.”

- 3. p18, lines 2-3: How much does snow cover or ice albedo change? It is a questionable assumption that the degree day factor remain does not change significantly as surface conditions change over the summer. The interpretation in Figure 11c seems rather tenuous.**

R. That is a very good point. And indeed the signal we base our interpretation on, could arise due to changes in the degree-day factor through the season. Therefore, we have done further research to asses the variability of degree-day factors and computed the relative amplitudes using an independent proxy of melt variability coming from surface elevation measurements by a sonic ranger at the AWS location. To address this question, we have added a short section (section 2) to the supplementary material. The new section study the variability of degree-day factors, and computes the relative amplitude of Fig. 11c using surface lowering as proxy for melt amplitude instead of the standard deviation of the positive part of temperature.

- 4. The title is fine as it is, but it is worth considering the title somehow including some- thing about the importance of the disconnected/weakly connected system in the interpretation, as this is a primary result.**

R. We have changed it to:

“Channelized, distributed, and disconnected: subglacial drainage under a valley glacier in the Yukon”

- 5. As mentioned above, the borehole results section is quite long.**

R. We have reduced the results by moving section 3.6 to section 1 of the supplementary material as suggested by referee #3. References to it were added to the Methods and Discussion.

Specific Comments

- Abstract seems a little short given the length of the paper, but it does hit the most significant highlights of the paper.**

R. We agree, but given the consideration that it does hit the most significant highlights of the paper, we will keep it unchanged.

- 1, 22: basal "slip" may be considered the preferred term here (Cuffey and Paterson, 2010), to acknowledge the ice is not sliding differentially from the substrate at its sole.**
“A similar effect is observed on glaciers resting on a till layer, where a lower N reduces the yield stress of the till, and therefore also enhances basal sliding”

R. We have added in parentheses: “sliding is here intended to include motion at shallow depths within the till layer as well as at the ice-till interface”. From the perspective of large-scale ice

motion, both processes appear as the same thing.

- **2, 6: No comma here.**

R. Removed

- **2, 6-11: Interactions between subglacial hydrology and ice motion could be mentioned here as well (e.g., Hoffman and Price, 2014). And Gordon.**

“The extent to which water pressure is raised by increased water supply depends on both, the configuration of conduits and the storage capacity of the drainage system, which can act to buffer the effect of additional water supply. In turn, the conduits that make up the drainage system can change in response to changes in water input, as the associated changes in effective pressure affect the rate at which viscous creep closes subglacial or englacial conduits. Changes in discharge also affect the rate at which wall melting enlarges conduits. Over time, the response of the drainage system to the same water input pattern can therefore change (Schoof, 2010).”

R. That is something worth mentioning. And the new version of the paragraphs does it (relevant changes underlined):

“The extent to which water pressure is raised by increased water supply depends on the following three factors: the permeability of till underlying the glacier, the configuration of conduits, both at the bed and in the ice, and the storage capacity of the drainage system, which can act to buffer the effect of additional water supply. In turn, the conduits that make up the drainage system can change in response to changes in water input, as the associated changes in effective pressure affect the rate at which viscous creep closes subglacial or englacial conduits. Changes in sliding (themselves due to changes in effective pressure) will also affect the opening of basal cavities (Hoffman and Price, 2014), and changes in discharge affect the rate of conduit enlargement by wall melting. Therefore, over time, the response of the drainage system to the same water input pattern can change (Schoof, 2010)”

- **2, 29: missing "a" -> "to provide a less efficient"**

R. Added

- **2, 33: "do" should be removed.**

R. Removed

- **2, 32-34: (Creyts and Schoof, 2009) could be an appropriate additional reference for this topic.**

“Unlike channels, multiple cavities can co-exist in close proximity, because a larger cavity size facilitates faster creep closure rates, while the opening rate is generally assumed to do not depend significantly on size. Therefore, larger cavities will tend to close faster and converge to equilibrium with small ones (Kamb et al., 1985; Fowler, 1987).”

R. Citation added

- **3, 5: I believe you meant for the second "channels" on this line to be "conduits".**

“The formation of channels can be understood as an instability in drainage through a distributed network of channels,”

R. Yes, changed

- **3, 9-15: This is a nice summary of the complexity in borehole observations. A few suggestions for additional references: "widespread areas of high water pressure during winter": (Ryser et al., 2014; Wright et al., 2016) "large pressure gradients": (Fudge et al., 2008) "sudden reorganizations": (Gordon et al., 1998) "anti-correlated temporal pressure variations": (Andrews et al., 2014; Ryser et al., 2014)**

R. Great suggestions. We have included all of these.

- **3, 31: "in-deep" -> "in-depth"**

R. Corrected as suggested

- **5, 33: Could mention that many authors refer to this as "hydraulic head".**
“In the present paper, water pressure values will be reported in metres of water (the height of the water column that would produce that pressure).”

R. We would rather not change the text in this case, because “hydraulic head” includes the offset due to the elevation of the base of the glacier ($\text{base height} + \text{pressure}/(\rho_w * g)$), so just writing $\text{pressure}/(\rho_w * g) = \text{head}$ would be incorrect. Therefore, to avoid confusion we decided to describe what we mean instead of referring to the concept of "hydraulic head".

- **Figure 2: I recognize that showing so many different symbols and colors is challenging, but it is difficult to differentiate some of them. Perhaps removing the 3d shading on the symbols would help. In particular, the red symbols are hard to make out. Maybe put a circle around them or something to make them easier to see. Also, the black and blue lines are difficult to tell apart. Finally, the concept of "upstream area" from Schoof et al., (2014) should be briefly elaborated on (either in the caption or the text).**

R. We have made the symbols easier to differentiate, both by removing the shading effect and increasing the size. To explain better the “upstream area” concept we have changed the last sentence of the caption to “Grey shading indicates the upstream area, calculated assuming an hydraulic gradient given by an effective pressure equal to half of the ice overburden pressure, and computed using the D^∞ method described by Tarboton (1997)”

- **Figure 3: The figure is a bit small in my printout. In particular, the green dots are hard to see.**

R. We have changed the points by bars to make the visualization clearer.

- **7, 8: Consider changing "Fast-Flow" to "Fast Water Flow". When I first read this I interpreted this to be a region where ice velocity is fast.**

“On July 28th, 2013, while installing a sensor in the hole marked “Fast-Flow” in Fig. 2, strong periodic pulls were felt through the sensor cable, revealing a conduit with turbulent, fast flow in the bottom 50 cm of the borehole. This borehole was also the only one in which there was an audible sound of flowing water. The fast-flow hole was drilled at the very end of the field operations, and no further detailed on-site investigation was conducted.”

R. Due to the numerous references to the “Fast-flow” borehole we rather keeping that short name. However we agree that the way we present it in the first instance is confusing. Therefore, we have modified the above paragraph so that the context is better explained before introducing the “Fast-flow” short name. The final paragraph will read as follows:

“On July 28th, 2013, while installing a sensor at the bottom of a borehole, strong periodic pulls were felt through the sensor cable, revealing a conduit with turbulent, fast water flow in the bottom 50 cm of the borehole. This borehole was also the only one in which there was an audible sound of flowing water. The location of the hole is marked as “Fast-Flow” in Fig. 2, it was drilled at the very end of the field operations, and no further detailed on-site investigation was conducted.”

- **8, 31: bumper**

“After a data gap caused by a corrupted compact flash card, the records have become more dissimilar by August 2nd, but continue to exhibit common pressure variations.”

R. Indeed

- **Figure 4: The colors are a bit difficult to match to the map. Again, perhaps removing the 3d shading of the symbols on the map would help.**

R. We have enlarged the symbols and removed the 3D shading.

- **Figure 4 caption: in part c), it says two sensors were installed here, but I only see one line in the plot. Clarify if they are plotted on top of each other or if only one is plotted and, if so, which and why.**

“(c) Pressure in the fast-flow borehole (red) and its correlation with temperature in grey, computed for any given time over a 3-day running window. Note that two sensors were installed in the fast-flow borehole, offset vertically from each other by 70 cm.”

R. The two lines are indeed on top of each other most of the time, but they can be distinguished in the periods with no diurnal oscillations. We have changed the last sentence to: “...offset vertically from each other by 70 cm, making the two lines indistinguishable most of the time at the presented scale. Later in section 3.5, the complete record will be displayed, where the two curves are more distinguishable.”

- **Figure 5: Is correlation to temperature calculated for panel c here as it was for Figure 4? If not, mention that in the caption.**

“Panel c shows pressure in the slow-flow borehole (black) and three other boreholes in the same line.”

R. No, it wasn't, because all the lines in the panel undergo disconnection events, so it does not make sense to produce a mean of all of them, or to pick one. However, as the correlation is relevant to the discussion. Therefore we have picked one timeseries that remains connected over the whole interval and computed the correlation of it with the temperature record. The correlation data has been added to the figure and the relevant lines of caption modified to: “Panel c shows pressure in the slow-flow borehole (black) and three other boreholes in the same line. The correlation with temperature has been calculated using the only borehole that remains connected over the whole interval.”

- **11, 18: Should "ice" be "water" here?**

“...it is therefore possible that more boreholes intersect conduits with fast-flowing ice...”

R. Indeed. Corrected.

- **13, lines 1, 2, 3, 5, 7, 9: Include figure number with each panel reference.**

R. Good suggestion. The references to the panels have been changed to include figure numbers like “panel 8c”. The same change have been applied in many other instances for consistency.

- **Figure 8: Caption for g) refers to six digital sensors included in panel b, but panel b is the temperature record.**

R. Yes, it should have said “panel c”. Corrected.

- **15, 20: The second comma should be removed.**

R. Removed.

- **Figure 10: Panel c is pretty hard to make out details of. Perhaps this figure could be reorganized into two columns, or panel c could somehow be made a bit larger.**

R. This figure was reduced to fit in one page using the discussion paper template. In the current version it was enlarged to full size.

- **17, 3: Fig. 8b must be an incorrect reference - do you mean Fig. 10C?**

“We have described the apparent spatial patterning of the drainage system above. This patterning is however not fixed but evolves over time. In Fig. 8b, it is clear that all 42 boreholes show very coherent temporal pressure variations at the start of the observation period.”

R. Yes it was incorrect. It should say figure 8c. It was corrected.

- **Figure 13: Consider putting earlier on, perhaps with Figure 3.**

R. Good suggestion. We have moved it up, corresponding now to Fig. 3. And the following text was added to the end of the caption: “The interannual variability evident in the photo will be discussed in section 4.”

- **Section 3.6: The data quality section would be more natural in section 2 (methods), than late in the results section.**

R. As mentioned above, section 3.6 have been moved to section 1 of the supplementary material. The corresponding references were added to sections Methods and Discussion.

- **22, 10: I think you mean "120% of overburden", not "above".**

R. Indeed. Corrected.

- **22, 11: Consider replacing "and" with "however" or "yet" to make it clear you are arguing against sensor drift being able to explain these observations.**

R. Good suggestion. It was replaced by “yet”.

- **23, 12-14: This text would flow better with this sentence in parentheses.**

“We will refer to this initial state of the subglacial drainage system as stage 1. Note that the “stages” identified here are not the same as the “phases” discussed in Schoof et al. (2014), who focused only on the later part of the melt season and the subsequent winter; for instance, phase 2 in Schoof et al. (2014) corresponds to the transition from stage 2 to 3 here.”

R. Although we agree with the suggestion, we were previously advised by the editor to avoid sentences completely in brackets. So we will make no changes in consideration of the editorial guidelines.

- **25, 5: (Hubbard et al., 1995) could be an additional appropriate reference here.**

R. Good suggestion. Added.

- **25, 14: An aside: water pressure in nearby moulins/crevasses would be useful here. Something to consider if this field campaign continues.**

R. We agree. Unfortunately there are no moulins in the study area, and most of the crevasses in appear to be shallow (10-15 m deep) and generally do not having standing water in them. We have considered instrumenting the area below from a moulin in future work.

- **25, 21: Some discussion of bridging stresses leading to isolation of low pressure channels would be good here (Hewitt, 2011; Lappégard et al., 2006).**

“These observations are consistent with a highly developed channel with higher water discharge that has become hydraulically isolated from the neighbouring bed: the high effective pressures in the channel would favour the closure of cavities or other connections at the bed.”

R. It is indeed an important process to include. We have edited the above paragraph to the following:

“These observations are consistent with a highly developed channel with higher water discharge that has become hydraulically isolated from the neighbouring bed: the high effective pressures

in the channel would favour the closure of cavities or other connections in the surrounding bed. This closure may also be enhanced due to the effect of bridging stresses (Lappégard et al., 2006). Bridging stresses transfer part of the weight of the ice overlying the channel to its surrounding bed, effectively increasing the ice overburden in those regions above its mean value (Weertman, 1972).”

- **25, 23: Also, Figure 3.**

R. Correct. Cross reference added.

- **25, 29: Mention that high up-stream areas means a likely water flow accumulation path (see comment above about introducing the significance of this upstream area).**

“Using the channel end-member feature of diurnal oscillations with pressure dropping to atmospheric at night, we have identified seven other boreholes where the drainage system is likely to have evolved into a well-developed channel (Fig. 2, red symbols), in all cases during the second half of July or first days of August during years with relatively high cumulative PDD, which ought to favour channel formation. Their locations loosely match zones with high up-stream areas (Fig 2, dark shading).”

R. In addition to the details already added to the caption of Fig. 2, at the end of the above paragraph we will add:

“..., which correspond to portions of the bed likely to concentrate basal water flow due to the expected hydraulic gradients.”

- **26, 1-7: This discussion would benefit from inclusion of (Meierbachtol et al., 2016).**

“Initially, creep closure will reduce any volume still occupied by air in the borehole and pressure can rise gradually; once there is no air space left, changes in water pressure must reflect the pressure required to maintain the borehole volume constant (assuming no further freezing) while the borehole may still deform under anisotropic stress conditions. Intuitively, we would expect the borehole to become flattened perpendicular to the direction of greatest compressive stress, requiring a larger borehole pressure to maintain a constant volume, which could account for the slow rise observed in water pressure, and possible for slightly above-overburden values. Importantly, the pressure in an isolated borehole should depend on its shape and can, therefore, differ from borehole to borehole; abrupt creation of new storage volume for instance due to crevasse propagation could also lead to abrupt changes in pressure in isolated boreholes.”

R. Indeed a good reference. We have included it in “... may still deform under anisotropic stress conditions (see also Meierbachtol et al, 2016)”

- **26, 28: "fragment into subsystem" -> "fragmented into subsystems"**

R. Corrected

- **27, 3-7: Interesting discussion. I think the quotes around "phase lag" should be removed.**

R. Quotes removed

- **27, 21: Is the distance long enough relative to channel flow speed for a phase lag to be expected? The other complication is there could be additional inputs of water from the surface that help to "lock" the channel phase to the surface phase even in the presence of diffusion within the subglacial system.**

“The pressure time series along the inferred channel system in Fig. 4 (panels c, e and g) are merely suggestive of a hydraulic connection, but hardly identical. [...] Importantly, however, there is no systematic phase lag accompanying the decrease in amplitude, as would be predicted by a diffusion model (Hubbard et al., 1995).”

R. In a diffusive system, the observed drop in amplitude should (with a single water input) correspond to a predictable phase lag. Therefore, if we observe a given drop in amplitude, we can predict the phase lag. That calculation involves a modeling exercise that we have decided not to include in the paper to avoid adding to its already considerable length. The point about additional water inputs is a fair one. To address it we have added the following at the end of the paragraph:

“It is however conceivable that additional water input from surface sources along the flow path can have a significant effect on the phase of the pressure signal.”

- **27, 27-29: Consider (Meierbachtol et al., 2016) again here.**

“Usually, disconnection occurs during a drop in water pressure in the subsystem, and reconnection during an increase (figures 6 and 8). This is consistent with connection or disconnection resulting from viscous creep closing connections between individual cavities within the distributed system (Kamb, 1987). Disconnection could also be the result of cavities shrinking while remaining connected, if the borehole simply terminates on an ice-bed contact area between connected cavities and those contact areas are systematically larger than the ~ 10 cm diameter of our boreholes.”

R. We have added “This process has been observed previously by Meierbachtol et al., (2016).”

- **27, 32: There is an alternative hypothesis as well of passive cavity opening due uniform basal sliding (Bartholomaus et al., 2011; Hoffman and Price, 2014; Iken and Truffer, 1997).**

“The anti-correlated signals we observe in our data (Fig. 8e) have previously been explained by a mechanical load transfer mechanism, where the ice around a pressurized conduit redistributes normal load, reducing the normal stress over neighbouring areas of the bed. Therefore unconnected water pockets in those areas would experience a drop in water pressure (Murray and Clarke, 1995; Gordon et al., 1998; Lefeuvre et al., 2015). A 3D full Stokes model presented by Lefeuvre et al. (2018) supports this interpretation, and suggest that the anti-correlation pattern depends on the bed slope, which can be one of the factors affecting the observed distribution of borehole displaying this behaviour. Boreholes exhibiting those anti-correlated pressures must then be effectively isolated, so that a change in normal stress mainly causes changes in the pressurization of the borehole rather than water exchange. The load transfer mechanism is consistent with our observations.”

R. Good point. We have considered the alternative explanation by adding:

“An alternative explanation suggests that such signals are associated to enhanced cavity opening due to basal sliding changes (Bartholomaeus et al., 2011; Hoffman and Price, 2014; Iken and Truffer, 1997). However, it is unlikely that a variation in sliding would precisely mimic the local water pressure variations in the adjacent drainage subsystem, as suggested by Fig. 9e: the force balance that determines sliding velocities should be affected by changes in basal shear stress across a larger portion of the bed”

- **28, 8: These island sound like the system described by (Murray and Clarke, 1995).**
“It would be difficult to explain the anti-correlated signal in these boreholes by normal load transfer over larger distances, when other isolated boreholes nearby show no such behaviour. This suggests that the connected drainage system can contain fine structure (either as channels or narrow regions of distributed drainage) with lateral extents smaller than the ~ 15 m borehole spacing. The same is indicated by the formation of disconnected “islands” in lines of otherwise connected boreholes at the same spacing as seen in Fig. 6 for the August observation period.”

R. Indeed, we have added the following at the end of the paragraph: “(see also Murray and Clarke (1995), for analogous observations).”

- **28, 19: Wouldn't disconnected areas act as *slippery* spots since they maintain high water pressure?**
“As in Hoffman et al. (2016), such a slow evolution could be accounted for by flow through a relatively impermeable till aquifer underlying a much more effective but less pervasive interfacial drainage system, and the magnitude of that leakage could have a significant impact on basal sliding rates if disconnected areas act as sticky spots.”

R. It is indeed very important to explain dynamic effects of isolated cavities. With this propose in the Introduction we have added the following paragraph (After line 4, page 3):

“If a cavity becomes disconnected, its fixed volume will result in a water pressure drop if sliding accelerates. Conversely, decelerating basal sliding will lead to relatively high water pressure in order to prevent creep closure, reducing basal drag. In other words, isolated cavities can act either as sticky spots when basal sliding speeds up or as slippery spots when it slows down, working as a buffer for basal sliding variations (Iken and Truffer, 1997; Bartholomaeus et al., 2011).”

However, we want to avoid interpreting our isolated boreholes as representative of isolated cavities, the high water pressures we observe are probably not representative of “ambient” water pressures in the disconnected areas, at least not necessarily. If a borehole connects to nothing but an isolated section of the bed, its pressure would be a passive measure of how hard the borehole is being squeezed by the ice, including stresses acting on the vertical wall of the borehole, that tells us nothing about the bed. It's still quite conceivable that there is strong ice-bed coupling near such boreholes. The assumption that these boreholes connect to cavities at the bed is what we want to avoid.

To clarify this in the paper, we have added the following at the end line 7 in page 26

(Discussion):

“Therefore, we have to caution against interpreting the pressure in individual disconnected boreholes as an indication of the conditions in the unconnected parts of the bed: instead the borehole pressure may be controlled predominantly by local stresses in the ice, and the orientation, volume and shape of the unfrozen portion of the borehole.”

- **28, 22-26: This is a significant result and well-stated here.**

“Although it is possible that some boreholes do not connect because they were not properly drilled to the bed, we believe that the existence of persistently disconnected areas is robust. Non-spatially biased samples suggest that up to 15% of the bed could remain unconnected year round. The existence of such unconnected holes, and the possibility of dynamic connection and disconnection, represents a challenge to existing drainage models, which typically assume pervasive connections at the bed.”

R. Thanks

- **30, 3: "differential motion between ice and till": If basal slip is primarily due to till deformation, then there will not be differential motion between ice and till.**

“Nevertheless, the lifespan of a sensor buried in the till ought to be short if there is differential motion between ice and till, causing the signal cable to tear.”

R. To clarify we will rephrase it as “... if there is differential motion between ice and the sensor placement in the till (e.g. Engelhardt and Kamb, 1998), causing the signal cable to tear.”

- **31, 11: Is there a significance to the designation 'K' or is it just an arbitrary letter choice?**

R. “K” is for Kamb, “R” is for Rothlisberger. To clarify, in that first mention of 'K'-conduits we now refer to them as “'Kamb' (K) conduits”.

- **31, 11: Please define n_c .**

R. See answer to next comment.

- **31, 11: Consider adding "along that edge" after " n_c-1 'K' conduits" to emphasize that this treatment is per edge.**

“Along each network edge ij , we assume one ‘R’-conduit that can behave either as a Röthlisberger (R) channel or a cavity, as in Schoof (2010), with average cross-section $S_{R,ij}$. To mimic the sheet of Werder et al. (2013) and avoid the pitfall of having to resolve every basal conduit, we also assume there are $n_c - 1$ ‘K’-conduits that behave only as cavities, and are not subject to enlargement by melting.”

R. The paragraph have been edited to: “Along each network edge ij , we assume there are n_c conduits connecting node i to node j : One ‘R’-conduit that can behave either as a Röthlisberger (R) channel or a cavity, as in Schoof (2010), with average cross-section $S_{R,ij}$, and n_c-1 ‘K’-conduits that behave only as cavities, and are not subject to enlargement by melting. This

configuration mimics the sheet of Werder et al. (2013) and avoid the pitfall of having to resolve every basal conduit”

- **Equations: It seems odd to use lettered sub-equations rather than a new number for each equation.**

R. Indeed, it is pointless in this case. We have changed the numbering to one number per equation.

- **31, 21: Also define Psi here.**

“We associate a nominal effective pressure N_i with each node, defined as overburden minus basal water pressure. Hydraulic potential Φ_i at each node and hydraulic gradient along the conduits are then given by”

R. The above paragraph have been modified to “We associate a nominal effective pressure N_i with each node, defined as overburden minus basal water pressure. Hydraulic potential Φ_i at each node and hydraulic gradient Ψ along the network edges are given by...”

- **Eq. 1d/e: A minor quibble: It would seem more intuitive if the threshold size also contributed to flow once the threshold is reached (which is not the case in 1d/1e). However I doubt the choice of how to treat that affects the results in a qualitative way, so either approach is defensible.**

R. We don't fully understand the meaning here. The threshold size does appear in the formula for flux even once the threshold is exceeded: in that case, discharge Q is proportional to $(S - S_P)^\alpha$, where S is conduit size and S_P the relevant threshold (we have omitted the other subscripts for implicitity).

- **Eqn. 1f/1g: Mention this is describing mass conservation to aid the reader. Also, this is a single equation so there should be a single label.**

“To account for conservation of mass, we also associate half the volume of water stored in a conduit between two nodes with each node, and likewise account for half the water created by wall melting in an R-conduit as water supply to each node. Consequently we impose”

R. To emphasize that just before presenting the equation, we have modified the last sentence to “Consequently we impose mass conservation in the form”

- **32, 17: This is a run-on sentence. How about ending it at "nodes" and starting a new sentence with "We".**

“To close the model, we need to relate the conduit effective pressure $P_{\{e,ij\}}$ to the nominal effective pressures N_i at network nodes, we write this in the form”

R. Changed as suggested.

- **33, 7: Is (Dow et al., 2015) meant here?**

“A key component that the model above continues to miss is the ability to open conduits due to

overpressurization of the system (Schoof et al., 2012; Hewitt et al., 2012; Bueler and van Pelt, 2015; Dow et al., 2016).”

R. Yes, corrected.

- **5.2 It would be clearer to call this section "Model Results".**
“5.2 Results”

R. Changed as suggested.

- **36, 1: "eventually" should be "eventual".**
“The eventually complete shut-down of the entire drainage system at the end of the summer season is presumably the result of low water supply: high effective pressure and low dissipation rate in channels allow basal conduits to close.”

R. Indeed, changed.

- **37, 11: The word "a" should be removed.**
“We have implemented this approach in a simple model, allowing us to reproduce qualitatively some of the main features of our data set: a sharply-defined drainage subsystems with insignificant diffusive pressure signal attenuation and the existence of isolated areas (See section 5.1).”

R. Removed

- **Data availability: What about model and model configuration and output? Mention it is included in the SI.**
“Data availability. The presented data set will be made publicly available in the future. Ongoing work is taking place to meet the format and create the ancillary data and documentation required for the release, that is expected to happen fully or partially by the end of 2018. In the meantime, it can be accessed on request to the corresponding author.”

R. We have added “The model code in Matlab and model configuration parameters are included in the supplementary material.”

Supplemental Material

- **paper_movie.mpg does not play for me.**

R. We have re-encoded it to a widely compatible format, and it is attached to this submission.

- **It would be more natural to switch the order of sections 1 and 2 to match the order these topics were presented in the main text.**

R. It does make sense. We have switched the order.

- **The SI material, particularly the modeling part, has some very useful information. I would like to see the main text refer to the SI in more places, with brief descriptions of what is found there.**

R. We have added multiple references to the supplementary material where pertinent. In particular there are five references to the Continuum model formulation.

Answers to referee #2 (Brad Lipovsky)

1. Additional questions about the observations/interpretation (Sections 2-4)

- a. **Given the complexity of the spatial patterning, would it be possible to make a movie that plots all the data? I envision the map in Figure 2 with each symbol having a color that is associated with a pressure scale. This should be feasible given the low sampling rate. There's only so much that can be conveyed with words.**

R. We have indeed considered and tried such visualization. However, we have decided to include it in a follow-up paper tackling the challenge of automatic clustering of time series for identification of boreholes subsystems. The reason for this is that the large variability of the unconnected sensors, the heterogeneity in the behaviours across short distances and the dynamism of the hydraulically connected subsystems, makes impossible to really distinguish any patterns in a visualization like the ones you propose unless we ignore/fade selected sensors and wisely color the subsystems of interest. Therefore, as the techniques we have developed for the identification and follow up of subsystems in time were beyond the scope of this paper, and are required to justify the decisions that have to be made to make such visualization useful, we have decided to do not include it here, but it will accompany our next paper.

- b. **How long does drainage of the borehole take upon connection to the bed? This timescale is mentioned only qualitatively in the manuscript. Early work by Kamb and Englehardt used this timescale to estimate properties of subglacial conduits.**

R. Unfortunately, the drilling rod used does not have the capability to record water pressure at the tip and we did not deploy any instrumentation to record water level during the drilling process. Therefore, we were not able to measure the water level drop during drainage events. For that reason, drainage events were treated qualitatively, and we did record whether they happened or not and at what approximate depth was the drill tip at that moment. To clarify this, after the sentence starting on line 6 on page 15:

“Drainage events occurred during drilling at all depths, but more frequently at greater depths, with 60% (59%) happening in the lower half of the boreholes. This remains true for the 2012 drilling campaign, where the first sensors were installed before the spring event and observations are likely to reflect winter conditions.”

We have added the following:

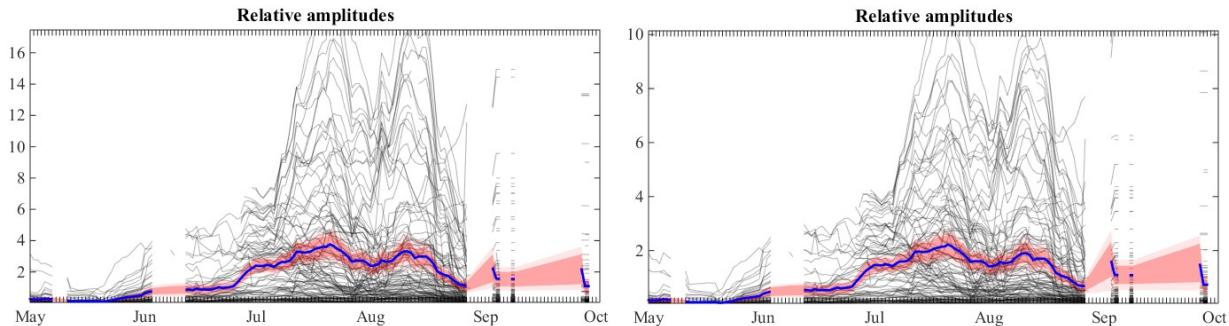
“Unfortunately, water level change and duration of drainage events were not recorded.”

- c. **Relative amplitude of pressure and temperature. Interquartile ranges (instead of standard deviations) may be more useful given the orders of magnitude variability.**

R. Indeed IQR would be more resilient to outliers. As per your suggestion we have tried IQR. The following two figures are a rough version of figure 11, panel c, the left one uses standard deviation, and the right one uses IQR

As can be seen, the differences are subtle and IQR does not provide a substantial improvement. On the other hand, it is a less common way to measure data dispersion, that might not be known

to many readers. For that reason, we have decided to keep the current definition of relative amplitudes using standard deviations.



d. Is it possible to quantify how fast switching events or connection/disconnection occur? For example, on page 27 line 26 [24]: “very abruptly in time”. What does that mean, exactly? Do transitions ever occur faster than the sampling resolution?

“We have referred to boreholes that cease to exhibit diurnal pressure variations as having disconnected. Connection and disconnection typically manifest themselves very abruptly in time (Fig. 6, see also Fig. 5 of Murray and Clarke (1995)).”

R. We mention the rough timescale when introducing the concept of switching event on page 19, line 3:

“In most cases, however, the transition is abrupt, and the same is true of boreholes connecting with each other: a rapid change in water pressure can occur over the course of a few hours or less as a connection is established. We term such abrupt transitions “switching events”, following Kavanaugh and Clarke (2000).”

We do not want to go much deeper into the details of switching events, but we do agree that it is important to mention the lower limit of the timescale and relate it to our sampling frequency. For that reason we have added the following after the paragraph on page 27 lines 23-24 cited above:

“This transition usually takes from few tens of minutes to a few hours. However, the initiation of the transition, often identified as a clear change in the rate of change of pressure with respect to time, can in many cases have the appearance of an instantaneous phenomenon, even at our shortest sampling interval of one minute. Therefore, it is unclear if these time scales can be associated with the connection or disconnection process, as they might only represent how fast the system responds to a perhaps instantaneous switch between connected and disconnected states.”

e. What does the pressure sensor response curve look like with and without the snubbers? Do the snubbers limit the ability of the sensor to measure high-frequency water pressure oscillations?

R. That is indeed an important consideration. We have now addressed it by changing line 29 on page 5 to:

“Most transducers installed from summer 2013 onwards were equipped with a Ray 010B ¼”

brass piston snubber that act as protection against transient high-pressure spikes, without altering the signal at the sensor sampling frequencies as verified by doubly-instrumented boreholes (see Supplementary Material Section 1).”

In the supplementary material, we have added the following text at the end of Section 1 (previously Section2: “Doubly instrumented boreholes: a test of pressure measurement reliability”):

“Doubly instrumented boreholes also allow us to assess the effect of pressure snubbers on pressure records. In figures 3, 4, and 7 to 11, sensor P1 (blue) was equipped with a snubber and P2 (orange) was not. In figures 1 and 2, both sensors had snubbers, and in figures 5 and 6 neither of them did. In the cases where only one sensor had a snubber, it can be seen that no smoothing of the pressure signal is observed. Close examination of the pressure time series shows that even spikes lasting a few minutes are well-reproduced by both records. Therefore, at the sampling frequencies of our sensors (1 to 20 minutes), the effects of the snubber are negligible. By contrast, among the sensors not equipped with a snubber, one out of 48 suffered large, “instantaneous” pressure offsets, contrasting with only one in 174 experiencing the same among sensors equipped with a snubber. Therefore, pressure snubbers seem to be effective at filtering out the transient high-pressure spikes (“fluid hammer”) that are thought to be responsible for those offsets through damaging the sensor diaphragm, but without affecting the accuracy of the instruments for measuring slower pressure variations.”

2. Questions about the model (Section 5)

a. A broader question regarding this type of modeling (i.e., also applicable to Schoof, 2010; Werder et al., 2013): Are conduit models convergent under grid refinement? Werder et al. (2013) in their Appendix A discuss grid densification. As those authors pointed out, this creates complexities associated with changing the domain geometry. But what refinement is undertaken in such a way that more grid nodes are added only at the midpoints between existing grid nodes. Does the model converge under this narrower sense of grid refinement?

R. Though the question is perfectly legitimate, the answer is really beyond the scope of the paper (and pertains as much to the Schoof 2010 and Werder et al 2013 papers as anything else). In short, network-based conduit models are not convergent under refinement, and are not intended to be. Effectively, they are intended to capture all the conduits at the bed individually. The reason for this should become apparent shortly.

Recognizing that capturing a large number of conduits may not be computationally feasible is what motivates the use of a continuum sheet overlain with a network of “potential channels” in Werder et al, and the use of the “K”-conduits of cross-sectional area S_K in the present case. The hope would be that, if we doubled the number of nodes and hence of network edges through any give line drawn through the domain, then halving the number n_c of total conduits per network edge would give some sort of effective convergence, although in practice the R and K conduits still behave sufficiently differently for that not to be entirely the case. The dependence on network orientation will of course remain, and is one of the bigger obstacles that remain in drainage modelling (in fact, it would be great to be able to evolve the geometry of channels and let them meander etc, but the real challenge in doing that would probably arise

when we try to couple them with other drainage conduits.

Based on what we have just said, the reason for not expecting convergence under “refinement” alone (meaning, just adding network edges) is therefore fairly straightforward – adding extra network edges then (without changing n_c) just corresponds to physically adding extra conduits.

The reason for using a non-continuum method (in the sense that we do not have convergence under refinement in the usual sense) is that channels that actually behave as R-channels (whose size is dictated by a balance of dissipation-driven thermal erosion and creep closure) cannot co-exist in close proximity. Consequently, channelization is intrinsically a process that does not lend itself to standard continuum description, where intensive quantities (like a channel density) would need to be used. The problem is that only a single channel will ultimately survive locally, while a density-based description would allocate a number $n = \text{density} \times (\text{grid cell size})$ of such channels to a given grid cell, and that has no hope of convergence, as the flux going through those channels, and hence the rate of wall erosion, then depends intrinsically on grid cell size.

b. What are the smallest scales that must be resolved by the spatial discretization? Do these length scales have practical significance for glacier modeling?

R. As per the above, a conduit model with a single conduit per network edge would have to resolve the scale of individual conduits. That is, the scale between adjacent conduit junctions. While that may be very small, it is the price that has to be paid to capture channelization. In our approach, as in that of Werder et al, we try to sidestep that slightly by lumping n_c conduits onto the same network edge, to allow realistically a coarser “resolution” (i.e. spacing between nodes). See above re: the meaning of resolution, however.

c. Is the model stable to perturbations of all wavelengths? This question is motivated by the observed “very abrupt” pressure changes. Consider, for example, Equation 17 in the supplement to Schoof 2010. The term v_m depends on the effective pressure gradient, which suggests that large effective pressure gradients may change the sign of the term in parentheses, and therefore destabilize flow. Is this analysis correct? If so, at what wavelengths does destabilization occur? How are these related to the wavelengths in the previous point.

R. As before, the model is not a continuum model, so the notion of continuous wavelength may be mistaken. Suffice it to say the following: If we took a one-dimensional “network” (effectively, “nodes on a string”), the model as formulated would be a legitimate finite-volume-type discretization of a pde model for a single channel, provided we make the parameter V_p proportional to the mean distance from the node in question to its neighbours (effectively, it has to represent storage capacity per unit length of the channel in that case, integrated over a single cell in the finite volume discretization). The corresponding one-dimensional pde problem is well-posed, in the sense that it is stable to short-wavelength perturbations (and that includes the action of the v_m term mentioned above). For longer wavelengths, we can get an instability (whose onset depends on the storage capacity per unit length) that can be explained physically – in fact, this instability is related to how jokulhlaups work and has been explored partly in Schoof et al 2014; a more theoretical take on this has been sitting on one (CS) of our desks for the last three years. That instability, which occurs for sufficiently long domains and sufficiently large storage capacities, is however not the point of the question, we suspect.

Instead, we assume that “wavelength” refers to the wavelength of perturbations in the cross-flow direction, and here the point about the model not being a continuum model in that sense becomes important. A more refined version of our model would solve the one-dimensional single conduit pde model referred to above on each network edge, treated as a line segment, so there would have to be many “grid points” on each network edge, resolving the spatial variations in N and S_R , S_K between the nodes of the network. At the nodes in our network, the individual conduits would join and be coupled through mass conservation and continuity of N . (As an aside, note that this approach can actually be fitted into our numerical framework, by putting additional network nodes connected to only 2 network edges between the nodes we already have, which generally have more than two edges connected to them. That procedure is generally overkill, in the sense that it yields a more accurate solution, but not one that is substantially different from the simpler network we are using in practice.)

What the more refined version of the model cannot do is solve a generalization of our single-conduit pde model to two dimensions (Note that this is a very different idea from a network of connected one-dimensional conduits; the change in dimensionality of the domain is what matters). A two-dimensional continuum model would not be well-posed, in the sense that it would be unstable to arbitrarily short wavelength perturbations. (The appendix to Schoof et al 2012 may be more instructive in that regard.)

Once more, the network model tries in effect to resolve individual conduits, not an actual continuum sheet. In that network, the channelizing instability will in fact typically involve some channels growing at the expense of their immediate neighbours, which in a sense is the equivalent of a short wavelength instability in a continuum model, except there is a “shortest scale” in our network problem (as opposed to the continuum counterpart), set by the spacing of individual channels. Instability at that discrete scale is not evidence of ill-posedness, while short-wavelength instability in its continuum counterpart would be.

In the long run, the instability in the network model leads to a coarsening of the channel structure: initially, very closely spaced channels grow, for instance as a pattern of alternating growing and shrinking channels. However, competition between nearby growing channels eventually leads to one channel winning out over its nearby competitors, so that locally only one channel survives. This is evident for instance in figure 3 of Schoof 2010, or in the supplementary movies #1 and #7 for that paper (where initially quite a dense channel structure emerges, which then coarsens). An attempt to understand the length scale for the coarsening (that is, of the length scale over which a single channel will no longer emerge victorious but at which different channels can co-exist) can be found in section 4.2 of the supplementary material to that paper. Obviously, the coarsening is a nonlinear effect that is not covered by any standard linearization techniques.

As we have pointed out, this really pertains to some of the existing literature on which our model builds, rather than the model development in the paper itself, so we have not incorporated any of the material above into the paper.

d. This line of questioning is based in part on my experience with subglacial hydrology modeling in the paper Lipovsky and Dunham (2015, JGR). In that paper we showed that there is no flow destabilization (at least not at glaciological flow velocities) in a sheet configuration without melting when elastic effects are taken into account (and with other assumptions).

R. We suspect there is a difference in scales being assumed here. We are interested in pre-existing “conduits” separated by areas of ice-bed contact, rather than an actual sheet, and the conduits are large enough to allow sufficient drainage to be potentially subject to enlargement by dissipation-driven melting, in the same way an R-Channel works.

e. Some small points: should the symbol S in Equation 1a be $S_{\{R,ij\}}$? Or is S another quantity? Same with Equation 1b. Also, $S_{\{K0\}}$ is not defined in the text.

R. Yes, S should have been $S_{R,ij}$ and $S_{K,ij}$ in (1a) and (1b), respectively. This has been corrected. We have also amended the text below the equations to say “and S_{R0} as well as S_{K0} are cavity-size cut-offs at which further conduit enlargement drowns out bed obstacles”

3. Connections between observation and model

a. I was disappointed by Section 5.2. Up to this point, I was carried along in the narrative of the paper: the reader learns about a dizzying array of new data, their broader interpretation, and then the formulation of a model improvement. But then I’m not sure what I’m supposed to learn from these simulations. Is the fit to data good? Does it capture some of the aspects of the field observations and not others? Given the ambitious scope of the paper, a much more extensive discussion of these topics is warranted.

R. We have fully rewritten section 5.2, adding a second model run without the size cut-off as requested, and making sure to state clearly the insights provided by the model.

b. I would strongly recommend the creation of a new “Section 5.3: Discussion of the Simulations”. There were so many observations in Section 3 that I had a difficult time keeping track of all of them (see later comment). As written, there is no relationship drawn between Figures 16 and 17 and the main observational results/figures.

R. We have expanded significantly on the description of model results (see above). Because the simulations we report on are motivated by trying to address specific features of the drainage observations, we have not created a separate section.

c. Near the last line of the paper it is stated, somewhat belatedly, that “However, the ability of the system to fully shut-down requires the incorporation of other physical process that could allow the reactivation of the drainage system during the spring event, something that is probably accomplished by over-pressurization.” This should be included earlier, in a potential model discussion section.

R. We have included this in the description of the drainage model results (section 5.2).

d. Is the model capable of describing stage 1, 2, and 3 as defined in Section 4?

R. The model is not capable of describing the beginning of stage 1, where a widespread set of new connections needs to be generated quickly, see the point identified immediately above:

“However, the ability of the system to fully shut-down requires the incorporation of other physical process that could allow the reactivation of the drainage system during the spring event, something that is probably accomplished by overpressurization”.

The model also requires a more careful treatment of normal stress redistribution, in particular in association with isolated and closely spaced cavities of very different water pressures. This is left for future work. In the future, we also hope that it will be possible to test models like the one presented here or more sophisticated versions of it, against detailed borehole datasets such as that from South Glacier.

The remaining stages pertain to channelization and focusing of flow, which pre-existing network models are known to be able to do (see Schoof 2010 for instance, as well as the Werder et al 2013 model). The only novelty (compared to these pre-existing network models) we require here is the ability to create fully disconnected regions that can, however, still evolve. That is why we have focused on the ability of the model with a percolation cut-off to cause switching events and evolving disconnected regions.

We also explicitly state that rapid, large-scale connection at near zero effective pressure cannot be captured by the modified model, see the new Model Results section.

e. Does the observed spatial heterogeneity (Section 3) factor into the choice of smoothing length scale?

R. Not directly. There are three smoothing length scale that one could justify physically: the linear transverse dimensions of a conduit, the spacing between conduits, and the ice thickness. In typical continuum models of cavity formation (e.g. Schoof 2005, Gagliardini et al 2007), the first two (conduit size and conduit spacing) are assumed to be comparable, and the effect of one cavity is felt roughly within that distance, so it makes sense to use conduit spacing as the averaging length scale, which is effectively what we do. Without more detailed knowledge of the detailed conduit configuration at the bed, it is difficult to be sure that this is what the observed spatial heterogeneity actually shows – our suspicion is that, if anything, we undersample that heterogeneity in the field. We are currently trying to test some of this using a record of switching events in the data (specifically, whether we can predict switching events using only pressure data in the vicinity of boreholes that switch on and off repeatedly), but that work will be reported elsewhere.

f. The bottom panels of Figure 17 would be better plotted in terms of water pressure (units equivalent water height) so that they can be easily compared to the rest of the figures in the paper...

R. As we state in the revised results section, our intention for the model is to investigate the qualitative behaviour of the model with a percolation cut-off. We do not have sufficient data on surface melt production or, more importantly, surface melt routing, in order for our calculations

to have anything more than a qualitative relation with the observed field data. Moreover, the actual magnitude of pressures depends not only on the water supply rates but also on the parameters in the model. As discussed in the appendix to Schoof et al (2014), the closure rate parameter c_2 in particular is not well constrained, but ultimately dictates the pressure scale. We have chosen Pa as units in order not to give too great a weight to the absolute pressure values calculated here, in addition, they are values of effective pressure in contrast of water pressure as in the rest of the paper. That said, 100 m of water are equivalent to 1 MPa.”

g. ...Which of the various observed time series should the reader associate with the four panels Figure 17d-g?

R. As before, the runs are idealized and so a direct comparison is not appropriate. However, we now make clear at the start of the results section that our motivation is in the switching events of stage 2 – in particular, the abundant switching events evident in Figure 10g (see also Figure 8c) during the part of the drainage season that we have associated with a potentially channelized drainage system.

4. Comments on the writing

a. There are so many important points in Section 3 that I had a difficult time sorting through all of them. I suggest adding a writing device to emphasize the most important ones. This is partially a stylistic choice. One option would be to enumerate the points at the start. Another option would be to align subsection headings with main points.

R. It is a very reasonable concern and it have been points by other referee too. After considering multiple possibilities we have included an extended overview at the end of the introduction. The following text has been added after line 32 of page 3:

“To help the reader to navigate through the numerous observations presented in this paper, we provide below an extended overview of its contents, highlighting the most important points to be considered:

- The observed drainage system consists of three main components (section 3.1)
 1. Channelized: efficient, turbulent drainage at low water pressure
 2. Distributed: slow water velocities, damped response to diurnal meltwater input, high water pressure
 3. Disconnected: near-overburden mean water pressure with no diurnal variations
- The “disconnected” areas display a small but statistically significant and sustained drop in mean pressure during the melt season, suggesting weak connections potentially through porewater diffusion in till (section 3.1 & 4.2).
- The connected drainage system consists of spatially distinct parts (subsystems) that appear to act independently. Each is characterized by a common diurnal pressure variation pattern that differs markedly from other subsystems (section 3.2 & 4).
- Pressure variations in boreholes in disconnected areas can also occur due to bridging effects and potentially due to ice motion, the latter giving rise to low-amplitude, high frequency pressure variations shared by distant boreholes (section 3.2, 4.2 & 4.3).

- Observations suggest the existence of a dense network of englacial conduits, but it is unclear if these can transport water over extended distances horizontally (section 3.3 & 4.2).
- During a spring event, a large distributed drainage system quickly develops over a large fraction of the bed. This splits into an increasing number of subsystems over the summer season, each potentially focusing around a channelized drainage axis. The extent of disconnected areas of the bed grows as a result (section 3.4 & 4).
- The transition from connected to disconnected is abrupt, with the connected parts of the bed having a high hydraulic diffusivity ([new] section 3.5 & 4.2). Disconnection and reconnection “events” typically occur as water pressure is falling and rising, respectively. These observations motivate the modification of existing drainage models presented in section 5.
- The timing and degree of channelization reached by the subglacial drainage system varies widely depending on weather and surface conditions during summer, and the spatial pattern of drainage can change from year to year ([new] section 3.6 & 4.1).
- Abrupt growth of the distributed drainage system, analogous to that observed during the spring event, can be observed during the summer in response to a sudden, abundant meltwater input following an extended hiatus, the latter usually caused by a mid-summer snowfall event (section 4).”

b. The manuscript, especially Section 3 and 4, would be improved by revision for brevity. There is a lot of repetition, particularly in Section 3. The authors mention at least four times, for example, that clustering is subjective.

R. Indeed, we have moved section 3.6 to section 1 of the Supplementary material for brevity. And the clustering criteria is now addressed only by the paragraph starting on line 7 of page 8. To which the following text was added:

“All borehole groupings presented in the following figures were manually selected using the same criteria as described for Fig. 5.”

Answers to referee #3

General comment

The authors report a new set of observations of water pressure at the base of a glacier. The amount and quality of data acquired in this study are particularly impressive and unique. Based on this comprehensive dataset, a thorough analysis is conducted in order to distinguish typical behaviors of the subglacial hydrology network based on analyzing characteristic spatio-temporal patterns in the measurements. Observations are generally in agreement with expectations from theory, except the finding that many portions of the bed are observed to be hydraulically isolated, a feature that yet is not accounted for in subglacial hydrology models. To overcome this lack, the authors present a modelling framework (based on the adaptation of existing theory) that allows explicitly treating these hydrologically isolated parts of the bed.

Overall, I find the study particularly interesting and novel, since it provides new observational constraints on subglacial hydrology, as well as a unique and comprehensive dataset of interest by a large community. For these reasons I strongly recommend this paper for publication. However, before so, significant revision is needed in order to clarify text in places, better structure observations and clarify results. Below I provide specific comments that hopefully will help the authors to improve this. Moreover, the complexity and lengthiness of the paper is further reinforced by the inclusion of a modelling part at the end. Although I clearly appreciate the modelling effort, I am not convinced that this section really fits in this observational paper. As is I feel like lots of readers won't even notice the modelling part of the paper, especially given the strong imbalance between the long and extensive analysis of data and the short modelling analysis provided at the very end. For these reasons I strongly recommend the authors to consider publishing this modelling work separately, and my comments below are limited to the observational part.

Detailed comments

Section 2

- **Some context information about the glacier and its environment is missing. I think this information is needed for the reader to make best sense on what type of general glacier and hydrology regime.**
 - **What are the typical values for glacier surface speed (in winter versus in summer)?**
 - **What are the expected sliding velocities (even rough estimates would be useful to know)**

R. After line 14 on page 5 the following has been added:

“Surface velocities were measured with a GPS array (Flowers et al., 2014), and display a strong seasonal contrast. The velocity at the GPS tower at the centre of the array (see Fig. 2) varied from 30.6 to 17.9 m/year between summer 2010 and early spring 2011. Modelled basal motion in our study area accounts for 75–100% of the total surface motion (see Fig. 6b in Flowers et al. (2011), where our study area is located between 1600 and 2500 metres)”.

- **Can the authors give a qualitative sense on the potential effects of basal water pressure on glacier dynamics for this glacier and at this particular location where water pressure is monitored?**

R. The most plausible cause of the variations mentioned in the previous point, is the effect of varying basal water pressure, as mentioned generically in the introduction. The lack of direct evidence among the observations presented in the paper to support anything more specific makes us hesitant to postulate more detailed effects than those already described in the introduction.

- **What are typical outlet water discharge values and how much do they typically vary from winter to summer?**

R. At the end of Section 2 “Field site and methods” we have added the following paragraph:

“The limited available stream gauging data suggests typical summer flow around 1-2 m³/s, with maximum values around 5 m³/s and minima below the measuring capacity of the gauging station (Crompton et al., 2015). However, the outlet stream was never observed to run dry (J. Crompton, personal communication).”.

Since the the study is motivated by understanding the links between hydrology and sliding (see intro), I think it would be good to give a sense on these aspects to the reader, even if these statements are brief and qualitative.

- **There is also missing information about how the glacier evolved over the past 8 years during which basal water pressure has been monitored. In particular, did glacier thickness vary over the course of the 8 years of experiment? If yes please give an estimate about how much.**

R. After line 9 on page 5 we have added the the following:

“The average net mass balance over the whole glacier during the period 2008-2012 was estimated to be between -0.33 and -0.45 m/year water equivalent (Wheler et al., 2014), corresponding to 37-51 cm/year of average glacier thinning. Elevation changes in the study area derived from differential Global Positioning System (GPS) measurements of borehole locations (taken after drilling) suggest a thinning of 59 cm/year over the same period, and 37 cm/year in the period 2008-2015.”

Section 3

- **Figure 4: I find it quite complicated to identify which hole goes with which measurement. Would there be a way to improve clarity in this figure? Maybe zoom in the map, or make two map subsets to make the color code easier to see.**

R. As mentioned to referee #1, we have removed the 3D shading of the dots in the map and

increased the size of the markers to make identification easier.

- **Line 16 p 7 to line 6 p 8 : unclear text with long sentences.**

“Panel c of Fig. 4 shows the pressure recorded in the fast-flow borehole for the first 33 days after installation. Panel d shows the pressure records in three boreholes along the same line across the glacier at 15 m spacing. The lack of similarity between the fast-flow hole pressure record and those from other nearby boreholes differs from the behaviour of most boreholes that display diurnal pressure oscillations: typically, such boreholes show a signal similar to one or more neighbouring boreholes, forming a cluster that extends some distance laterally across the glacier (see section 3.2). In the case of the fast-flow borehole, somewhat similar temporal pressure patterns were observed at a much larger distance downstream, as shown in panels e and g of Fig. 4, and less so in panel h, while a set of boreholes exhibiting very different variations close to those in panel d is shown in panels f. For reference, panel i shows the remaining pressure time series recorded in the same area, highlighting the diversity of pressure patterns observed. No systematic time lags were found between peaks on the fast-flow borehole and pressure peaks of boreholes displayed in panels e and g.”

R. The text has been changed to:

“Panel c of Fig. 5 shows the pressure recorded in the fast-flow borehole for the first 33 days after installation, and panel 5d shows the pressure records in three boreholes along the same line across the glacier at 15 m spacing. Note the lack of similarity between the fast-flow hole pressure record and those from other nearby boreholes. This lack of similarity contrasts with the typical behaviour of boreholes exhibiting diurnal pressure oscillations. Such boreholes usually share a similar pattern of pressure oscillations with one or more neighbouring boreholes, forming a cluster that extends some distance laterally across the glacier (see section 3.2).

However, in the case of the fast-flow borehole, somewhat similar temporal pressure patterns were observed downglacier and at much larger distances than the 15 m lateral borehole spacing, as shown in panels 5e and 5g, and less so in panel 5h. By contrast, a set of boreholes exhibiting very different variations close to those in panel 5d is shown in panels 5f. For reference, panel 5i shows the remaining pressure time series recorded in the same area, highlighting the diversity of pressure patterns observed. No systematic time lags were found between peaks in the fast-flow borehole and pressure peaks of boreholes displayed in panels 5e and 5g.”

- **P 7 to p 8: the whole discussion on what aspects borehole measurements have been grouped is quite vague, and repetitive. It would be good to have a single, short paragraph explaining how boreholes have been grouped, even if the criteria are qualitative (by eyes is a good enough justification), and then go on with the description without repeating how the selection has been done.**

R. We have gather the information about the grouping criteria in one clear paragraph (starting on line 52 of page 6 of the new manuscript) as suggested.

- **Label of Fig 6: amplitude offset? Or phase offset? Looks like it's amplitude.**
“We have applied offsets to make the agreement between the records clearer. These are, in order, 27, 26, 24, and 29 meters in (a), and 27, 20, 22, and 27 in (b).”

R. They are pressure offsets, with no changes in amplitude (just adding a constant value but no multiplier). We will make that clear by changing the above paragraph to: “We have applied a constant value offset in pressure to each time series (meaning, added a constant to the directly measured pressure) to make the agreement between the records clearer. The offset values are, in order, 27, 26, 24, and 29 metres in (a), and 27, 20, 22, and 27 in (b).”

- **I suggest to split section 3.1 into two sections. One would be something like "global overview of the dataset" with Fig 4 and 5 and the other would be something like "Diurnal and seasonal cycles in slow and fast flowing water" (Fig 3, 6 and 7). I think this would make it easier to read.**

R. We considered ways of doing this but were consistently stumped by the fact that the diurnal and seasonal cycles (especially the diurnal ones) were the strongest indicators of drainage activity, and could not conceive of a satisfactory way of splitting the section.

- **Line 5 to 15, p 12: unclear paragraph. Too long sentences.**

“When the whole data set is viewed over a given time window during summer, it is often possible to identify multiple subsets of boreholes showing very similar temporal pressure variations within that subset (often recognizable by the way in which the amplitude of diurnal oscillations changes over time), but these temporal variations are different from other boreholes. One example of this phenomenon comes from the boreholes in Fig. 4f, where we can see a group of boreholes that display a very coherent signal but with a distinctive two-day period. The boreholes in panel f are directly adjacent to those in panel e, we have associated with the fast-flow borehole and which show a very different, diurnal pattern of pressure variations (see also panels c and g). Less clear-cut though indicative of the same phenomenon is Fig. 5, where we see boreholes in panels d–f that exhibit quite different diurnal pressure variations to those observed in the group associated with the slow-flow borehole in panel c. Figure 3 of Schoof et al. (2014) also shows an example of the same phenomenon during July and August 2011: borehole B in that figure is, in fact, one of a group of 5 that exhibit almost identical diurnal water pressure oscillations that are quite distinct from those in boreholes A1–A6 in the same figure.”

R. The paragraph has been edited as follows:

“When the whole dataset is viewed over a given time window during summer, it is often possible to identify multiple clusters of boreholes, each exhibiting a specific pattern of temporal pressure variations. Often, these patterns are defined by the way in which the amplitude of diurnal oscillations changes over time. While boreholes in a given clusters will share the pattern of temporal variability, this will differ significantly from the pattern of temporal variability in the other clusters. One example of this phenomenon comes from the boreholes in Fig. 5f, where we can see a group of boreholes that display a very coherent signal but with a distinctive two-day period. However, those boreholes in figure 5f are directly adjacent to those in 5e. The latter by contrast show a very different pattern of diurnal pressure variations (that we have associated with the fast-flow borehole, along with panels 5c and 5g). Less clear-cut, though indicative of the same phenomenon is Fig. 6, where we see boreholes in panels d-f that exhibit quite different diurnal pressure variations from those observed in panel c (the group associated with the slow-

flow borehole). Figure 3 of Schoof et al. (2014) also shows an example of the same phenomenon during July and August 2011: borehole B in that figure is, in fact, one of a group of 5 that exhibit almost identical diurnal water pressure oscillations that are quite distinct from those in boreholes A1–A6 in the same figure.”

- **Line 10 p 13: Comparing panel b with panel e in Fig 8 I do not see the "inverted" or anti-correlated relationship. . . Wording and support from figures is confusing here.**

R. We agree with the difficulty of distinguish the features we mention. Therefore, we have highlighted in black one line that clearly displays the anti-correlated feature within the group. Without that highlight, the details are lost due to the overlap between lines. The paragraph has been changed to:

“The group of 14 boreholes in panel e of Fig. 8 also shares common diurnal pressure variation patterns, though this is not immediately clear as the mean pressures and amplitude of pressure variations varies significantly. For that reason we have highlighted in black one line that shows these variations clearly. Notably, these variations are “inverted” versions of the pressure variations seen in panel b, with peaks becoming troughs and vice versa.”

- **Line 28 p 13: Fig. 9 is very lately introduced here. Actually figure 9 seems to help in the understanding of "inverted" or anticorrelated signals, but it comes too late. Perhaps to be place earlier?**

R. Figure 9 shows a different kind of anticorrelated signal – the particular features being highly correlated or anticorrelated high-frequency pressure variations, occurring over large spatial distances, which are distinct from those we were trying to highlight in Fig 8. As a result, in order to avoid misinterpretation, we don't want to present the figure earlier. However, we hope that the above changes in figure 8 and the clarification of the text will help in the understanding of anti-correlated signals.

- **P 17: I find the difference between the title of 3.4 (seasonal evolution) and title of 3.1 (annual cycle) to be too weak. . . As is I get lost trying to understand what's new in 3.4 that could not be observed or has not been said in 3.1.**

R. We attribute this confusion to badly chosen section titles. To set the right expectations regarding the content, and help the reader we have change the title of Section 3.1 (Annual cycle and water flow) to “Modes of water flow: fast, slow and unconnected”.

In addition, we have split Section 3.4 (Seasonal evolution) in two, that correspond now to sections 3.4 and 3.5. The new section 3.4 is titled “Seasonal development of the subglacial drainage system”. The new section 3.5 starts after line 6 of page 18, and it will be titled “Basal hydrology transitions and 'Switching events”.

- **Section 3.6: I suggest to put this section in supplementary material, and just have a single paragraph in the main text that states how and to which extent observations could be biased by changes in data quality. If kept in the main text, this paragraph could even be placed in a separate section before results are exposed.**

R. As mentioned above, section 3.6 was moved to section 1 of the Supplementary Material. References to it were added to the Methods section. Figure 15 was kept in the main text to be referenced by section 4.4, where we have also added part of the text of section 3.6 that was relevant to that figure. The paragraph starting on line 21 of page 29, now reads as follows:
“It is likely that with time, some sensors can become encased in ice, as suggested by the fact that older sensors are less likely to show diurnal oscillations (for that reason, old isolated sensors were often decommissioned before they ceased to produce a signal), and the observations in doubly-instrumented boreholes (see section 1 of the supplementary material). Digital confinement data suggest that in some cases, as in Fig. 15, the termination/initiation of diurnal oscillations is associated with an increase/decrease in confinement. This observation would also be consistent with ice encapsulation of the sensor during winter.”

Section 4

- **Would be good to have a section or a paragraph that summarizes all key observations, which would be placed outside the discussion section. Then the discussion section would only be based on the summarized, main observations. As is it is embedded and its makes it hard to read.**

R. This is a very similar concern than the one expressed by referee #2 on the first of his “Comments on the writing”. Please refer to the answer to that comment.

- **I don’t see what is the difference between 4.4 data interpretation and what’s discussed earlier. Isn’t the earlier discussion also data interpretation?**

R. Indeed the title is not appropriate. We have changed it from “Data interpretation” to “Data interpretation caveats”.

Section 5

- **I suggest to remove that section from the paper, and write a separate paper on the modelling aspects.**

R. Further work on models for dynamic connection and disconnection in drainage models is clearly desirable. As in Hoffman et al (2016), our stated goal here is to link our observations directly to the shortcomings of existing models. This motivates the introduction and structure of the paper. As a result, we believe that it is sensible to point out avenues by which they can be fixed. The model alteration we propose is not an enormous one, and we feel it's preferable to propose it in context than to write an overly short paper simply modifying a couple of equations in an existing model. We are also interested in putting the idea “out there” so that other groups might feel encourage to work on updating drainage models. We view this as analogous to the work in Hoffman et al (2016), in the sense that we do not aim to have the last word on the subject.

Channelised, distributed, and disconnected: subglacial drainage under a valley glacier in the Yukon

Subglacial characterization from eight years of continuous borehole data on a small valley glacier in the Yukon Territory, Canada

Camilo Rada¹ and Christian Schoof¹

¹Department of Earth, Ocean and Atmospheric Sciences, University of British Columbia. 2207 Main Mall, Vancouver, BC Canada.

Correspondence: Camilo Rada (camilo@rada.cl)

Abstract. The subglacial drainage system is one of the main controls on basal sliding, but remains only partially understood. Here we use an eight-year ~~data-set~~ dataset of borehole observations on a small, alpine polythermal valley glacier in the Yukon Territory to assess qualitatively how well the established understanding of drainage physics explains the observed temporal evolution and spatial configuration of the drainage system. We find that the standard picture of a ~~channelizing~~ channelising drainage system that evolves towards higher effective pressure explains many features of the ~~data-set~~ dataset. However, our ~~data-set~~ dataset underlines the importance of hydraulic isolation of parts of the bed. We observe how ~~isolated~~ disconnected portions of the bed systematically grow towards the end of the summer season, causing the drainage system to fragment into progressively more distinct subsystems. We conclude with an adaptation of existing drainage models that aims to capture the ability of parts of the bed to become hydraulically ~~isolated~~ disconnected due to basal cavities of finite size becoming disconnected from each other as they shrink.

1 Introduction

Basal sliding often accounts for about half of the observed surface speed of glaciers [e.g. *Gerrard et al.*, 1952; *Vivian*, 1980; *Boulton and Hindmarsh*, 1987; *Blake et al.*, 1994; *Harper et al.*, 1998]. The sliding rate typically shows a marked seasonal variation, with summer sliding speeds sometimes two or three times faster than winter averages [*Nienow et al.*, 1998a; *Sole et al.*, 2011;

Ryser et al., 2014; *Ryser et al.*, 2014a]. These variations are controlled by the subglacial drainage system [*Iken and Bind-schadler*, 1986; *Gordon et al.*, 1998; *Nienow et al.*, 1998b; *Mair et al.*, 2001; *Harper et al.*, 2005]. However, the physical processes controlling the magnitude and timing of sliding rate variations are still incompletely understood.

The main variable linking subglacial drainage processes to basal sliding is effective pressure N , defined as the difference between normal stress at the bed (averaged over the scale of any basal heterogeneities) and water pressure, where normal stress is usually taken to be equal to the overburden pressure. Increased basal water pressure reduces N and provides partial support for the weight of the glacier, reducing the contact surface with the underlying bedrock, and therefore enhancing basal sliding [*Lliboutry*, 1958; *Hodge*, 1979; *Iken and Bind-schadler*, 1986; *Fowler*, 1987; *Schoof*, 2005; *Gagliardini et al.*, 2007]. A similar effect is observed on glaciers resting on a till layer, where a lower N reduces the yield stress of the till, and therefore also enhances basal sliding (sliding is here intended to include motion at shallow depths within the till layer as well as at the ice-till interface) [*Engelhardt et al.*, 1978; *Iverson et al.*, 1999; *Tulaczyk et al.*, 2000; *Truffer et al.*, 2001]. Conversely, large effective pressures enhance the mechanical coupling at the bed interface and therefore reduce sliding.

The magnitude of N is controlled by the combined effect of the rate of ~~melt-water~~ meltwater supply and the configuration of the englacial and subglacial conduits that drain the water out of the glacier [*Iken and Röthlisberger*, 1983; *Kamb et al.*, 1985; *Iken and Bind-schadler*, 1986]. For a given conduit configuration, an increase in water supply is likely to

decrease effective pressure. Specifically, water pressure gradients must increase in order to evacuate the additional water input to the system, requiring larger water pressures near locations of water supply to the bed.

5 The extent to which water pressure is raised by increased water supply depends on ~~both the following three factors: the permeability of till underlying the glacier,~~ the configuration of conduits, ~~both at the bed and in the ice,~~ and the storage capacity of the drainage system, which can act to buffer 10 the effect of additional water supply. In turn, the conduits that make up the drainage system can change in response to changes in water input, as the associated changes in effective pressure affect the rate at which viscous creep closes subglacial or englacial conduits. Changes in ~~discharge-sliding~~ 15 ~~(themselves due to changes in effective pressure)~~ will also affect the ~~rate at which wall melting enlarges conduits.~~ Over opening of basal cavities [Hoffman and Price, 2014], and changes in discharge affect the rate of conduit enlargement by wall melting. Therefore, over time, the response of the 20 drainage system to the same water input pattern can therefore change [Schoof, 2010].

Current drainage models have succeeded in reproducing observed variations of glacier velocities at a seasonal scale, and several features of the drainage system. These models 25 typically consider a system composed of two main types of conduits, R-(Röthlisberger) channels [Röthlisberger, 1972] and linked cavities [Lliboutry, 1968; Walder, 1986]. Other types of conduits and modes of water transport have been hypothesized-hypothesised [Alley et al., 1986; Walder, 1982; 30 Walder and Fowler, 1994; Ng, 2000; Boulton et al., 2007; van der Wel et al., 2013], but their relevance to alpine glaciers remain unclear.

R-channels grow by turbulent dissipation of heat and close due to ice creep. The creep closure of a channel is driven 35 by the effective pressure, and balanced by the melting of its walls by heat dissipated from turbulent water flow [Röthlisberger, 1972]. Multiple channels in close proximity are unstable. In such configuration, one channel that is slightly larger than its neighbours will also carry a larger discharge 40 resulting in higher dissipation and a faster opening rate. The creep closure rate will also be faster in the larger channel than the smaller one, but is less sensitive to size than the opening rate [Schoof, 2010]. Therefore, the larger channel will grow larger at the expense of the smaller ones. This process 45 tends to focus water flow into a few large channels, leading to the formation of an arterial drainage system covering a small fraction of the glacier bed [Fountain and Walder, 1998; Schoof, 2010; Hewitt, 2011, 2013; Werder et al., 2013].

In an R-channel, steady state is reached at a higher effective 50 pressure when the channel discharge (Q) increases, as a faster melt rate has to be offset by a faster closure rate. By implication, when water drains through channels, an increase in water supply should increase effective pressure around the channels, and slow the glacier down [Nye, 1976; Spring and 55 Hutter, 1982; Schoof, 2010].

On the other hand, linked cavity systems are thought to provide a less efficient transport mechanism, where slow water flow provides negligible heat dissipation. Cavities are kept open by the sliding of ice over bed roughness elements, which causes an ice-bed gap to open in their lee, while they 60 also close by viscous creep [Lliboutry, 1968; Kamb et al., 1985; Fowler, 1987].

Unlike channels, multiple cavities can co-exist in close proximity, because a larger cavity size facilitates faster creep closure rates, while the opening rate is generally 65 assumed ~~to do not not to~~ depend significantly on size. Therefore, larger cavities will tend to close faster and converge to equilibrium with small ones [Kamb et al., 1985; Fowler, 1987; Creyts and Schoof, 2009].

In contrast to channels, equilibrium in a linked cavity system is reached at lower effective pressure when Q increases: 70 cavities have to grow to accommodate additional discharge, and this requires creep closure to be suppressed by a reduced effective pressure. Therefore, an increase in Q should decrease effective pressure, and speed the glacier up [Kamb, 75 1987; Schoof, 2010].

If a cavity becomes disconnected, its fixed volume will result in a water pressure drop if sliding accelerates. 80 Conversely, decelerating basal sliding will lead to relatively high water pressure in order to prevent creep closure, reducing basal drag. In other words, isolated cavities can act either as sticky spots when basal sliding speeds up or as slippery spots when it slows down, working as a buffer for basal sliding variations [Iken and Truffer, 1997; Bartholomäus et al., 2011]. 85

The formation of channels can be understood as an instability in drainage through a distributed network of 85 channels-conduits, and can be expected to occur when water supply rates to the bed are sufficiently large [Schoof, 2010; Hewitt, 2011, 2013; Werder et al., 2013]. However, even then 90 the formation of a well-developed arterial channel network requires time and may not be fully complete in a single summer melt season.

Drainage models that include the above physics [e.g., Werder et al., 2013], still fail to reproduce direct borehole 95 observations of subglacial conditions [Flowers, 2015]. These include the existence of ~~isolated-disconnected~~ areas that show no signs of ~~basal-hydraulic-connections-flow-related~~ changes in water pressure [Hodge, 1979; Engelhardt et al., 1978; Murray and Clarke, 1995; Hoffman et al., 2016], the 100 development of widespread areas of high water pressure during winter [Fudge et al., 2005; Harper et al., 2005; Ryser et al., 2014b; Wright et al., 2016], large pressure gradients over short distances [Murray and Clarke, 1995; Iken and Truffer, 1997; Fudge et al., 2008; Andrews 105 et al., 2014], sudden ~~reorganizations-reorganisations~~ of the drainage system [Gordon et al., 1998; Kavanaugh and Clarke, 2000], high spatial heterogeneity, boreholes exhibiting anti-correlated temporal pressure variations [Murray and 110 Clarke, 1995; Gordon et al., 1998; Andrews et al., 2014;

New paragraph about the dynamical effect of disconnected cavities

Lefeuvre et al., 2015; *Ryser et al.*, 2014b], and englacial conduits [Fountain and Walder, 1998; Nienow et al., 1998b; Gordon et al., 1998; Fountain et al., 2005; Harper et al., 2010].

5 The relative scarcity of subglacial observations make it difficult to assess how common these phenomena are, and in some cases, the physical processes involved. In this paper, we take a holistic view of an eight-year ~~data set~~ dataset of borehole water pressure records and surface conditions obtained from a small polythermal valley glacier in the Yukon Territory, Canada. This ~~data set~~ dataset includes 311 boreholes with up to 150 being recorded simultaneously. We attempt to present a comprehensive picture of the evolution of the drainage system, incorporating all the main features of
15 the borehole record.

Our aim in this paper is to assess qualitatively the extent to which established understanding of drainage physics is compatible with our observations, and where existing models are in conflict with those observations. We will then
20 present a modification of a class of existing models intended to account for what appears to be the most significant missing physics: the development of hydraulically isolated patches of the bed *Hodge, 1979; Engelhardt et al., 1978; Murray and Clarke, 1995; Hoffman et al., 2016.*

25 The paper is laid out as follows: in section 2, we describe the field site and observational methodology. An overview of our observations is given in section 3, with a physical interpretation presented in section 4. Motivated by our observations, we present the model modification in section 5, focusing on the dynamic ~~organization~~ organisation of the drainage system into active and hydraulically isolated components. This will not provide a full account of the presented ~~data set~~ dataset, which also includes surface speed and other variables. An ~~in-deep~~ in-depth study of the evolution of the subglacial drainage system structure and its relationships with
35 measured surface speeds is ongoing and will be presented in upcoming papers.

40 To help the reader to navigate through the numerous observations presented in this paper, we provide below an extended overview of its contents, highlighting the most important points to be considered:

- The observed drainage system consists of three main components (sections 3.1)
 1. Channelised: efficient, turbulent drainage at low water pressure
 2. Distributed: slow water velocities, damped response to diurnal meltwater input, high water pressure
 3. Disconnected: near-overburden mean water pressure with no diurnal variations
- The “disconnected” areas display a small but statistically significant and sustained drop in mean

pressure during the melt season, suggesting weak connections potentially through porewater diffusion in till (sections 3.1 & 4.2).

- The connected drainage system consists of spatially distinct parts (subsystems) that appear to act independently. Each is characterised by a common diurnal pressure variation pattern that differs markedly from other subsystems (sections 3.2 & 4).
- Pressure variations in boreholes in disconnected areas can also occur due to bridging effects and potentially due to ice motion, the latter giving rise to low-amplitude, high frequency pressure variations shared by distant boreholes (sections 3.2, 4.2 & 4.3).
- Observations suggest the existence of a dense network of englacial conduits, but it is unclear if these can transport water over extended distances horizontally (sections 3.3 & 4.2).
- During a spring event, a large distributed drainage system quickly develops over a large fraction of the bed. This splits into an increasing number of subsystems over the summer season, each potentially focusing around a channelised drainage axis. The extent of disconnected areas of the bed grows as a result (sections 3.4 & 4).
- The transition from connected to disconnected is abrupt, with the connected parts of the bed having a high hydraulic diffusivity (sections 3.5 & 4.2). Disconnection and reconnection “events” typically occur as water pressure is falling and rising, respectively. These observations motivate the modification of existing drainage models presented in section 5.
- The timing and degree of channelisation reached by the subglacial drainage system varies widely depending on weather and surface conditions during summer, and the spatial pattern of drainage can change from year to year (sections 3.6 & 4.1).
- Abrupt growth of the distributed drainage system, analogous to that observed during the spring event, can be observed during the summer in response to a sudden, abundant meltwater input following an extended hiatus, the latter usually caused by a mid-summer snowfall event (section 4).”

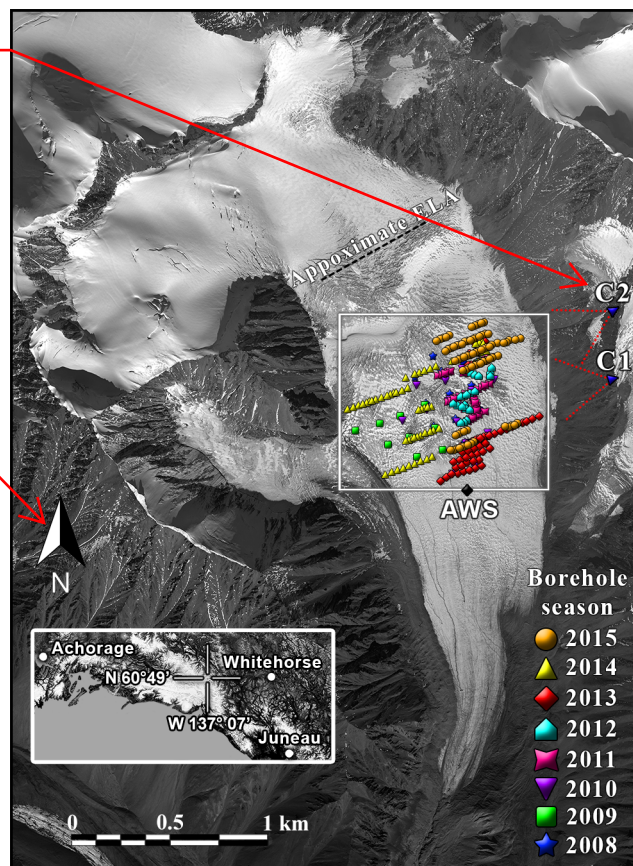
2 Field site and methods

All observation presented were made on a small (4.28 km²), unnamed surge-type alpine glacier in the St. Elias Mountains, Yukon Territory, Canada, located at 60° 49' N, 139°

New extended overview of contents



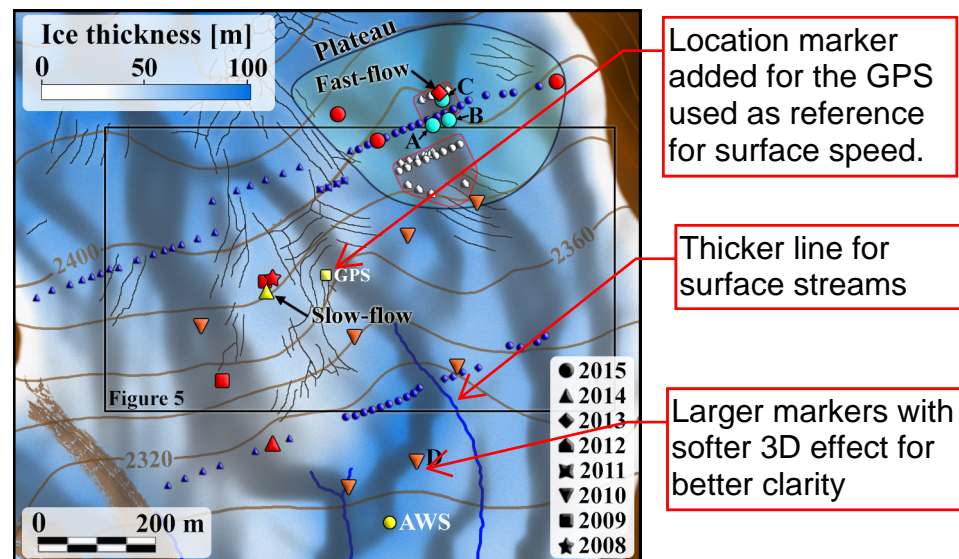
Labels added to
Time-lapse cameras



North arrow added

Figure 1. WorldView-1 satellite image of South Glacier taken on September 2nd, 2009. Borehole positions are marked according to the year of drilling, showing the most recent year in repeatedly drilled locations. ~~Time-lapse~~ camera positions (C1 & C2), Automatic Weather Station (AWS) approximate equilibrium line (ELA) are also indicated. The inset map shows the general location in the Yukon. The white box corresponds to the area shown in Fig. 2. Note that the different symbols indicating years of borehole drilling are used systematically through the text.

8° W (Fig. 1). We will refer to the site as “South Glacier” for consistency with prior work [Paoli and Flowers, 2009; Flowers et al., 2011, 2014; Schoof et al., 2014]. Surface elevation ranges from 1,960 to 2,930 m above sea level (asl), with an average slope of 12.6°. The equilibrium line altitude (ELA) lies at about 2,550 m [Wheler, 2009]. Bedrock topography at the site has been reconstructed from extensive ground-penetrating radar (GPR) surveys [Wilson et al., 2013], reporting an average and maximum thickness of 76 m and 204 m respectively. Direct instrumentation and radar scattering [Wheler and Flowers, 2011; Wilson et al., 2013] reveal a polythermal structure with a basal layer of temperate ice. Exposed bedrock in the valley consists mainly of highly fractured Shield Pluton granodiorite [Dodds and Campbell, 1988; Crompton et al., 2015]. Borehole videos have also shown the presence of granodiorite cobbles in the basal ice,



Location marker
added for the GPS
used as reference
for surface speed.

Thicker line for
surface streams

Larger markers with
softer 3D effect for
better clarity

Figure 2. Detailed map of the study area. The following symbols indicate specific boreholes: those used for non spatially-biased statistics (blue symbols), displaying behaviour similar to the fast-flow hole in Fig. 5 (red symbols), re-drilled ones (light blue symbols), and those used in Fig. 10 (orange symbols), the 2014 slow-flow borehole in Fig. 6 (yellow triangle), and the location of the Automatic Weather Station (yellow circle), and the central GPS tower shown in Flowers et al. [2014] (yellow square). The red outlines encompass all the boreholes displayed in figure 14, shown here using coloured and white markers. Black lines indicate major crevasses, blue lines surface streams. Contours show surface elevation, blue shading ice thickness. Grey shading indicates the upstream area ~~calculated as in panel b of Fig. 2 in Schoof et al. [2014], calculated assuming an hydraulic gradient given by an effective pressure equal to half of the ice overburden pressure, and computed using the D_∞ method described by Tarboton [1997].~~

and highly turbid water near the bottom of freshly drilled boreholes. Frozen-on sediments and a basal layer of till of unknown depth are visible in some borehole imagery, and till thicknesses in excess of two meters are exposed near the snout.

~~Boreholes were drilled in the upper ablation area of the glacier, between 2,270 and 2,430 m asl (Fig. 1), covering an area of approximately 0.6 km², with an average ice thickness of 63.4 m and a maximum of 100 m. No moulins are visible in or above this area. Instead, surface melt is routed into the glacier through abundant crevasses (Fig. 2). The basal layer of temperate ice in the study area extends up to 30–60 m above the bed.~~

An automatic weather station (AWS) operated at 2,290 m next to the lower end of the study area between July 2006 and August 2015 [MacDougall and Flowers, 2011] as part of a simultaneous energy balance studies study [Wheler and Flowers, 2011]. ~~The average net mass balance over the whole glacier during the period 2008–2012 was estimated~~

Paragraph
relocated at the
bottom of next
page

New paragraph
about mass balance
and thinning

Figure relocated
(previously Fig.13)

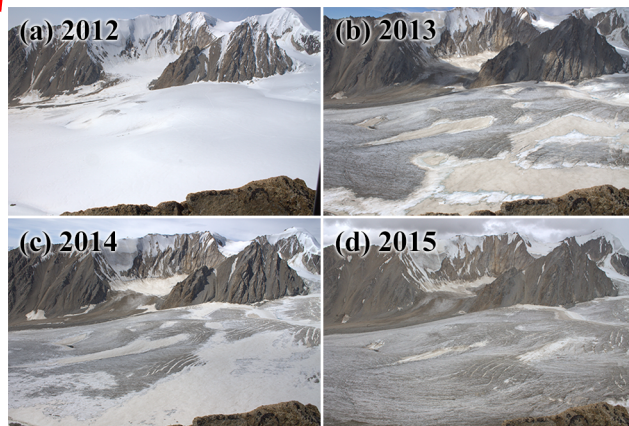


Figure 3. Photographs of the study area taken from camera C1 (see Fig. 1) on July 19th, 2012–2015, as indicated in each panel. The interannual variability evident in the photo will be discussed in section 4.

to be between -0.33 and -0.45 m/year water equivalent [Wheler *et al.*, 2014], corresponding to 37–51 cm/year of average glacier thinning. Elevation changes in the study area derived from differential Global Positioning System (GPS) measurements of borehole locations (taken after drilling) suggest a thinning of 59 cm/year over the same period, and 37 cm/year in the period 2008–2015.

We use air temperatures (specifically positive air temperatures, meaning the maximum of measured temperature and 0° C) and Positive Degree Days (PDD, defined in the usual way as the integral with respect to time over positive air temperatures) as the main proxy of the water input into the subglacial drainage system. Temperature estimates after the August 2015 removal of the on-glacier AWS were calculated by a calibrated linear regression of data from a second AWS operated since 2006 by the Geological Survey of Canada and the University of Ottawa 8.8 km to the Southwest, at an elevation of 1845 m.

Surface velocities were measured with a GPS array [Flowers *et al.*, 2014], and display a strong seasonal contrast. The velocity at the GPS tower at the centre of the array (see Fig. 2) varied from 30.6 to 17.9 m/year between summer 2010 and early spring 2011. Modelled basal motion in our study area accounts for 75–100% of the total surface motion (see Fig. 6b in Flowers *et al.* (2011), where our study area is located between 1600 and 2500 metres).

Between 2008 and 2015, 311 boreholes were drilled to the bed [Schoof *et al.*, 2014] and instrumented with pressure transducers in the upper ablation area of the glacier between 2,270 and 2,430 m asl (Figs. 1 and 3), covering an area of approximately 0.6 km^2 , with an average ice thickness of 63.4 m and a maximum of 100 m. No moulines are visible in or above this area. Instead, the surface meltwater is routed into the glacier through abundant crevasses (Fig. 4)2). The basal

layer of temperate ice in the study area extends up to 30–60 m above the bed.

Boreholes were instrumented with pressure transducers providing continuous subglacial water pressure records, with up to 150 boreholes being recorded simultaneously. The inclination of the boreholes was not measured, but the drilling technique used aims to ensure minimal deviations from vertical. A comparison with GPR data shows that borehole lengths were generally in agreement with ice thickness within a 6% margin [Wilson *et al.*, 2013]. Contact with the bed was deemed to have been established if water samples taken from the bottom of the holes showed significant turbidity. Otherwise, a borehole camera was used to assess bed contact visually; a significant number of additional, unsuccessful drilling attempts terminated at englacial cobbles near the bed. With only a few exceptions, sensors were installed only in holes that we were confident had reached the bed, and placed 10–20 cm from the bottom. Boreholes typically froze shut within one to two days, becoming isolated from the surface. The spatial distribution of new boreholes varied each year, not following a regular pattern. However, they were generally 15–60 m apart along cross-glacier lines, with lines 60–120 m apart. A map of all boreholes drilled is shown in Fig. 1. The region labelled as the “plateau” in Fig. 2 was re-drilled every year between 2011 and 2015.

Pressure data were acquired using Barksdale model 422-H2-06 and 422-H2-06-A and Honeywell model 19C200PG5K and SPTMV1000PA5W02 transducers. Each sensor was embedded in clear epoxy to provide mechanical strength and waterproofing. Most transducers installed from summer 2013 onwards were equipped with a Ray 010B $\frac{1}{4}$ " brass piston snubber as protection against transient high-pressure spikes, without altering the signal at the sensor sampling frequencies as verified by doubly-instrumented boreholes (see supplementary material section 1). Data were recorded by Campbell Scientific CR10, CR10X and CR1000 data loggers, set to log at intervals of 2 minutes during summer for CR10(X) loggers, switching to 20 minutes for the rest of the year, and at intervals of 1 minute for CR1000 loggers year-round. In the present paper, water pressure values will be reported in metres of water (the height of the water column that would produce that pressure).

During the summers of 2014 and 2015, a total of 10 custom-made digital sensor pods was installed in boreholes. These pods were built based-on-around an ATmega328P microprocessor and communicated via the RS-485 protocol with custom-made data loggers built-constructed using the Arduino Mega open-hardware platform. The sensor pods recorded pressure, conductivity, turbidity, reflectivity in five spectral bands, tilt, orientation, movement, temperature, and confinement. The latter is a measure of the magnitude of the acceleration produced by an internal vibrating motor, used to assess whether the sensor was hanging freely in water, or tightly confined within solid walls. Seven of the digital sensors were installed in the same boreholes as the standard ana-

New paragraph
about surface
speed

logue transducers to assess data quality ([see section 1 of the supplementary material](#)).

We have not used data from a stream gauge at the outlet of the glacier, maintained for part of the observation period by the Simon Fraser University glaciology group, for two reasons: first, several surface melt streams and at least one major lateral stream enter the glacier below the study site. Second, the instrumentation at the stream site was destroyed on multiple occasions by flood waters, and a continuous record is not available.

The limited available stream gauging data suggests typical summer flow around 1–2 m³/s, with maximum values around 5 m³/s and minima below the measuring capacity of the gauging station [Crompton et al., 2015]. However, the outlet stream was never observed to run dry (J. Crompton, personal communication).

3 Results

3.1 Annual cycle and Modes of water flow: fast, slow and unconnected

Despite a large diversity of borehole pressure records, a few general patterns are easy to identify. The most common is the contrast between an inactive winter regime and an active summer period. During winter, most sensors show stable, high (near overburden) water pressures, interrupted only during a 2–4 months period of summer activity starting in June–July (Fig. 4). The onset of the active summer period (or “spring event”) occurs during rapid thinning of the snowpack under high summer temperatures. After the spring event, 20% of sensors show a drop in diurnal running mean pressure, and most start displaying diurnal oscillations.

Pressure records alone do not allow us to determine the characteristics of water flow at the bed, and visual observations at the bottom of boreholes often fail due to the high turbidity of the water after drilling. However, in a few exceptional cases, we were able to observe water flow at the bed directly. We will describe the two most clear-cut cases.

On July 28th, 2013, while installing a sensor in the hole marked “Fast-Flow” in Fig. 2 at the bottom of a borehole, strong periodic pulls were felt through the sensor cable, revealing a conduit with turbulent, fast water flow in the bottom 50 cm of the borehole. This borehole was also the only one in which there was an audible sound of flowing water. The fast-flow hole location of the hole is marked as “Fast-Flow” in Fig. 2, it was drilled at the very end of the field operations, and no further detailed on-site investigation was conducted.

The fast-flow borehole was 93 m deep and drained at a depth of 87 m during drilling. On the first recorded diurnal pressure peak, the water reached a pressure of about 5.2 m (6% of ice overburden; we will consistently express pressures in metres of water in this paper). A water sample retrieved from the bottom showed moderate turbidity. Two pressure

sensors were installed in this borehole, 10 and 80 cm above the bed, the upper one with a snubber and the lower one without one.

Panel c of Fig. 5 shows the pressure recorded in the fast-flow borehole for the first 33 days after installation. Panel d shows the pressure records in three boreholes along the same line across the glacier at 15 m spacing. The lack of similarity between the fast-flow hole pressure record and those from other nearby boreholes differs from the behaviour of most boreholes that display. This lack of similarity contrasts with the typical behaviour of boreholes exhibiting diurnal pressure oscillations: typically, such boreholes show a signal similar to. Such boreholes usually share a similar pattern of pressure oscillations with one or more neighbouring boreholes, forming a cluster that extends some distance laterally across the glacier (see section 3.2). In

However, in the case of the fast-flow borehole, somewhat similar temporal pressure patterns were observed at a much larger distance downstream down-glacier and at much larger distances than the 15 m lateral borehole spacing, as shown in panels e and g of Fig. 5, 5e and 5g, and less so in panel h, while 5h. By contrast, a set of boreholes exhibiting very different variations close to those in panel 5d is shown in panels 5f. For reference, panel 5i shows the remaining pressure time series recorded in the same area, highlighting the diversity of pressure patterns observed. No systematic time lags were found between peaks in the fast-flow borehole and pressure peaks of boreholes displayed in panels e and 5e and 5g.

The grouping of boreholes into panels in Fig. 5 was done on the basis of spatial proximity in panel c, and on the basis of a commonality of diurnal pressure variations in the remaining panels, in particular, a. In particular, we have clustered the records on the basis of commonality in how the amplitude of diurnal pressure variations changes in time. For instance, the similarity between the records in panel 5g should be obvious. However, note that there can be subtler similarities: panels e, e and 5c, 5e and 5g at least partially share a period of larger diurnal amplitudes leading up to August 3rd, a hiatus lasting until August 10th punctuated by a diurnal pressure peak late on August 6th, and a period of renewed diurnal oscillations lasting until August 17th; this differs from the pattern of diurnal oscillations seen in panel 5h. Grouping boreholes in this way is partially a subjective measure, and we will present a more systematic clustering method (which has helped to guide the groupings here) in a separate paper (see also Gordon et al. [1998]; Huzurbazar and Humphrey [2008]).

Gordon et al. [1998]; Huzurbazar and Humphrey [2008]). All borehole groupings presented in the following figures were manually selected using the same criteria as described for Fig. 5.

Several features stand out in the pressure record from the fast-flow borehole: sharp diurnal pressure peaks and a small

New paragraph about stream gauging data

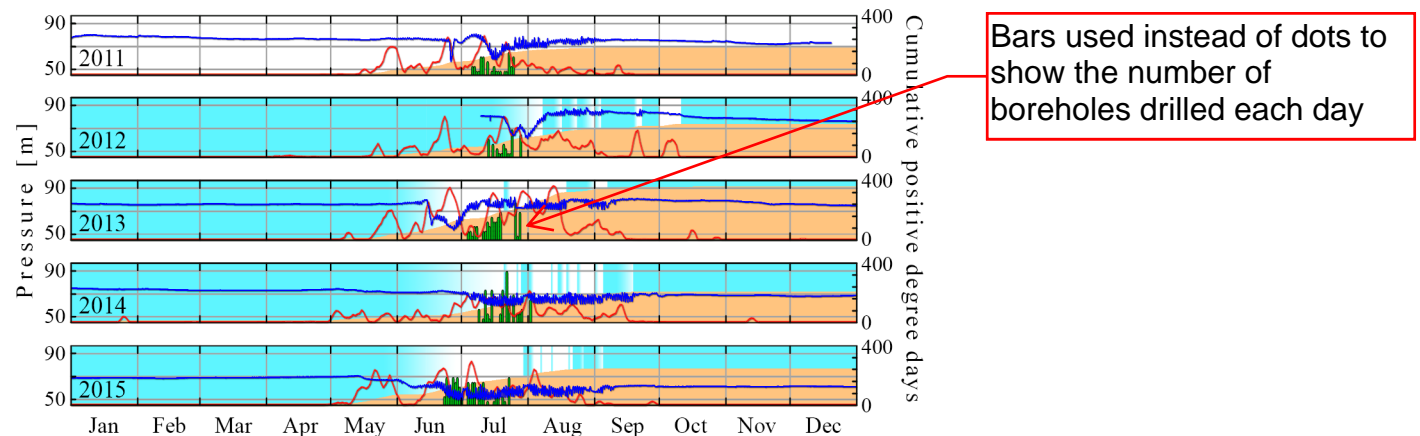


Figure 4. Example pressure time series recorded in one borehole (D in borehole D of Fig. 2) from 2011 to 2015 (blue line). Daily PDD values are shown as a red line, annual cumulative positive degree days as orange shading, and fresh snow cover determined from time lapse imagery as light blue shading. The fading blue at the end of the winter indicates the appearance of larger snow-free patches and the filling of a perennial supraglacial pond in the study area, rather than the complete disappearance of the winter snowpack. Green bars indicate the count of boreholes drilled each day on a scale from zero to 13.

time lag between peak surface temperatures and diurnal water pressure maxima (1-3 hours), as well as the general similarity between the temporal variations in pressure and temperature pattern. The correlation between the two, computed over a moving window, stayed above 0.8 for several days (Fig. 5bc, grey shading). This high correlation was more pronounced late in the season, also coinciding with the water pressure dropping to atmospheric values at night.

A contrasting observation of water flow was made on July 23rd, 2014, when a clear water sample was retrieved from the bottom of a borehole (“Slow-flow” in Fig. 2) and the borehole camera was deployed. The resulting borehole video (see supplementary material) reveals a slowly-flowing thin layer of turbid water at the borehole bottom overlaid with clear water, an unusual condition that allowed the observation, as the water in a bed-terminating hole is usually highly turbid due to the basal sediments disturbed by the drill jet.

The slow-flow borehole was 62 m deep, and the first recorded diurnal pressure peak reached 48 m (85% of ice overburden). One pressure transducer with snubber was installed 6 cm above the bed. Figure 6c shows the pressure recorded in the slow-flow borehole (black line). Pressure records from three other boreholes in the same across-glacier line and one sensor downstream are shown in red in the same panel, while the record of a fifth borehole in the same line is shown in panel 6d. Note that there are four virtually indistinguishable records in panel 6c during July 23rd-25th (see also figure 7). After a data gap caused by a corrupted compact flash card, the records have become more dissimilar by August 2nd, but continue to exhibit common pressure variations. The pressure time series from the borehole that is part of the line immediately below the slow-flow hole by contrast

has significantly higher mean water pressure and the diurnal pressure variations have a much smaller amplitude. We have included it in panel 6c because it is the only one in that lower line that matches one of the other pressure records in panel e-well-6c well, if we remove their means and scale them to have unit variance. As discussed above, the grouping into panels is somewhat subjective, and we have grouped boreholes whose diurnal oscillations resemble each other; mostly that resemblance is obvious without any scaling, but not always.

Most boreholes showing diurnal pressure oscillations share the general features displayed by the slow-flow borehole, specifically 1) smooth pressure peaks and troughs, 2) pressure patterns well differentiated from the atmospheric temperature pattern, 3) mean pressures during periods with diurnal oscillations that lie between 55-120% of the overburden ice pressure (much higher than in the fast-flow hole), 4) peak pressures that typically lag peak temperatures by 2-8 hours and 5) patterns of temporal pressure variations that are often similar to neighbouring boreholes both in the along-and across-glacier-along- and across-glacier direction.

On average, during summer, 71% of sensors showed the behaviour observed in the slow-flow borehole at some point, as assessed visually from the presence of smooth diurnal pressure oscillations. Only 8 boreholes (3% of the total, shown as red markers in Fig. 2) exhibited water pressures dropping to atmospheric pressure, one of the key characteristics of the fast-flow borehole. Six of them were found during the three years with the highest cumulative positive degree day count in the data-set dataset (2013: 437 °C days, 2009: 386 °C days, 2015: 297 °C days).

These figures may however not be representative as drilling was concentrated in some areas. For this reason,

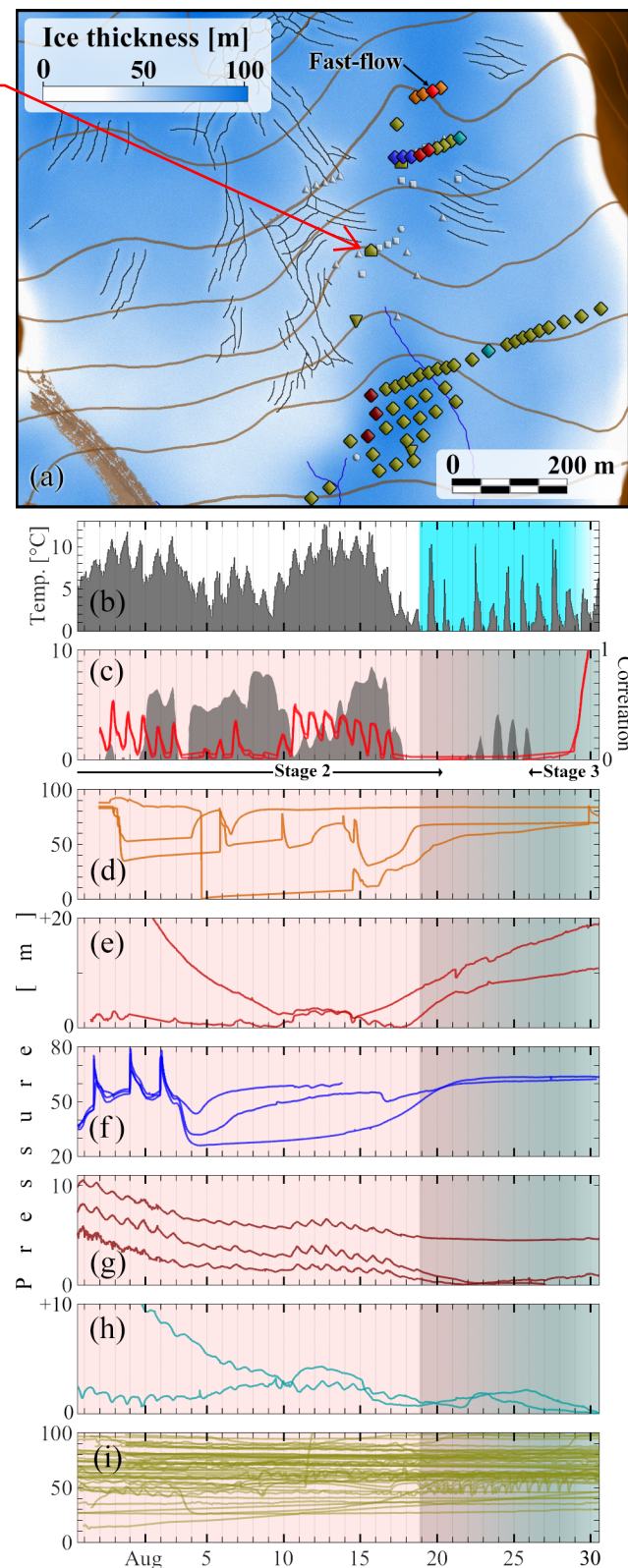


Figure 5. Locations and pressure time series ~~of for~~ the boreholes associated with the fast-flow borehole during the summer of 2013. (a) The map uses the same scheme as Fig. 2, but omits the upstream area shading. (b) Temperatures (grey) and fresh snow cover deter-

mined from time lapse imagery (light blue shading, fading colour indicates partial cover). (c) Pressure in the fast-flow borehole (red) and its correlation with temperature in grey, computed for any given time over a 3-day running window. Note that two sensors were installed in the fast-flow borehole, offset vertically from each other by 70 cm, making the two lines indistinguishable most of the time at the presented scale. Later in section 3.5, the complete record will be displayed, where the two curves are more distinguishable. (d-i) Pressure records from other boreholes marked on the map. The colour of plots corresponds to borehole marker colours on the map; the same convention is used in all subsequent figures. Symbol shapes represent drilling years as in Fig. 2, uncoloured (grey) markers correspond to boreholes with active sensors during the displayed period whose pressure time series are not shown in the figure.

we have selected 70 boreholes in two across-glacier profiles (blue markers in Fig. 2). Among those, 81% show a behaviour qualitatively similar to the slow-flow borehole, and 4% that of the fast-flow one. Note however that even these statistics remain biased, as borehole spacing along these lines is concentrated in areas that were of interest due to likely drainage activity, and crevassed areas are under-represented as ~~sensors~~ sensor signal cables typically have a short life span there.

We emphasise that the borehole in which fast flow was observed initially displayed a relatively smooth diurnal cycle, and the statistics above are based on the identification of diurnal pressure oscillations reaching atmospheric pressure at night: it is therefore possible that more boreholes intersect conduits with fast-flowing ieewater, without the observed pressure records indicating as much.

The remaining 26% (or 15% ~~of in~~ the two cross-glacier lines in Fig. 2) of boreholes do not show any significant diurnal pressure oscillations at any point during the year. These “isolated” “disconnected” boreholes usually show year-round mean pressures between 90-120% of ~~the ice overburden pressure. Isolated ice overburden. Disconnected~~ boreholes frequently show a near-constant pressure signal, but not always, with some exhibiting difficult-to-interpret temporal variability. In 2016 there were 55 ~~isolated sensors~~ disconnected boreholes, allowing us to treat their behaviour statistically. Despite only slight differences in mean pressures between winter and summer there is, however, a slow but statistically significant decrease in water pressure during summer, starting around the spring event and amounting to about 6% of the overburden pressure in total (Fig. 8).

3.2 Spatial patterns in water pressure variations

When the whole ~~data-set~~ dataset is viewed over a given time window during summer, it is often possible to identify multiple ~~subsets of boreholes~~ showing very similar clusters of boreholes, each exhibiting a specific pattern of temporal pressure variations ~~within that subset~~ (often recognizable). Often, these patterns are defined by the way in which the

Larger markers with softer 3D effect for better clarity

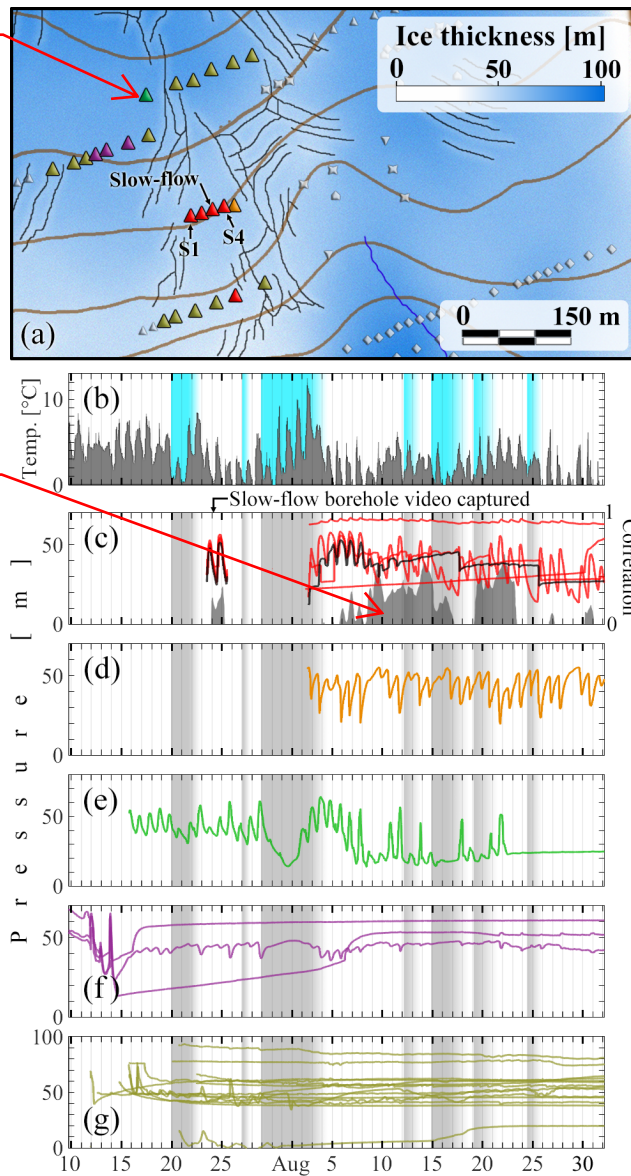


Figure 6. Locations and pressure time series ~~of~~ for the boreholes associated with the slow-flow borehole on July and August 2014, with the same plotting scheme as Fig. 5 (see corresponding caption). Panel c shows pressure in the slow-flow borehole (black) and three other boreholes in the same line. The correlation with temperature has been calculated using the only borehole that remains connected over the whole interval. The remaining panels show pressure time series from other nearby holes as indicated by the line and borehole marker colours. The time series from boreholes S1–S4 are shown in more detail in Fig. 7.

amplitude of diurnal oscillations changes over time), but ~~these temporal variations are different from other boreholes.~~ While boreholes in a given clusters will share the pattern of temporal variability, this will differ significantly from the pattern of temporal variability in the other clusters.

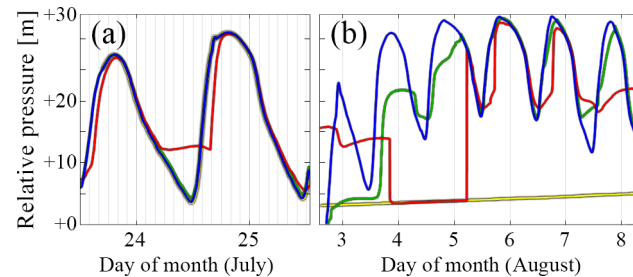


Figure 7. Pressure records from the four sensors marked S1–S4 in 6b in July (a) and August (b) 2014. Colour coding is red (S1), yellow (S2), green (S3) and blue (S4). We have applied offsets—a constant value offset in pressure to each time series (meaning, added a constant to the directly measured pressure) to make the agreement between the records clearer. ~~These~~ The offset values are, in order, 27, 26, 24, and 29 ~~meters~~ metres in (a), and 27, 20, 22, and 27 in (b). Note that the S2–S4 time series in panel (a) agree so well with each other that they are barely distinguishable.

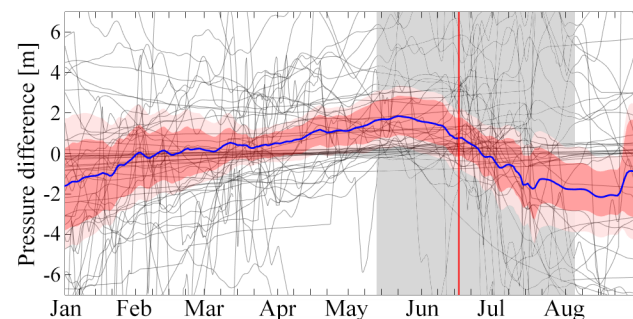


Figure 8. Mean water pressure computed over a 1-day running window for each of the 55 sensors that did not display diurnal oscillations during 2016, shown in black. For legibility, we have subtracted the mean over all sensors and the time window shown. The blue line shows the mean over all the black lines at a given time (i.e. over all the sensors) and the bootstrap confidence intervals [Efron and Tibshirani, 1993] of 90 and 99% (dark and light pink shading, respectively). Gray shading represent the period over which the initiation of diurnal oscillations was observed in connected boreholes, and the red vertical line is the median time at which diurnal oscillations first appeared in the 70 boreholes that did experience such oscillations during 2016.

One example of this phenomenon comes from the boreholes in Fig. 5f, where we can see a group of boreholes that display a very coherent signal but with a distinctive two-day period. ~~The boreholes in panel~~ However, those boreholes in figure 5f are directly adjacent to those in ~~panel e,~~ we have associated with the fast-flow borehole and which 5c. The latter by contrast show a very different ~~, diurnal pattern of~~ pattern of diurnal pressure variations (see also panels c and ~~that we have associated with the fast-flow borehole, along with panels 5c and 5g).~~

Less clear-cut, though indicative of the same phenomenon is Fig. 6, where we see boreholes in panels ~~d–f–d–f~~ that ex-

hibit quite different diurnal pressure variations ~~to~~ from those observed in panel c (the group associated with the slow-flow borehole in panel e). Figure 3 of Schoof *et al.* [2014] also shows an example of the same phenomenon during July and August 2011: borehole B in that figure is, in fact, one of a group of 5 that exhibit almost identical diurnal water pressure oscillations that are quite distinct from those in boreholes A1–A6 in the same figure.

The spatial patterning of the drainage system into distinct subsets-clusters becomes much clearer when a dense borehole array with good spatial coverage is available. During the summer of 2015, there were 88 boreholes with active sensors on the plateau indicated in Fig. 2, and 66 further downstream. The corresponding pressure records are presented in Fig. 9. Between June 26th and August 27th, 42 boreholes on the plateau (panel 9c) and 11 boreholes downstream (panel 9d) showed a highly coherent pressure signal that was qualitatively different from the atmospheric temperature signal (panel 9b) and the majority of other boreholes in the two areas (panel 9f). There was no consistent time lag between sensors in the plateau and downstream. However, there was a clear drop in amplitude of diurnal oscillations between the plateau and downstream sensors (panels e and panels 9c and 9d), where the latter showed amplitudes around 15-30% of those seen in the plateau.

Five of the sensors on the plateau were capable of conductivity measurements (panel 9g). We emphasize-emphasise that, in general, the spatial patterning was recognizable-recognisable only in the pressure records, and pressure oscillations were not associated with conductivity changes. Although all five sensors showed very similar temporal variations in pressure (panel 9c), the conductivity time series bear far less similarity to each other, with only a handful of abrupt conductivity changes common to three of the sensors (S2 and S4 marked in panel 9g).

The group of 14 boreholes in panel e of Fig. 9g also shares common diurnal pressure variation patterns, though this is not immediately clear as the mean pressures and amplitude of pressure variations varies significantly. Specifically for that reason we have highlighted in black one line that shows these variations clearly. Notably, these variations are “inverted” versions of the pressure variations seen in panel 9b, with peaks becoming troughs and vice versa. These anti-correlated boreholes, in contrast to those in panels e-and 9c and 9d, have smaller diurnal oscillations amplitudes, and the oscillations are super-imposed-superimposed on a signal with near-constant running mean and high mean pressure, usually close to overburden. Therefore, if diurnal variations were filtered out, these pressure records would resemble the winter regime. At 15 meters-metres spacing between boreholes, we do not observe sequences of boreholes smoothly transitioning from correlated to anti-correlated, in the sense that there appears to be no continuous change in phase and amplitude from borehole to borehole: we observe a sharp boundary between correlated and anti-correlated boreholes,

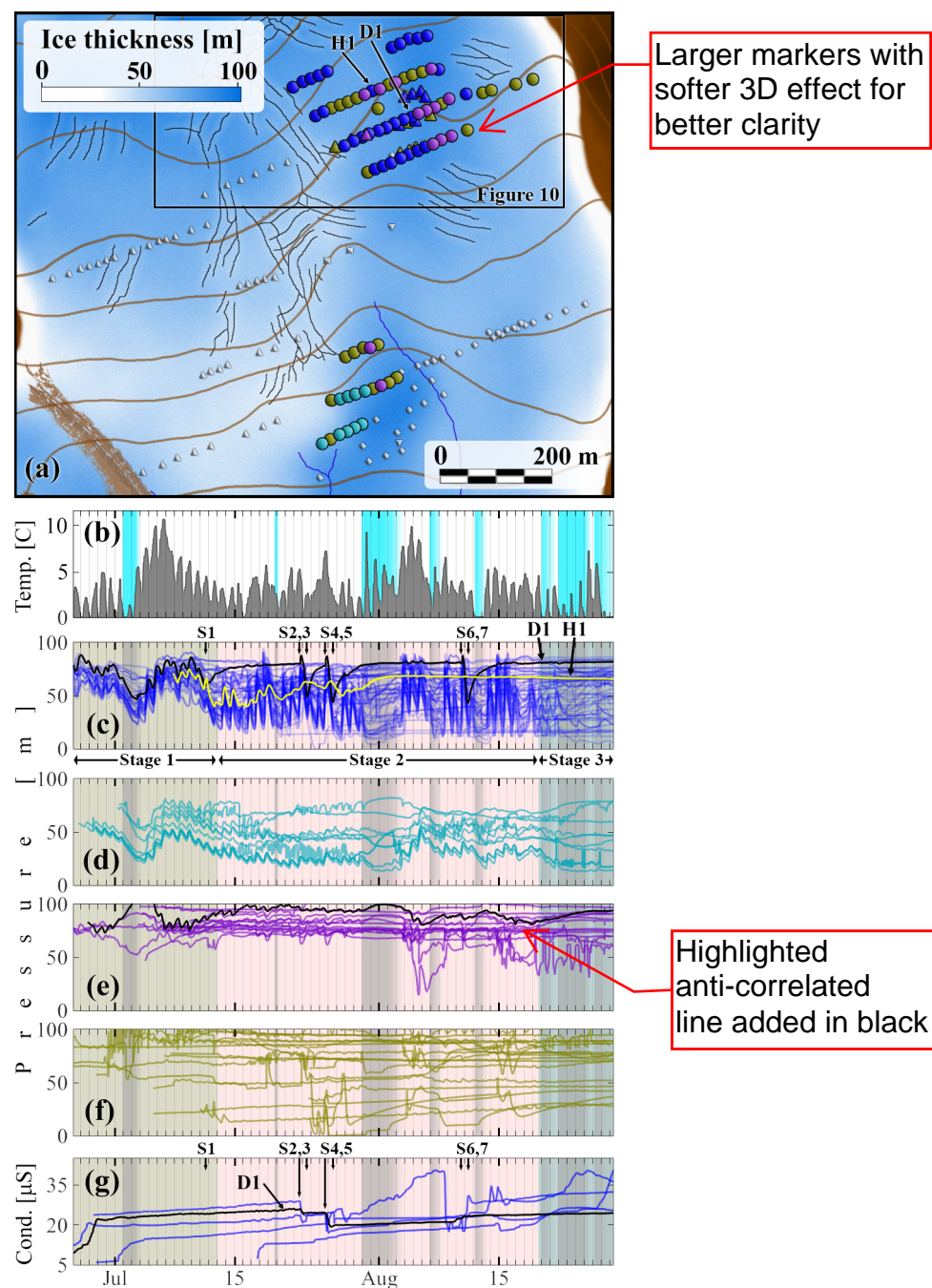


Figure 9. Locations and pressure time series ~~from~~ for all 82 boreholes on the plateau area and 20 boreholes down-glacier during June–August 2015, plotted using the same scheme as Fig. 5. (b) Temperatures (grey) and fresh snow cover (light blue shading), (c) Pressure in 42 boreholes on the plateau that ~~share~~ shared similar diurnal-water pressure variations during at least part of the observation period. The highlighted time series are from boreholes D1 (black) and H1 (yellow line). Both boreholes are indicated on the map. S1–S7 indicate ‘switching events’ in the D1 record (see section 3.4). (d) Boreholes downstream of the plateau showing similar pressure variation to those in (b). (e) Pressure records that are anti-correlated to those on panels (c)–(d). (f) Pressure records from the remaining boreholes on the map, (g) Conductivity records from the six digital sensors included in panel bc.

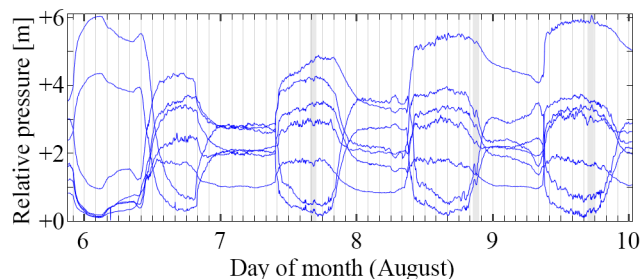


Figure 10. Relative pressure variations in 7 boreholes (orange symbols in Fig. 2) displaying common small amplitude diurnal oscillations with high-frequency content during August 2011. To make these visible in the same plot, we have applied offsets of 93, 71, 64, 61, 63, 66 and 27 meters-metres to the measured pressures. Three common high-frequency features are highlighted by grey vertical bands.

or correlated boreholes and boreholes exhibiting no diurnal oscillations. Note that one of the records in panel f of Fig. 6 also anti-correlates strongly with the record in panel e of the same figure 6e during the later part of the time window shown, and the record in panel 6d anti-correlates strongly with the record from the adjacent borehole S4 during August; anti-correlation of this kind is a common feature of the data-setdataset, often but not always involving boreholes in close proximity.

There is typically another set of boreholes that show very similar diurnal variations in water pressure super-imposed on near-constant or slowly changing diurnal running mean values. The diurnal variations for this set have very small amplitude (typically 0.2–0.6 m, exceptionally up to 6 m), and resemble a square-wave with super-imposed high-frequency variations. Matching oscillations can be observed in multiple boreholes spread over large distances, both along and across the glacier, and both diurnal and much higher frequency features in the pressure signal are preserved between these boreholes. An example from 2011 involving boreholes across the width of the study area, and recorded by different data loggers, is shown in Fig. 10. Clearly, the oscillations can be both correlated or anti-correlated with each other. Not shown in Fig. 10 is the longer-term evolution of water pressure in the same boreholes. While they share short-time-scale temporal variability, their long-term pressure variations are generally not well correlated.

3.3 Three-dimensional drainage structures

The pressure observations primarily give us a two-dimensional picture of the drainage system. The drilling process itself as well as borehole camera investigation provides additional information on englacial connections [Fountain et al., 2005; Harper et al., 2010]. 37% of all the boreholes drilled-drained completely or partially during the drilling process, as did 39% of those in the cross-glacier lines marked as

blue symbols in Fig. 2. For simplicity, we will give statistics for the entire data-set-dataset in running text below, and the corresponding figure for the cross-glacier lines in parentheses. Of the boreholes that drained during drilling, only 14% (0%) drained when reaching the bed, and the remaining 86% (100%) drained at some point during the drilling process, suggesting connections to englacial conduits or voids. Such connections were also observed on multiple occasions using the borehole camera. Drainage events occurred during drilling at all depths, but more frequently at during drilling, but with a slight preference for greater depths, with 60% (59%) happening in the lower half of the boreholes. This remains true for the 2012 drilling campaign, where the first sensors were installed before the spring event and observations are likely to reflect winter conditions. Unfortunately, water level change and duration of drainage events were not recorded.

During the borehole re-freezing process, 29% (11%) of the boreholes showed a pressure spike typically about 1.3 times overburden pressure, suggesting that freezing happened in a confined space. In total, 62% (73%) of these initially confined boreholes showed diurnal oscillations during the first week, suggesting that some degree of connection was developed with a drainage system experiencing diurnal-daily varying water input.

In 2014 and 2015, three one-year-old boreholes were re-drilled, and the sensor-was-sensors were recovered (boreholes A, B and C in Fig. 2). During this process, we found that holes A and C had sections about 8–12 m long near the bed that had remained unfrozen for the entire year, suggesting that boreholes, as well as natural englacial conduits close to the bed, could remain open through the winter. In borehole A, the contact with the bed had erroneously been assumed after the initial drilling based on highly turbid water. However, borehole video footage taken after re-drilling showed that the original borehole had terminated at an isolated rock. From the depth of nearby boreholes, we estimate that the sensor was installed approximately 4 m above the bed. Nonetheless, the diurnal water pressure oscillations recorded in borehole A continued to mimic other nearby bed-terminating boreholes that were drilled in 2014 and 2015, indicating a persistent connection. Fig. 11 shows the pressure record in borehole A and the point at which the re-drilling took place.

3.4 Seasonal evolution/development of the subglacial drainage system

We have described the apparent spatial patterning of the drainage system above. This patterning is however not fixed but evolves over time. In Fig. 9bc, it is clear that all 42 boreholes show very coherent temporal pressure variations at the start of the observation period. During late July and August, some the pressure variations in some of the boreholes become more distinct until, by late August, there is no longer

a common signal and all boreholes show dissimilar temporal pressure variations.

In Fig. 9c, this emerging patterning is evident only in the more disordered appearance of the plot for later times. In Fig. 11, we show the 42 boreholes of Fig. 9b separated into subgroups. ~~As in figures 5 and 6, the grouping is somewhat subjective; a paper on a more systematic clustering approach that has guided our choices here is in preparation. We have attempted to group boreholes whose diurnal water pressure oscillations during late July and early August closely resemble each other.~~

~~Even within~~ Within these groupings, it is clear that boreholes can switch from having closely correlated pressure records to behaving independently and, less frequently, to being strongly correlated again (panels d–h in particular); For simplicity, we refer to boreholes as being “connected” while they exhibit the same temporal pattern of pressure variations, and as “disconnected” otherwise. For each grouping, we have computed a mean pressure displayed in black, including only the boreholes that are connected at a given time; in some cases, no boreholes were connected to each other, and we used the last borehole still to exhibit diurnal oscillations to define the set of connected boreholes. In that case, the black mean curve ~~obscured~~ obscures the corresponding, coloured borehole pressure time series. These mean curves for each panel are re-plotted in the corresponding borehole marker colour in panel 11c.

The major dichotomy in Fig. 11 is between the groupings in panels d–g and i on one hand and panel k on the other. The distinctions between panels d–g in particular are more subtle, and generally relate to the absence or subdued nature of certain diurnal peaks in them: for instance, panels d–f all show diurnal oscillations on August 1st and 2nd, while the larger group in g does not; there are other examples close to the end of the summer season. For all groupings in panels d–g, it appears that the early season records resemble each other more closely than those late in the season, as was already evident in Fig. 9b, and that fewer boreholes have disconnected early in the season.

At a much smaller scale, a similar fragmentation of the drainage system is shown in Figs. 6b and 7, where we see four boreholes that are initially very well connected during late July having become much less well connected in August, although with the diurnal pressure oscillations still showing some similarities between several of the boreholes. Interestingly, one borehole (S2, yellow) has ceased to exhibit oscillations by August, but is straddled by two that still do (S1 and S3, 15 m to either side), suggesting a relatively fine-scale structure to the drainage system locally.

In addition to spatial patterning, Figs. 9 and 11 hint at an overall evolution towards lower mean water pressures and larger diurnal oscillations. The seasonal evolution of the drainage system may be evident not only in its spatial extent, but also in the evolution of mean water pressure and its response to surface melt input. Perhaps the simplest measure of

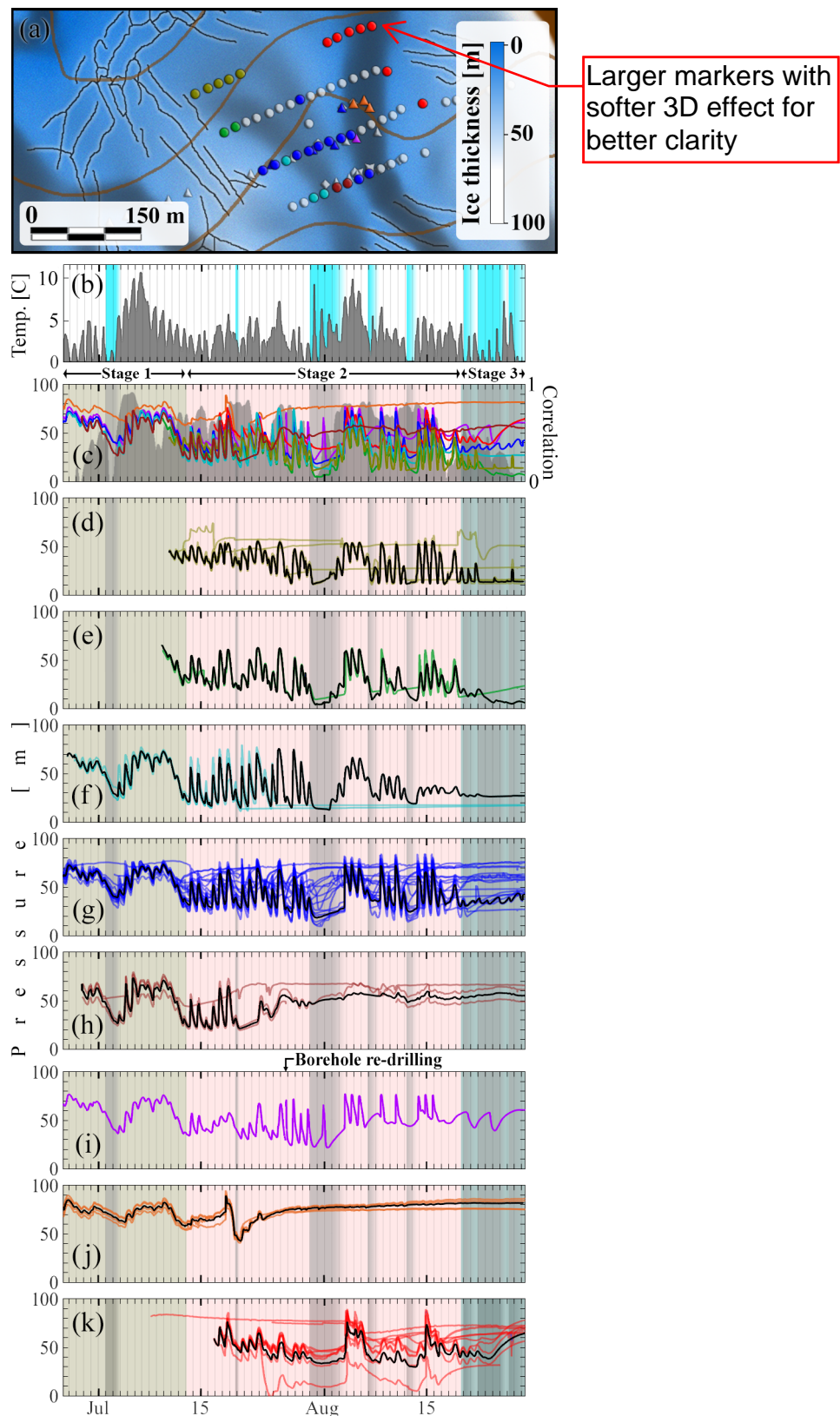


Figure 11. Locations and pressure time series ~~of for~~ all 42 boreholes shown in Fig. 9b, grouped according to the similarities between their diurnal pressure variations in July–August 2015, same

plotting scheme as in Fig. 5. (a) The map area is indicated as a box in figure 9a. Grey shading is the upstream area shown in Fig. 2 (b) Air temperature (grey) and fresh snow cover (light blue). (d–k) borehole pressure time series, colour of plots corresponds to colour of borehole marker on the map. Black lines are the mean pressure in each panel, computed only over those boreholes that are “connected” at a given time (see main text); the black lines frequently obscure one of the borehole time series. (c) The black “mean” curves from panels (d–k), plotted in the corresponding borehole marker colour. The maximum cross-correlation coefficients, allowing for time lags of up to six hours, between all pressure records and air temperature computed over a moving three-day window is shown in dark grey.

sensitivity to surface melt input is what we term the relative amplitude of pressure to temperature oscillations: we compute standard deviations of pressure time series from boreholes that exhibit diurnal oscillations at some point of the season, and also standard deviations of positive air temperatures (the maximum of air temperature and $0\text{ }^{\circ}\text{C}$). We compute these standard deviations over one-day running windows, and define the ratio of the two running standard deviations to be the relative amplitude of pressure to temperature variations. Taking the running standard deviation of air temperature as a marker of surface melt rate variability (see section 2 in the supplementary material for a discussion about this assumption), the relative amplitude defined in this way gives an indication of how sensitive the drainage system is to variations in water input.

In Fig. 12, we see that the running standard deviation in pressure only vaguely tracks its temperature counterpart. However, the relative amplitude systematically increases during much of the season (Fig. 12c), except during an interval of colder weather and surface snow around the beginning of August, while the mean water pressure also decreases (Fig. 12d).

3.5 Basal hydrology transitions and “Switching events”

Above, we have seen that boreholes can become disconnected from each other, going from a state in which they undergo synchronous and virtually identical pressure variations over time to a state in which borehole pressure appears to evolve independently. The reverse change also happens, though less frequently (except during the spring event). The change from connected to disconnected and its reverse can take different forms. In a few cases, disconnection is gradual, with the boreholes continuing to exhibit similar diurnal pressure oscillations that progressively become more dissimilar in amplitude, phase and mean water pressure. The record from H1 in Fig. 9c (yellow line in panel c) is one such example. In most cases, however, the transition is abrupt, and the same is true of boreholes connecting with each other: a rapid change in water pressure can occur over the course of a few hours or less as a connection is established. We term such

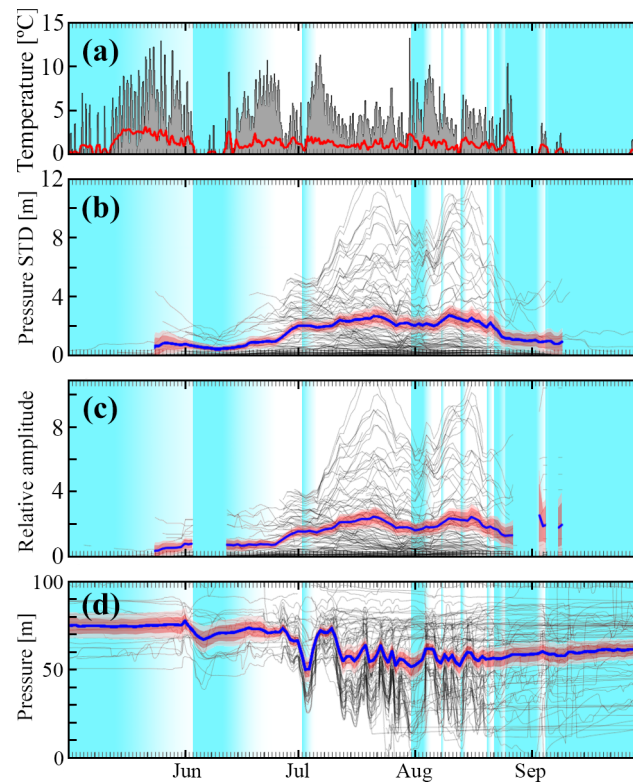


Figure 12. Relative amplitudes of pressure and temperature diurnal oscillations from May to September 2015. (a) Positive air temperature (grey), and its standard deviation over a 1-day running window (red). (b) Standard deviation of pressure over a 1-day running window (thin black lines) for each borehole in the plateau area, and the mean of these standard deviations (blue) with bootstrap confidence intervals of 90 % (dark pink) and 99% (light pink). (c) Ratio between pressure and temperature standard deviations shown in (a) and (b), computed only where standard deviation of air temperature is non-zero. (d) Mean pressure computed over a 1-day running window. Light blue shading represents fresh snow on the glacier surface.

abrupt transitions “switching events”, following *Kavanaugh and Clarke* [2000].

Figure 7 shows multiple examples in the boreholes labelled S1–S4 in Fig. 6c, spaced 15 m apart. Perhaps unsurprisingly, the majority of switching events involving new connections seem to occur while water pressure is increasing or after a recent increase, while disconnections tend to occur as water pressure is falling (see Fig. 11c,d,f for several obvious examples), though the two are rarely symmetric, with disconnection usually occurring at a lower water pressure than the original connection. The record from sensor D1 in Fig. 9c is one such example, where arrows labelled S1–S7 mark multiple switching events. The borehole originally disconnected from the main group on July 11th, but reconnects on several occasions during periods of high water pressure in the active drainage system, disconnecting when water pressure subsequently drops. Note that for the first two recon-

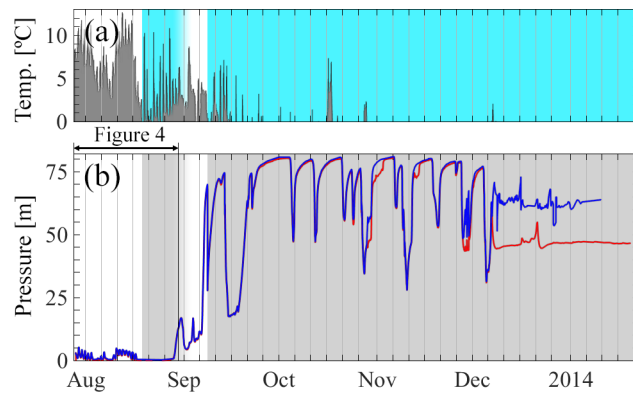


Figure 13. Extended pressure time series from the 2013 fast-flow borehole (Fig. 5). (a) air temperature (grey) and fresh snow cover (light blue). (b) Pressure recorded by two sensors installed 10 cm and 80 cm above the bed (red and blue respectively).

nections, S2 on July 21st and S4 on July 24th, the switching events are clearly associated with large drops in conductivity as seen in panel g, suggesting an inflow of [melt-water](#) [meltwater](#) that has spent less time in contact with the bed [\[Oldenborger et al., 2002\]](#).

Towards the end of the melt season, most boreholes have become disconnected from each other, and water pressure in them typically rises again towards overburden, remaining nearly constant through the winter. However, in some cases, we observe quasi-periodic pressure variations in winter as previously reported in [Schoof et al. \[2014\]](#). Figure 13 shows the winter pressure record for the two sensors installed in the fast-flow borehole, extending the summer record shown in Fig. 5c. As in other boreholes, we see water pressures rising at the end of the summer season. This is briefly interrupted during early September, when surface snow cover temporarily disappears, and a drop in water pressure occurs in the borehole, accompanied by the resumption of diurnal oscillations. This is followed once again by the termination of diurnal oscillations and a sharp rise in water pressure towards overburden once the surface becomes snow-covered again. Unlike in most other boreholes, that rise towards overburden is however interrupted by oscillations lasting from 2–12 days. During these oscillations, water pressure can drop rapidly to as little as a quarter of the overburden, followed by a slower rise in pressure back towards overburden, [stabilization](#)[stabilisation](#), and a renewed rapid drop.

3.6 Inter-annual variability

As observed in Fig. 4, there is large inter-annual variability in positive air temperatures and hence, presumably, in surface melting, both in terms of onset and intensity. In addition, we expect that differences in the snow-pack can also affect water delivery to the englacial system; presumably, a thicker snow-pack can store or refreeze surface [melt-water](#)[meltwater](#), and

[leads to higher average surface albedo during the summer](#). Figure 3 shows a view of the study area from an automated camera on July 19th in 2012–2015. These images illustrate very significant differences in surface snow cover at the height of the summer melt season: the visible snow cover in each image is part of the remaining winter snowpack.

Alongside the inter-annual variability in temperature and snow cover, there are also significant season-to-season differences in the water pressure records. Differences in drilling objectives from season to season make year-to-year comparisons difficult except in one part of the study area. Figure 14 shows a compilation of pressure records from a set of boreholes drilled in almost the same locations every year in the lower plateau area from 2012 to 2015, as indicated by two red polygons in Fig. 2. There are four boreholes (surrounding the fast-flow hole in Fig. 5) included here for 2013–2015 that were not drilled in 2012, and four that were drilled in 2012 but not in later years. Alongside air temperatures and snow cover, we also indicate the total PDD count prior to June 15th, and at the end of September. Also shown are the median of the dates on which diurnal oscillations appear and disappear over all boreholes with functioning sensors (red lines). The latter are clearly a crude measure of drainage system evolution as they are biased by borehole locations and drilling dates. Despite these differences, the borehole pressure records clearly indicate some systematic differences, with a relative absence of diurnal pressure oscillations in 2012 and 2013, though accompanied by very low water pressures associated with the fast-flow borehole in 2013 (see also Fig. 5), and a larger number of “connected” boreholes with large-amplitude diurnal oscillations in 2015. We also note that we drilled new boreholes in 2014–2015 in the location of the 2013 fast-flow hole without encountering more evidence of turbulent water flow.

3.7 Data quality

~~There are numerous mechanisms by which a sensor can become corrupted. An obvious cause is a damage to the signal cables, which is sometimes visible at the glacier surface due to crevasse opening. We have visually identified records that show signs of such corruption, such as large, random jumps in pressure between successive measurements, and large negative water pressures.~~

~~Transient high-pressure spikes [Kavanaugh and Clarke, 2000](#) are likely to have caused abrupt calibration changes in four of the recorded pressure time series. From 2013 onwards, most sensors were equipped with snubbers, and only one sensor displayed this issue afterwards. In all four cases, instantaneous offsets were manually identified and corrected.~~

~~All presented pressure values were computed from differential voltage readings using a linear transformation. The two corresponding constants are referred as the offset and the multiplier. Our reported measurements rely on~~

Section moved into section 1 of the Supplementary Material

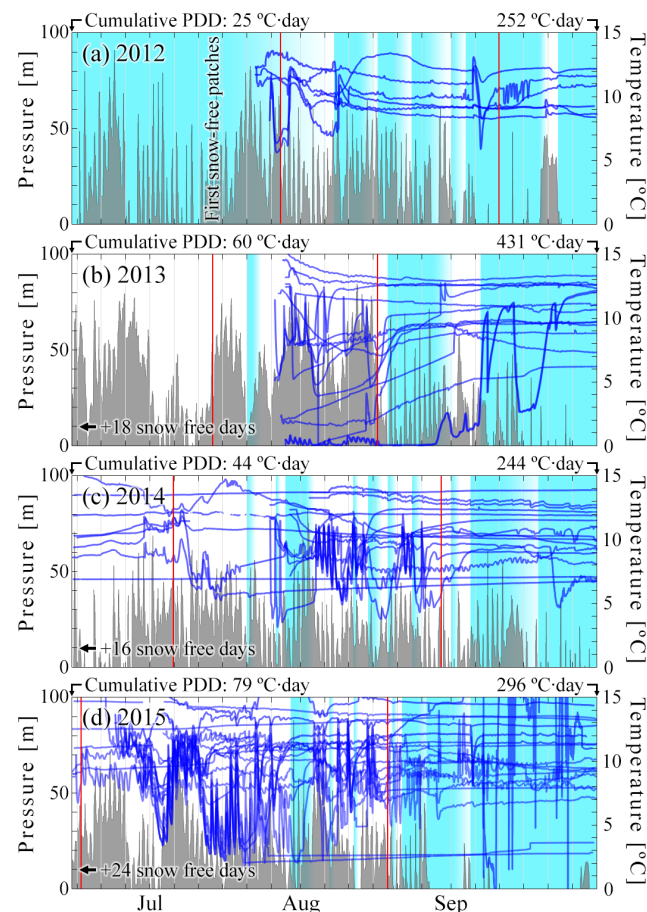


Figure 14. Overview of pressure variations on the lower portion of the plateau area from 2012 to 2015. Each panel includes air temperature (grey), coverage of fresh snow (light blue), and vertical red lines displaying the median date of initiation and termination of diurnal oscillations on all active sensors each year. Cumulative positive degree days are displayed for the beginning and end of the shown interval.

pre-installation calibrations, and assume no change in calibration constants.

To assess data quality as well as drift in the offset and multiplier, eleven boreholes were equipped with two sensors, logged independently (see the supplementary material for details). These sensors recorded in total more than 13 years of duplicated data. Seven of the boreholes included a digital transducer, in which the measurement is made in the sensor, while the remaining sensors were analogue sensors, which rely on voltage measurements at the surface and can, therefore, be corrupted by damage to the signal cable introducing partial short circuits. Doubly-instrumented boreholes indicate that calibration drift can start developing 3–4 months after installation (in October–November), but differences in measured pressures always remain below 15 m even after two years. Therefore, they can only explain pressures readings around 120 above overburden for most

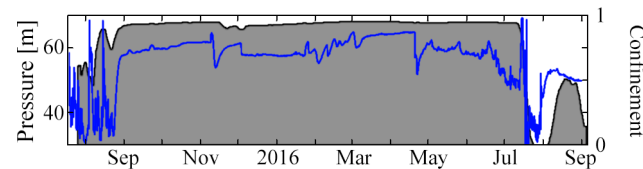


Figure 15. Confinement data (grey) and pressure (blue) for one of the digital sensors in Fig. 9b,c from July 2015 to September 2016.

boreholes, and a few analogue sensors in the data set reached values as high as 130–200 of overburden. Test of the sensors extracted by re-drilling after one year also found that small offsets had developed, in all cases smaller than 3 m. Multiplier changes were also observed, but they account for an even smaller effect within the measured pressure range. The observation of a few sensors gradually drifting up to nearly 200 of overburden is therefore difficult to explain and may be due to errors in calibration or hard-to-diagnose sensor damage. We were not able to correct for this effect; one possible cause of large calibration errors developing could be permanent deformation of the sensing diaphragm by ice formation against it.

Instrumental accuracy and precision aside, our interpretation below will rely on water pressures having been measured at the bed, except in cases where the sensor is known to have been installed englacially (such as hole A in Fig. 2). Recall that sensors were typically installed 10–20 cm above the bed; we are relying on the connection to the bed not becoming closed off. We observe that sensors in doubly-instrumented boreholes can start to exhibit independent pressure variations during winter, sometimes reverting to a common signal. One example can be seen in Fig. 13, where the red and blue curves are measured by two different sensors in the same hole. One possible explanation for the mismatched data could be the sensors becoming encased in ice during the winter, and thus separated from each other in the doubly-instrumented borehole, where the sensors are vertically offset from one another.

There is direct evidence for processes that could lead to sensors becoming enclosed in ice. Digital confinement data suggest that in some cases, as in Fig. 15, the termination/initiation of diurnal oscillations is associated with an increase/decrease in confinement: this is measured as the response of an accelerometer on board the sensor pod to an internal motor being activated, and expressed as one minus the ratio of the acceleration recorded by the sensor to the calibration acceleration recorded when freely hanging in water. Note that the fraction of boreholes showing diurnal variation in their second summer season decreases compared with the first, dropping from 71 in the first season to 58 in the second. This could also be a consequence of sensors becoming encased in ice or otherwise isolated from the bed.

4 Discussion

The seasonal evolution of the drainage system we observe is broadly consistent with existing ideas about drainage physics. A drainage system forms annually, triggered abruptly by the delivery of ~~melt-water~~ meltwater to the bed in a “spring event” [Iken and Bindenschadler, 1986]. The timing of the spring event varies significantly from year to year, taking place when most of the glacier surface is still snow covered, but always after the appearance of the first ~~sizeable~~ ~~sizable~~ snow-free patches (Fig. 3, see also Nienow *et al.* [1998b]). This suggests that the development of drainage pathways through the surface snow cover is a precursor to water delivery to the bed, with the timing most likely dictated by snow depth, temperatures, and early season melt rates [see also Harper *et al.*, 2005]. Additionally, the appearance of bare ice will significantly lower albedo, and could lead to a significant increase in melt production. After the spring event, most boreholes show strongly correlated diurnal pressure variations, suggesting extensive hydraulic connections, and at least a slight drop in water pressure. However, ~~if~~ ~~when~~ compared with late-season diurnal pressure fluctuations, these early season pressure oscillations have smaller amplitudes and lower correlation with the inferred surface melt rates, suggesting a relatively inefficient drainage system. We will refer to this initial state of the subglacial drainage system as stage 1. Note that the “stages” identified here are not the same as the “phases” discussed in Schoof *et al.* [2014], who focused only on the later part of the melt season and the subsequent winter; for instance, phase 2 in Schoof *et al.* [2014] corresponds to the transition from stage 2 to 3 here.

Later in the season, the drainage system becomes more focused, in what we will call stage 2. During this stage, the mean water pressure in the system drops, and the magnitude of diurnal pressure variations increases (see Fig. 12, also Harper *et al.* [2002]). Different parts of bed still exhibit diurnal oscillations but cease to be mutually well-connected, as also observed by Fudge *et al.* [2008]. We will refer to the parts of the bed that remain internally well-connected as hydraulic subsystems (Fig. 5 panels f and g, Fig. 6 panels c and f, and Fig. 11d–h, j and k are examples of this behaviour, with panels d–g in the latter sharing many features but appearing quite distinct from panel k). Subsystems progressively shrink, shutting down drainage over an increasing fraction of the bed. At most boreholes, the drainage shut-down is marked first by the sudden disappearance of diurnal cycles in a switching event, often followed by a sustained increase in pressure that takes approximately one to a few weeks to ~~stabilize~~ ~~stabilise~~ at a value close to overburden.

In high-melt years, the fragmentation of the drainage system can be extreme. Figure 5 shows only a handful of boreholes exhibiting diurnal oscillations towards the end of stage 2. Our data suggest these boreholes may align with down-glacier drainage axes. Had we sampled the glacier bed dif-

ferently, we could have had no boreholes showing diurnal oscillations during this period. This widespread drainage shut-down around highly focused drainage subsystems would explain why the end of diurnal oscillations in most boreholes precedes the decline in inferred meltwater supply and proglacial river runoff as observed by Harper *et al.* [2002] and Fudge *et al.* [2005].

The distinct response of different subsystems to the same surface conditions must be the result of peculiarities of each subsystem. The amplitude of the diurnal pressure cycle typically varies over periods of several days, but the temporal pattern of amplitude variations differs between subsystems, and generally, does not reproduce corresponding variations in diurnal melt amplitude (Fig. 11 here and Fig. 3 of Schoof *et al.* [2014]).

The systematic increase throughout stages 1 and 2 of the relative amplitude of diurnal pressure and inferred melt oscillations (Fig. 12), and the correlation with positive temperatures (Figures 5 and 11) is consistent with an increase in the drainage system efficiency.

A widespread termination of diurnal oscillations in the remaining connected holes is typically triggered by a marked drop in meltwater supply, usually coincident with a snow-fall event. We label this as the start of stage 3 in Figs. 5 and 9, 11; in Fudge *et al.* [2008], this is referred to as the “fall event” (though their data makes connections with ~~snow~~ ~~fall~~ ~~snowfall~~ less easy to establish). The termination of diurnal oscillations is often followed by a rise in borehole pressures towards overburden, marking the beginning of the winter pressure regime, where pressure variations are no longer closely correlated, suggesting an absence of hydraulic connections.

The shrinking and fragmentation process during stage 2, and possibly the onset of stage 3, may, however, be partially reversed by brief episodes in which the reconnection of at least some boreholes is observed. These reconnection episodes are often associated with strong increases in meltwater supply, usually on hot days when temporary snow cover clears. During 2015, snow events during late July and early August led to several episodes in which most boreholes shown in Fig. 9 appeared to disconnect from each other, pressures in them not only ceasing to exhibit diurnal oscillations but also evolving independently. These episodes ended with surface snow cover disappearing and melt supply resuming, leading to widespread and often abrupt reconnection at high basal water pressures.

Similarly, we cannot exclude the possibility that highly focused drainage subsystems remain open during the early parts of stage 3: the borehole array cannot sample all conduits directly, and we are only certain of having intersected a main conduit in one instance. That conduit, the 2013 “fast-flow” borehole, remained at close to atmospheric pressure for nine days at the start of stage 3 (Fig. 5). Subsequently, water pressure started to rise, but even then, the disappearance of snow cover and continued melting led to a pressure drop and

renewed diurnal pressure oscillations correlated with surface temperatures from September 1st to 6th (Fig. 13).

We have referred to snow cover on the glacier being a good indicator of a drop in water supply to the bed. Often this snow cover persists for a period of days in positive temperatures. With the data we have, we cannot state unequivocally whether the reduction in water supply is primarily due to the high albedo of snow suppressing melt, or due to water retention in the snowpack.

The spatial evolution of the drainage system is consistent with the drainage system becoming **channelized** channelised during the melt season. By this, we mean the formation of individual R thlisberger-type ("R") channels, incised into the base of the ice by dissipation-driven melting [*R thlisberger, 1972*]. Formation of channels should cause the mean water pressure to drop, as the focusing of water discharge causes larger channel wall melt rates that have to be offset by faster creep closure, driven by larger effective pressures [*Nye, 1976; Spring and Hutter, 1982*]. It can also account for the increased sensitivity of the pressure response to the inferred melt input, and the reduction of dye tracer transit time observed in other glaciers [*Nienow, 1993*].

The clustering of boreholes into drainage subsystems indicates good hydraulic connections between them. However, as channels cannot coexist stably in close proximity [e.g. *Schoof, 2010; Hewitt, 2011*], it is unlikely that all boreholes that sample the same drainage subsystem are located in R-channels, or in an R-channel at all. A more obvious explanation is that in stage 2, each independent subsystem contains a channel surrounded by a distributed drainage system consisting of linked cavities or a similar conduit configuration [*Kamb, 1987; Fowler, 1987; Hubbard et al., 1995; Schoof, 2010; Hewitt, 2011*]. Such a distributed system is consistent with the observation of slow-moving water in the 2014 slow-flow borehole. In addition, the existence of narrow R-channels within those systems is also consistent with the finding of the 2013 fast-flow borehole in stage 2.

Pressure records alone are insufficient to determine if there is water flow and whether a sensor is in a channel or a distributed system, even if the distributed system is hydraulically well-connected. The pressure record shown in Fig. 5 is the one record of which we know that it almost certainly reflects pressure variations in a channel. We know that highly turbulent flow occurred in the bottom 50 cm of the borehole, which we take to be the height of the channel, but its width is unknown. The first week of that time series resembles the smooth pressure variations observed in many other boreholes (albeit at fairly low water pressures), while it develops very distinct features later: water pressure drops to atmospheric at night, and there are unusually small time lags relative to and very high correlation with inferred surface melt rates.

The 2013 fast-flow borehole does not connect hydraulically to other nearby ones that lie along an across-glacier line (Fig. 5d), but appears to connect to a narrow set of boreholes extending 500 m downslope (Fig. 5 e and g). The pressure

time series from those boreholes differ somewhat from that measured in the channel, so there is probably a narrow distributed system close to the channel, the width of that system being less than the 15 m borehole spacing.

These observations are consistent with a highly developed channel with higher water discharge that has become hydraulically isolated from the neighbouring bed: the high effective pressures in the channel would favour the closure of cavities or other connections ~~at the bed~~ in the surrounding bed. This closure may also be enhanced due to the effect of bridging stresses [*Lappegard et al., 2006*]. Bridging stresses transfer part of the weight of the ice overlying the channel to its surrounding bed, effectively increasing the ice overburden in those regions above its mean value [*Weertman, 1972*].

The 2013 season was marked by high net inferred melt: the total PDD at the end of that season exceeded the PDD for 2014 and 2015 by 46% or more (Fig. Figs. 4 and 14). The high inferred melt rates are consistent with **channelization** channelisation reaching an end-member state. The rapid flow of water in the borehole also made identification easier; it is unclear if a smaller channel would have been as easy to identify.

Using the channel end-member feature of diurnal oscillations with pressure **doping** dropping to atmospheric at night, we have identified seven other boreholes where the drainage system is likely to have evolved into a well-developed channel (Fig. 2, red symbols), in all cases during the second half of July or first days of August during years with relatively high cumulative PDD, which ought to favour channel formation. Their locations loosely match zones with high up-stream areas (Fig 2, dark shading), which correspond to portions of the bed likely to concentrate basal water flow due to the expected hydraulic gradients.

Late in the season, the shut-down of the now well-developed basal drainage system during a period of dwindling inferred melt supply is consistent with high effective pressures causing the closure of subglacial connections, especially as disconnection events often occur at low observed water pressures. Different boreholes appear to become hydraulically isolated from each other during this process. We interpret the subsequent evolution of pressure records after disconnection as reflecting the response of an isolated water pocket in the borehole, presumably containing a fixed (or nearly fixed) volume of water exposed to the ambient stress field. Initially, creep closure will reduce any volume still occupied by air in the borehole and pressure can rise gradually; once there is no air space left, changes in water pressure must reflect the pressure required to maintain the borehole volume constant (assuming no further freezing) while the borehole may still deform under anisotropic stress conditions [*Meierbachtol et al., 2016*]. Intuitively, we would expect the borehole to become flattened perpendicular to the direction of greatest compressive stress, requiring a larger borehole pressure to maintain a constant volume, which could account for the slow rise

observed in water pressure, and possible for slightly above-overburden values. Importantly, the pressure in an ~~isolated disconnected~~ borehole should depend on its shape and can, therefore, differ from borehole to borehole; abrupt creation of new storage volume for instance due to crevasse propagation could also lead to abrupt changes in pressure in ~~isolated boreholes, disconnected boreholes~~. Therefore, we have to caution against interpreting the pressure in individual ~~disconnected boreholes as an indication of the conditions in the unconnected parts of the bed; instead the borehole pressure may be controlled predominantly by local stresses in the ice, and the orientation, volume and shape of the unfrozen portion of the borehole.~~

During winter, a handful of boreholes exhibited large-scale ~~aperiodic quasi-periodic~~ pressure oscillations as detailed in *Schoof et al.* [2014] and shown in Fig. 13. We have previously ~~hypothesized hypothesised~~ that these multi-day winter oscillations indicate ongoing drainage in a few locations, with the oscillations driven by the interaction between conduit growth and distributed water storage in smaller water pockets, basal ~~erevassess crevasses~~ and moulins; such oscillations could be triggered when water supply drops below a critical value in combination with a steady background water supply [*Schoof et al.*, 2014]. Winter oscillations are common in boreholes that showed end-member channel behaviour at the end of the summer, as ~~it is~~ the case for our 2013 fast-flow borehole ~~as seen shown~~ in Fig. 13, and borehole D in *Schoof et al.* [2014]. However, similar winter oscillations can occur also in boreholes that were ~~isolated disconnected~~ or belonged to ~~distributed drainage systems a distributed drainage system~~ during the previous summer.

4.1 Interannual variability

The timing of spring events and speed at which the evolution of the drainage system occurs appears to be linked systematically to the availability of meltwater. Cool, snowy summers are most obviously linked to a poorly developed drainage system with weak diurnal cycles (2012) and poor correlations between boreholes, as well as the absence of a sharp spring event (Fig. 14).

The spatial structure of the drainage system also varies from year to year. The plateau area reliably has drainage activity, though upstream area pattern in Fig. 2 does not directly agree with the observed drainage structure (Fig. 11), but is merely suggestive. Channel formation is influenced by pressure gradients controlled by surface and bed topography. However, changes in water supply geometry and the instability inherent in channel growth and competition between emerging channels implies that channels need not form in the same location every year, ~~as evidenced in~~. This is consistent with our failure to find in 2014 and 2015 a channel at the 2013 fast-flow borehole location.

4.2 Challenges to current subglacial drainage models

Boreholes do not only disconnect from or reconnect to each other during the summer: a significant number of boreholes never connect at all. Others disconnect from the drainage system as it becomes more focused and ~~fragment into subsystem~~ ~~fragmented into subsystems~~ during stage 2. Some boreholes even disconnect and reconnect multiple times (figures 7, 9 and 11).

There is typically a very clear distinction between connected holes showing a similar response to the diurnal input, and disconnected ones that do not. Within a given drainage subsystem, there is typically no gradual phase shift or diminution of oscillation amplitudes from borehole to borehole, as would be expected if the drainage system were a diffusive system with a finite diffusivity [*Hubbard et al.*, 1995]: effectively, our data suggest that, if the distributed system is diffusive, its diffusivity is very high, or zero where the system has become disconnected.

This observation contrasts with the interpretation of data in *Hubbard et al.* [1995], who identify a gradual phase shift and decay in amplitude of diurnal pressure oscillations away from an inferred subglacial channel location. In our view, the ~~“phase lag” phase lag~~ in their Fig. 5, can however also be interpreted as showing diurnal switching of their borehole from being well-connected with their boreholes 29 and 35 to being disconnected. The latter interpretation would be consistent with *Murray and Clarke* [1995], and with Fig. 7 here also showing an example of switching events with similar characteristics on South Glacier.

Hubbard et al. [1995], suggest that the bed substrate at their study site is composed of glacial till of varying grain size distributions, acknowledging that “a network of small channels” on a hard bed could also account for their observations. However, in terms of hydrology, till and a distributed drainage system at the ice-bed interface share many characteristics: we expect both to give rise to a diffusive model for water pressure if water storage in the distributed system is an increasing function of water pressure. The primary difference is in how the permeability of that system evolves. In the ‘hard-bed’ view, the permeability evolves over time in response to changes in effective pressure, whereas for a granular till, porosity and therefore permeability are simply functions of effective pressure and therefore respond instantly to changes in it [*Flowers, 2015*]. The main inconsistency of appealing to drainage through continuous till layer as the main pathway for water flow is that we would expect to see more standard diffusive behaviour, and certainly no sharp switches between connected and disconnected portions of the bed. In addition, till with a sufficient coarse-grained fraction of cobbles and boulders would probably be capable of supporting the formation of cavities in the lee of those larger grains. In short, if till is capable of creating cavities, or is interspersed with bedrock bumps or somehow capable of supporting switching

New paragraph about the effects of basal till

events by other means, then our interpretation would not be affected by assuming a hard or granular bed.

Pressure measurements at South Glacier therefore suggest that the distributed parts of each drainage subsystem are hydraulically well-connected, with all connected boreholes showing almost identical pressure variations. The limited electrical conductivity and turbidity measurements however also ~~indicated~~ indicate that relatively little water might actually flow in the distributed system ~~:- unlike~~ [Oldenborger et al., 2002]. Unlike in the data in *Hubbard et al.* [1995], there are no diurnal variations in electrical conductivity. With a hydraulically well-connected system, this has to correspond to a low water storage capacity, so that substantial variations in water pressure need not be accompanied by the similarly large changes in stored water. Alternatively, that storage capacity could be relatively ~~localized~~ localised, so that water need not flow everywhere. Oldenborger et al. [2002] shows how water pressure variations with no corresponding change in conductivity can be observed over an impermeable bed. However, the proposed mechanism requires the boreholes to be disconnected, and would not operate on hydraulically connected boreholes as in this case.

While there are typically insignificant cross-glacier differences in diurnal pressure response within well-defined drainage subsystems, the same is not true in the down-glacier direction, even where we believe a hydraulic connection can be identified. The pressure time series along the inferred channel system in Fig. 5 (panels c, e and g) are merely suggestive of a hydraulic connection, but hardly identical. The amplitude of pressure variations decreases markedly downstream from the fast-flow borehole, which would be consistent with a diffusive system, though it is unclear whether the change in amplitude occurs along the length of the channel, or within a putative distributed system flanking the channel, since the holes further down-glacier most likely did not sample the channel directly. Importantly, however, there is no systematic phase lag accompanying the decrease in amplitude, as would be predicted by a diffusion model [*Hubbard et al.*, 1995]. It is however conceivable that additional water input from surface sources along the flow path can have a significant effect on the phase of the pressure signal.

We have referred to boreholes that cease to exhibit diurnal pressure variations as having disconnected. Connection and disconnection typically manifest themselves very abruptly in time (Fig. 7, see also Fig. 5 of *Murray and Clarke* [1995]). This transition usually takes from few tens of minutes to a few hours. However, the initiation of the transition, often identified as a clear change in the rate of change of pressure with respect to time, can in many cases have the appearance of an instantaneous phenomenon, even at our shortest sampling interval of one minute. Therefore, it is unclear if these time scales can be associated with the connection or disconnection process, as they might only represent how fast the system responds to a perhaps

instantaneous switch between connected and disconnected states.

Usually, disconnection occurs during a drop in water pressure in the subsystem, and reconnection during an increase (figures 7 and 9). This is consistent with connection or disconnection resulting from viscous creep closing connections between individual cavities within the distributed system [*Kamb*, 1987], or presumably with elastic gap opening or closing if sufficiently rapid. Disconnection could also be the result of cavities shrinking while remaining connected, if the borehole simply terminates on an ice-bed contact area between connected cavities and those contact areas are systematically larger than the ~ 10 cm diameter of our boreholes. This process has been observed previously by Meierbachtol et al. [2016]. It however seems unlikely that this effect, which should be random, would lead to a ~~recognizable~~ recognisable spatial structure of narrow drainage regions flanked by increasing large disconnected regions. Instead, we would expect a random distribution of apparently connected and disconnected boreholes.

The anti-correlated signals we observe in our data (Fig. 9e) have previously been explained by a mechanical load transfer mechanism, where the ice around a ~~pressurized~~ pressurised conduit redistributes normal load, reducing the normal stress over neighbouring areas of the bed. ~~Therefore unconnected~~ Unconnected water pockets in those areas would ~~therefore~~ experience a drop in water pressure [*Murray and Clarke*, 1995; *Gordon et al.*, 1998; *Lefeuvre et al.*, 2015]. A ~~3D full-Stokes model presented by three-dimensional Stokes flow model~~ Lefeuvre et al. [2018] supports this interpretation, and suggest that the anti-correlation pattern depends on the bed slope, which can be one of the factors affecting the observed distribution of borehole displaying this behaviour. Boreholes exhibiting ~~those~~ anti-correlated pressures must ~~then be effectively isolated~~ be effectively disconnected, so that a change in normal stress mainly causes changes in the ~~pressurization~~ pressurisation of the borehole rather than water exchange. The load transfer mechanism is consistent with our observations.

An alternative explanation suggests that such signals are associated to enhanced cavity opening due to basal sliding changes [Bartholomaeus et al., 2011; Hoffman and Price, 2014; Iken and Truffer, 1997]. However, it is unlikely that a variation in sliding would precisely mimic the local water pressure variations in the adjacent drainage subsystem, as suggested by Fig. 9e: the force balance that determines sliding velocities should be affected by changes in basal shear stress across a larger portion of the bed.

Note that we observe anti-correlated signals in boreholes that are not immediately adjacent to boreholes showing a correlated signal (purple and blue markers in Fig. 9). It would be difficult to explain the anti-correlated signal in these boreholes by normal load transfer over larger distances, when other ~~isolated~~ disconnected boreholes nearby show no such behaviour. This suggests that the connected

New paragraph about switching events time scale

New paragraph about the alternative hypothesis for anti-correlated signals

drainage system can contain fine structure (either as channels or narrow regions of distributed drainage) with lateral extents smaller than the ~ 15 m borehole spacing. The same is indicated by the formation of disconnected “islands” in lines of otherwise connected boreholes at the same spacing as ~~see seen~~ in Fig. 7 for the August observation period (~~see also Murray and Clarke [1995], for analogous observations~~).

We have referred to a borehole as ~~isolated~~ ~~when observations suggest that there is effectively no water transport into or out of the borehole~~ ~~disconnected~~ ~~when observations show that pressure variations on a diurnal timescale are not communicated to a borehole~~. However, the evolution of the mean water pressure in disconnected boreholes is consistent with a residual amount of water leakage into the connected drainage system: during the summer, that mean pressure gradually decreases. The end of the monotonic increase in water pressure of disconnected boreholes observed in Fig. 8, coincides with the spring event, followed by a slow decrease. The large sample obtained in summer 2016 supports this trend up to a 99% confidence despite the large variability of the observations.

As in Hoffman *et al.* [2016], such a slow evolution could be accounted for by flow through a relatively impermeable till aquifer underlying a much more effective but less pervasive interfacial drainage system, and the magnitude of that leakage could have a significant impact on basal sliding rates if disconnected areas act as sticky spots.

Widespread ~~bed hydraulic isolation~~ ~~hydraulic isolation of the bed~~ in winter is supported by high recorded water pressures and the marked pressure drop at the spring event observed in 20% of boreholes. In contrast, theories based on a remnant ~~“distributed”~~ ~~“distributed”~~ system would ordinarily suggest relatively low water pressures in winter (Schoof, 2010; Hewitt, 2013). Although it is possible that some boreholes do not connect because they were not properly drilled to the bed, we believe that the existence of persistently disconnected areas is robust. Non-spatially biased samples suggest that up to 15% of the bed could remain unconnected year round. The existence of such unconnected holes, and the possibility of dynamic connection and disconnection, represents a challenge to existing drainage models, which typically assume pervasive connections at the bed.

In addition to conduits at the bed interface, englacial conduits are known to exist inside temperate glaciers [Fountain and Walder, 1998; Nienow *et al.*, 1998b; Harper *et al.*, 2010]. However, it is unclear whether they allow mostly vertical water transport, or if horizontal water transport over significant distances is also possible through them. Frequent drainage events during drilling (also observed by Iken and Bindenschadler [1986]) suggest the existence of a large number of englacial conduits, and borehole re-drilling observations show that upward conduits can remain open through the winter season in a layer extending several ~~meters~~ ~~metres~~ above the bed. However, we have no evidence of significant along-glacier drainage in winter, while we know that englacial con-

nections can remain. This suggests that the englacial connections remain isolated from each other during winter. It is unclear if they can connect in summer and establish an englacial drainage system capable of supporting significant down-glacier drainage. The persistence of conduits through winter is most likely related to the basal layer of temperate ice [Wilson *et al.*, 2013], and hydraulic isolation preventing creep closure. The apparent ubiquity of englacial conduits suggests a need to assess their role in downstream water transport in future; if significant, this represents another area of improvement for drainage models.

4.3 Mechanically connected boreholes

Strong correlations over long distances were observed in boreholes displaying all the features of ~~isolated~~ ~~disconnected~~ boreholes except a superimposed low-amplitude diurnal pressure variations with high-frequency variations (Fig. 10). From their wide spatial distribution, it appears impossible for them to be connected by hydraulic conduits. As such conduits would need an extremely high diffusivity to preserve the observed high-frequency features over large distances (>500 m as seen in Fig. 2). Moreover, a high diffusivity is at odds with the diverging evolution of ~~temporally~~ smoothed borehole water pressures in the same holes.

These signals do not seem to be instrumental artifacts, and in many cases were recorded by independent data loggers. We have also considered effects due to induction on non-twisted signal cable coils, temperature, or solar irradiation. However, in those cases, such signals should also be superimposed on records from distributed drainage systems, contrary to our observations. Possible explanations must be related to periodic large-scale stress changes in the ice compressing ~~isolated~~ ~~disconnected~~ boreholes whose volume must remain constant, thereby eliciting an instant water pressure response. The most likely cause of such large-scale stress changes would appear to be the occurrence of periodic diurnal basal slip events as suggested by Andrews *et al.* [2014].

4.4 Data interpretation caveats

We generally assume that the sensors at the bottom of boreholes measure the water pressure at the bed. However, this may not always be the case if the sensor becomes encased in ice, is connected to an englacial conduit, or if the borehole did not reach the bed or has penetrated into the basal till.

It is likely that with time, some sensors can become encased in ice, as suggested by the fact that older sensors are less likely to show diurnal oscillations ~~and by~~ ~~confinement data showing in some cases a correlation with the initiation/termination of diurnal pressure oscillations (Fig. 15)~~. ~~For this reason, old isolated sensors (for that reason, sensors in old disconnected boreholes~~ were often decommissioned before they ceased to produce a signal), ~~and the observations in doubly-instrumented boreholes~~

(see section 1 of the supplementary material). Digital confinement data suggest that in some cases, as in Fig. 15, the termination/initiation of diurnal oscillations is associated with an increase/decrease in confinement. This observation would also be consistent with ice encapsulation of the sensor during winter.

Although the upper end of the boreholes typically freezes shut within few days, the abundance of englacial conduits ~~described above~~ opens the possibility that the sensors could connect to an englacial conduit through the lower portion of the borehole while it is still open. In such a case, the pressure record could at least partially reflect the evolution of englacial conduits instead of the basal drainage system.

Alternatively, in the absence of englacial connections, a sensor in a borehole that fell short of the bed would appear as ~~isolated~~~~disconnected~~, even if the underlying bed is not. However, we believe this is not a common situation due to the strict procedures followed to assess whether a borehole reached the bed or not (see section 2).

Observations by *Hart et al.* [2015] using wireless pressure sensors installed across the basal till layer in a glacier in Norway showed that, while a sensor ~~in at~~ the ice-till interface shows clear diurnal variations, another one placed a short distance away inside the till layer can show a signal very similar to our ~~isolated~~~~disconnected~~ boreholes. This could be a problem affecting some of our sensors, as borehole drilling could eventually penetrate the till. Nevertheless, the lifespan of a sensor buried in the till ought to be short if there is differential motion between ice and ~~the~~ ~~the sensor placement in the~~ till [e.g. *Engelhardt and Kamb, 1998*], causing the signal cable to tear. Indeed, one sensor that was accidentally installed directly on the bed with limited (1 m) cable slack, rather than suspended just above the bed, survived for only just over a month, and showed uncharacteristic high-frequency noise superimposed on a smooth diurnal oscillation (see the lowest curve in Fig. 5g).

~~We also reiterate that calibration~~ Calibration drifts may affect in-situ sensors over time, and differences in measured water pressure may not be reflective of an actual pressure gradient between two boreholes (~~section ??~~ ~~supplementary material section 1~~); consequently, we have taken similarity in response to diurnal forcing as our indicator of connections, rather than looking directly at the evolution of pressure ~~differences~~ ~~gradients~~.

5 Modelling

Our data show that the glacier bed not only contains regions that remain disconnected from the subglacial drainage system during the melt season, but that those regions can evolve in time, and that disconnection from or reconnection to the drainage system can be quite abrupt. By itself, that insight is not new. Previous observational studies [*Murray and Clarke, 1995*; *Gordon et al., 1998*; *Andrews et al., 2014*; *Meierbach-*

tol et al., 2016] have pointed out the same set of phenomena. Most models in their present form [*Schoof, 2010*; *Hewitt, 2011*; *Schoof et al., 2012*; *Hewitt et al., 2012*; *Hewitt, 2013*; *Werder et al., 2013*; *Bueler and van Pelt, 2015*] however do not capture them: water can flow everywhere in the domain, although the permeability of the distributed system varies with position and over time. The expected signature of the distributed system in borehole records is then a progressive decrease in amplitude of diurnal oscillations away from subglacial channels, with a corresponding phase lag (see Fig. 8 of *Werder et al. 2013*): the sheet behaves as a diffusive system, in which the diffusivity varies smoothly in space and time and evolves as sheet thickness does [see also *Hubbard et al., 1995*]. This contrasts with the possibility of abrupt disconnection from the drainage system that appears to be the main feature of our field data, rather than a slow, diffusive attenuation of pressure signals.

The only exception is the model of *Hoffman et al.* [2016], which contains a ‘weakly connected’ component that exchanges water with the active remainder of the drainage system through highly inefficient connections. Diurnal pressure variations in that weakly connected system are primarily due to the effect of ice motion rather than through the exchange of water, as we have also inferred for the groups of boreholes in our data that show common, mechanically transferred pressure variations (Fig. 10). The spatial extent of individual weakly connected parts of the bed is however left unresolved in *Hoffman et al.* [2016], and water exchange with the distributed system occurs locally, as is also the case in dual-porosity models [*de Fleurian et al., 2014*]. Instead of prescribing the physics by which the connection between distributed and weakly connected systems evolves, a simple linear increase in the exchange coefficient is assumed to occur during the summer.

Here we take a different approach and try to construct a model that can resolve connected and unconnected (or weakly connected) regions explicitly, and track their evolution. Our basic premise is the following: models of distributed drainage [*Hewitt, 2011*; *Schoof et al., 2012*; *Werder et al., 2013*; *Bueler and van Pelt, 2015*] typically describe a system of cavities, and model the mean cavity size at any given location. Crucially, these cavities are assumed to connect whenever they have non-zero size. Here, we replace that assumption by a percolation limit: cavities only form a connected system once they have reached a critical size. We describe the implementation of such a limit in the context of a discrete network-based model for subglacial drainage, and discuss the relatively straightforward equivalent continuum formulation in [section 3 of the supplementary material](#).

5.1 Model Formulation

We assume an arbitrary network of conduits connecting nodes labelled by a single index i ; the edge connecting nodes i to j is identified by the double index ij . The basic set-up

of the model, with a handful of alterations identified below, proceeds as in *Schoof* [2010].

Along each network edge ij , we assume ~~one~~ there are n_c conduits connecting node i to node j : One 'R'-conduit that can behave either as a Röhrlisberger (R) channel or a cavity, as in *Schoof* [2010], with average cross-section $S_{R,ij}$. ~~To mimic the sheet of Werder et al. [2013] and avoid the pitfall of having to resolve every basal conduit, we also assume there are~~, and $n_c - 1$ 'K'-conduits 'Kamb' (K) conduits that behave only as cavities, and are not subject to enlargement by melting. ~~This configuration mimics the sheet of Werder et al. [2013] and avoids the pitfall of having to resolve every basal conduit.~~ We denote their average cross-sectional area by $S_{K,ij}$. The conduits evolve according to

$$\frac{dS_{R,ij}}{dt} = c_1 Q_{R,ij} \Psi_{R,ij} + u h_R (1 - S_{R,ij}/S_{R0}) - c_2 S_{R,ij} |P_{e,ij}|^{n-1} P_{e,ij} \quad (1)$$

$$\frac{dS_{K,ij}}{dt} = u h_K (1 - S_{K,ij}/S_{K0}) - c_2 S_{K,ij} |P_{e,ij}|^{n-1} P_{e,ij} \quad (2)$$

Here $Q_{R,ij}$ is discharge from node i to j in the R-conduit, and $\Psi_{R,ij}$ the hydraulic gradient along the R-conduit. u is sliding velocity, h_R the size of bed obstacles supporting cavity formation, and S_{R0} is a as well as S_{K0} are cavity-size cut-off cut-offs at which further conduit enlargement drowns out bed obstacles. $P_{e,ij}$ is the effective pressure driving conduit closure (related to N_i as described by equation 7 below), and c_1, c_2 are the same constants as in *Schoof et al.* [2014]. Subscripts K refer to equivalent quantities for the K-conduits.

We associate a nominal effective pressure N_i with each node, defined as overburden minus basal water pressure. Hydraulic potential Φ_i at each node and hydraulic gradient ~~along the conduits are then given by~~ Ψ along the network edges are given by

$$\Phi_i = \Phi_{0,i} - N_i, \quad \Psi_{R,ij} = \frac{\Phi_i - \Phi_j}{L_{ij}}, \quad \Psi_{K,ij} = \frac{\Phi_i - \Phi_j}{TL_{ij}} \quad (3)$$

where $\Phi_{0,i} = \rho_i g s_i + (\rho_w - \rho_i) g b_i$ is the geometrical contribution to hydraulic potential, ρ_i and ρ_w being the densities of ice and water, g acceleration due to gravity, s_i and b_i ice surface and bed elevation at the node. L_{ij} is the length of the network edge and $T \geq 1$ is the tortuosity of the K-conduits. ~~K-conduits~~, relative to the R-conduits. In a departure from previous models, we assume a percolation cut-off for flow along the conduits ~~, and write~~

$$Q_{R,ij} = c_3 \max(S_{R,ij} - S_{PR}, 0)^\alpha |\Psi_{R,ij}|^{\beta-2} \Psi_{R,ij}$$

$$Q_{K,ij} = c_3 \max(S_{K,ij} - S_{PK}, 0)^\alpha |\Psi_{K,ij}|^{\beta-2} \Psi_{K,ij}.$$

and write

$$Q_{R,ij} = c_3 \max(S_{R,ij} - S_{PR}, 0)^\alpha |\Psi_{R,ij}|^{\beta-2} \Psi_{R,ij} \quad (4)$$

$$Q_{K,ij} = c_3 \max(S_{K,ij} - S_{PK}, 0)^\alpha |\Psi_{K,ij}|^{\beta-2} \Psi_{K,ij} \quad (5)$$

Here c_3 is the same constant as in *Schoof et al.* [2012], and α and β are constant exponents as in *Werder et al.* [2013], while S_{PR} and S_{PK} are the constant thresholds that conduit sizes must reach before water can flow in the conduits. For linked cavities, such a threshold is easy to justify: while S_K may be the average cross-sectional area of cavities along the network edge, the local cavity size will naturally vary as bed obstacles are uneven, and it is natural to expect that cavities with non-zero size may fail to connect. We apply the threshold equally to the R-conduit as it can act as either a channel or a cavity, and a cut-off must apply self-consistently in its cavity state. A node that is connected to others purely by conduits that are all below the percolation threshold is then hydraulically disconnected from the drainage system.

At each node, water can be stored in englacial void space connected to the node, with volume storage capacity per unit water pressure V_p [see also *Werder et al.*, 2013; *Schoof et al.*, 2014; *Brinkerhoff et al.*, 2016]. Water can also be supplied externally to each node at a locally-defined rate m_i , and flows along network edges through R- or K-conduits, or possibly through a permeable porous substrate if the conduits are closed. To account for conservation of mass, we also associate half the volume of water stored in a conduit between two nodes with each node, and likewise, account for half the water created by wall melting in an R-conduit as water supply to each node. Consequently ~~we impose~~, we impose mass conservation in the form

$$V_p \frac{dN_i}{dt} + \sum_j [Q_{R,ij} + (n_c - 1)Q_{K,ij} + k_{\text{leak}} \Psi_{ij}] = \sum_j \frac{\rho_i}{2\rho_w} c_1 Q_{R,ij} \Psi_{R,ij} L_{ij} + m_i \quad (6)$$

where k_{leak} represents the possibility of a substrate (till) with non-zero permeability. Sums over j are taken over nodes connected to node i .

To close the model, we need to relate the conduit effective pressure $P_{e,ij}$ to the nominal effective pressures N_i at network nodes. ~~we~~. We write this in the form

$$P_{e,ij} = \sum_k G_{ijk} N_k \quad (7)$$

where the sum is over all node indices k in the network, and G_{ijk} is a suitable positive averaging kernel that satisfies $\sum_k G_{ijk} = 1$; in our network model below we put $G_{ijk} = 1/2$ if $k = i$ or $k = j$ and $G_{ijk} = 0$ otherwise for simplicity; this is however a surprisingly key assumption (see also

Single number equation labels

the [Supplementary Material section 3 of the supplementary material](#)). Suppose we have $k_{\text{leak}} = 0$ and no hydraulic connection at all between adjacent nodes. This can lead to arbitrarily large effective pressure gradients. The usual assumption of cavity formation models [Fowler, 1987; Schoof, 2005; [Gagliardini et al., 2007](#)] breaks down, namely that adjacent cavities are subject to the same nominal effective pressure, defined as overburden pressure (or far field normal stress) minus a common water pressure. The rate of opening or closing of a cavity is unlikely to be a function of its own nominal effective pressure alone, and is likely to be affected by stresses around other nearby cavities (and hence dependent on their nominal effective pressure: the observation of anti-correlated water pressure records in our [data set dataset](#) indicating a load transfer of overburden onto highly [pressurised](#) parts of the bed [Murray and Clarke, 1995] also supports this assumption. We try to capture this load transfer effect by the averaging kernel G above.

More practically, if conduit opening and closing were driven by a local effective pressure variable alone, then the [generalization-generalisation](#) of our model to a distributed sheet [Werder et al., 2013] would result in disconnected parts of the bed potentially never reconnecting. In order for a disconnected region to reconnect, sheet thickness in the disconnected region needs to change. On the absence of leakage through the substrate, the only way that can happen in a way that is driven by the hydrology of the connected regions is through a non-local sheet closure term, or through the sliding velocity u . We expand on this in [section 3](#) of the supplementary material, but note here that conduit closure must involve a non-locally defined effective pressure in order for our percolation model to function as intended, allowing for expansion as well as the contraction of a connected region at the bed.

A key component that the model above continues to miss is the ability to open conduits due to [overpressurization-overpressurisation](#) of the system [Schoof et al., 2012; Hewitt et al., 2012; Bueler and van Pelt, 2015; [Dow et al., 2016](#) [Dow et al., 2015](#)]. While not necessary to explain switching events during the main melt season, this is likely to be key in establishing a drainage system at the start of the melt season: unlike existing sheet models, in which a distributed system always exists and can simply be expanded through water supply in the spring, the percolation limit model above allows the system to shut down completely, and rapid re-establishment through a spring event is likely to require [overpressurization-overpressurisation](#). We discuss the extension of the approach in Schoof et al. [2012] and Hewitt et al. [2012] further in [section 3](#) of the supplementary material.

Table 1. Parameters used in [simulationthe simulations](#)

Symbol	value
c_1	$1.35 \times 10^{-9} \text{ m}^3 \text{ J}^{-1}$
c_2	$3.44 \times 10^{-24} \text{ Pa}^{-3} \text{ s}^{-1}$
c_3	$4.05 \times 10^{-2} \text{ m}^{9/4} \text{ Pa}^{-1/2} \text{ s}^{-1}$
k_{leak}	0
n	3
α	5/4
β	3/2
ρ_i	910 kg m^{-3}
ρ_w	1000 kg m^{-3}
g	9.8 m s^{-2}
S_{PR}, S_{PK}	$2.65 \times 10^{-3} \text{ m}^2$
S_{R0}, S_{K0}	3.32 m^2
uh_R, uh_K	$3.47 \times 10^{-6} \text{ m}^2 \text{ s}^{-1}$
T	1
n_c	2
V_p	$2.53 \times 10^{-5} \text{ m}^3 \text{ Pa}^{-1}$

New Model results section

5.2 ResultsModel results

~~We show results here for Network-based models for drainage channelisation (e.g. Schoof [2010]; Hewitt [2013]; Werder et al. [2013]) have been used previously to model the seasonal evolution of drainage systems. In particular, they have been used to model the evolution of a drainage system supplied through discrete moulins, focusing on channelised system from a more spatially extensive one as in stages 1 and 2 identified in this paper, and the subsequent shut-down of the system as in stage 3. See figure 3 of Schoof [2010], figure 5 of Hewitt [2013], and figure 12 of Werder et al. [2013] for examples of seasonal drainage evolution. What these models are missing is the ability to capture the formation of disconnected regions at the glacier bed and the subsequent ability of parts of the bed to connect and disconnect to the drainage system, which is what we focus on here.~~

Instead of attempting to model a full seasonal cycle, we focus here on the effect of time-dependent water input ~~to a fully developed, into a fully~~ channelised drainage system. ~~A list of model parameters is given in Table ??; unlike in Hoffman et al. [2016], we do not consider feedbacks with ice velocity u , which we hold constant. The shape of the domain is indicated, in order to test whether our modification of existing models can capture the qualitative behaviour of the switching events such as those in Fig. 11 (see in particular panel g). In other words, we focus on the behaviour of the drainage system in stage 2. Our simulation is an idealised run, not based on the specific geometry or properties of the South Glacier field site and does not claim to reproduce observations beyond their generic features. Work to use proxies for surface melt rates and likely surface water supply routing in an inverse model for the drainage system is currently underway and will be reported elsewhere. Our aim here is simply to study the qualitative features of our forward~~

model, modified from existing ones found in the literature, and to compare them equally qualitatively with our borehole records.

The rectangular domain is 5 km long and 1 km wide. The ice and bed surfaces are used with contour lines in panels a3 and b3-c and g of Fig. 16, where black lines are surface contours at 100 m intervals, and grey lines are bed contours at the same intervals. Zero inflow is prescribed at the sides and top of the domain, and zero effective pressure at the lower end of the domain $y=0, y=0$. The network geometry is the same as indicated in Fig. 1 of the supplementary material to Hewitt [2013], with a total of 201×201 nodes. The location of the

We allow water to be supplied in 40 moulins is indicated by red dots in panels a4 and b4 of Fig. 16, the size of each dot scaled to the instantaneous water supply discrete locations (effectively, moulins). Each moulin undergoes a diurnal cycle whose amplitude varies over several days, with mean water supply rates also varying over several days; the dominant period of the cycle is the same for each moulin but the ratio of diurnal amplitude to mean water supply is chosen randomly (while maintaining positive water supply rates at all times), and we have allowed for slight phase shifts between moulins. The time series of water supply to all moulins are shown in panel e of Fig. 16i.

We show two different simulations. Both use the parameter values shown in table 1, except that the percolation cut-offs S_{PR} and S_{PK} have been set to zero in one of the simulations (to identify the effect a percolation limit has on our results), and uh_R and uh_K are also set to one-tenth the value given in table 1 in the same simulation (without a percolation limit, cavities of the same size will permit larger discharge, so we reduce the cavity opening rates uh_R and uh_K in order to limit cavity size).

Figure 16 shows two snapshots of a four-week drainage cycle, corresponding to the maximum and minimum extent of the one set of panels for each simulation, identified by the numbers 1 (no percolation cut-off) and 2 (finite percolation cut-off) in the panel labels. When referring to a specific panel for both simulations at the same time, we will identify it by the letter in the panel label. Both simulations start from a fully channelised steady state computed with moulin water supply set to constant values. Diurnal oscillations are subsequently superimposed on those constant water supply values. The system is run for several days to account for transients before the detailed results shown in Fig. 16 are computed.

The channelised configuration of the system does not change during the simulation (compare panels a and e in Fig. 16), although it differs slightly between the two simulations. Pressure oscillations result from the time-dependent water supply. These pressure variations are confined to the connected drainage system (compare panels c and g of 16, and see also the supplementary movie #2).

In simulation 2 (with non-zero percolation cut-offs), the extent of connected drainage system during that period. Panels a4 and b4 indicate the connected regions in each case in blue. Also indicated there are two squares that we treat as synthetic borehole grids. A video showing the continuous evolution of conduit sizes, effective pressure and connectivity is included in the supplementary material, also evolves, shown as blue areas in panels d2 and h2 of Fig. 16 and the supplementary movie #2. While pockets of water can move down-glacier essentially without connection to the channelised system (see the left-hand side of the main drainage axis in supplementary movie #2), the main feature here is the expansion of the connected system at times of large water supply and low effective pressures. The larger connected system in panel h2 of Fig. 16 corresponds to peak water supply, the smaller system in panel d2 to the minimum water supply in the cycle shown. This is at least qualitatively consistent with our observation of switching events, that establish connectivity during periods of increasing water supply.

Time series for water pressure in these borehole grids are shown in Fig. 17, we focus on what an array of boreholes would observe. The borehole array is located in the black rectangle shown in panel d2 of Fig. 16. Panels a2-c2 in Fig. 17 show the evolution of the connected parts of the bed within the borehole array, while panels d2-g2 show pressure time series, again grouped subjectively.

The presence of at least two distinct drainage subsystems is immediately obvious (circles and diamonds in panels a2-c2, corresponding to the time series shown in panels d2 and e2 respectively). These two subsystems correspond to two different drainage channels. The grouping of boreholes in panel f2 (triangles) is intermittently connected to the diagonal channel of panel e2 (diamonds), with different boreholes connecting and disconnecting at different times, through connection and disconnection are again typically favoured by low and high effective pressures, respectively. This is in qualitative agreement with our actual borehole data (see Fig. 11g). In addition, there is an additional grouping of persistently disconnected boreholes (Fig. 17 panel g2, crosses), although two of these become very poorly connected later in the cycle, permitting an excursion in effective pressure without obvious diurnal cycling.

One important aspect of the synthetic borehole records in panel f2 of Fig. 17. The character of diurnal pressure signal propagation is qualitatively more in line with that in our field data than, for instance, the equivalent, is the relatively minimal attenuation of amplitude and minimal phase lags observed within that distributed system relative to the channel (panel e2) to which the distributed system connects, and the abrupt switching to nearly constant effective pressures on disconnection. Compared with borehole data from South Glacier, we do not reproduce the tendency of disconnected boreholes to experience rising water pressure (i.e. falling effective pressure), which we believe is related

to the dynamics of disconnected boreholes incised upwards into the ice being squeezed by anisotropic stresses in the ice, an effect this drainage model is not designed to capture.

Removing the percolation cut-off for simulation 1 increases the ability of the distributed system to drain water (equations 4 and 5). To account for this we simultaneously lower conduit opening rates uh_R and uh_K to $3.47 \times 10^{-7} \text{ m}^2 \text{ s}^{-1}$, keeping all other parameters the same. In order to create comparable drainage structures in both simulations, simulation 1 was started from the same initial state as simulation 2. The percolation cut-offs and conduit opening rates were then gradually changed with water supply rates held constant until a new steady state was achieved, before imposing the same diurnal oscillations as in simulation 2 again (panel i of Fig. 8 in Werder *et al.* [2013]: switching events as well as clear differentiation into drainage subsystems are visible, while there is considerably less diffusive attenuation and development of phase lags. The synthetic time series however also provide a note of caution: As expected, connections usually happen during times of decreasing mean effective pressure, with the opposite true for disconnection events. In 16).

A small change in channel configuration results from removing the percolation cutoffs: two of the main drainage channels along the centre of the glacier in Fig. 16 panels a2 and e2 collapse onto a single channel in panels a1 and e1, as they are no longer isolated from each other by the percolation cut-off. The main difference in model results is however the much larger region over which the effect of oscillatory water input is felt away from the channels (compare Fig. 16 panels c1 and g1 with panels c2 and g2). This is a natural consequence of enforcing connectivity in the drainage system everywhere (see Fig. 16 panels d1 and h1).

On the left-hand side of Fig. 17 we use the same groupings of synthetic boreholes as for the simulation with a percolation cut-off (right-hand side of the same figure). The boreholes marked as diamonds produce an almost identical pressure time series as in the first simulation (compare panels e1 and e2 in Fig. 17), indicating that the behaviour of channelised drainage is not substantially affected by dispensing with the percolation cut-off. By contrast, the boreholes marked as circles in Fig. 17 experience higher mean effective pressures and bigger oscillations in panel d1 than d2. This is the result of the two channels on the left-hand edge of the domain in Fig. 17 panels a2-c2 having been merged into a single channel in panels a1-c1: the percolation cut-off allows subsystems to co-exist separately in closer proximity, in accordance with our observations at South Glacier.

The biggest difference is in the behaviour of the boreholes within the distributed system surrounding the channels (Fig. 17, all boreholes in panels e and f as well as two boreholes rendered in pink in g ultimately connect to the same channel, though a superficial assessment would not

necessarily identify that. panels f and g). Unlike in the case of the model with a percolation cut-off, the results in panels f1 and g1 no longer exhibit switching events, and there are no persistently disconnected boreholes. Instead, we see evidence of typically diffusive behaviour away from the channels: a reduction in the amplitude especially of the higher frequency (diurnal) forcing components with an attendant phase shift, and the absence of a sharp division between drainage subsystems. This behaviour mimics that in Fig. 8 of Werder *et al.* [2013], but contrasts with our field observations. Those observations indicate minimal variations in amplitude and phase shifts within drainage subsystems, with sharp boundaries separating different subsystems. The inability to explain those features of our field observations motivates the model modification we have proposed here.

A synthetic borehole grid. (a-c): enlargements of the inset box in Fig.16(a4) at times $t = 3.9$ (a), 7.8 (b) and 20.6 (c) days. Superimposed on the blue connectivity map is S_R conduit size, plotted using the same colour scheme as indicated by the colour bar in column 1 in Fig. 16-. Also shown are the locations of 16 synthetic boreholes, colour-coded by row, (d-g). Effective pressure time series from the boreholes, grouped according to borehole symbols: circles (d), diamonds (e), triangles (f), crosses (g). Each time series is colour-coded by row. That modification comes with one major drawback, which we do not attempt to resolve here. While the model is able to open drainage connections spontaneously, this is a slow process driven by viscous deformation, controlled by the non-local effective pressure term in equation 7. When the drainage system is subject to a rapid increase in water supply, the physics by which drainage connections are established may involve either elastic hydrofracture driven by overpressurisation (e.g. Tsai and Rice [2012]) or the large-scale uplift of ice at flotation as described in Schoof *et al.* [2012]. As we discuss in section 3 of the supplementary material, the latter is not straightforward to incorporate into our modified model, as is the former (which requires a blending of elastic and viscous effects). We identify this as an important area for future research.

6 Conclusions

While winter pressure record suggests that most boreholes remain isolated/disconnected during that period, the rapid spring increase in water supply produced when a rapid springtime increase in melt overwhelms the water storage capacity of the snowpack is overwhelmed, leads, leading to the sudden supply of water to the bed and activation of an extensive and well-connected/well-connected distributed drainage system. During this period, the majority of boreholes show similar diurnal pressure variations and experience modest water transport (see section 2.3.1).

New version of the figure comparing results from model runs with and without cavity-size cut-off

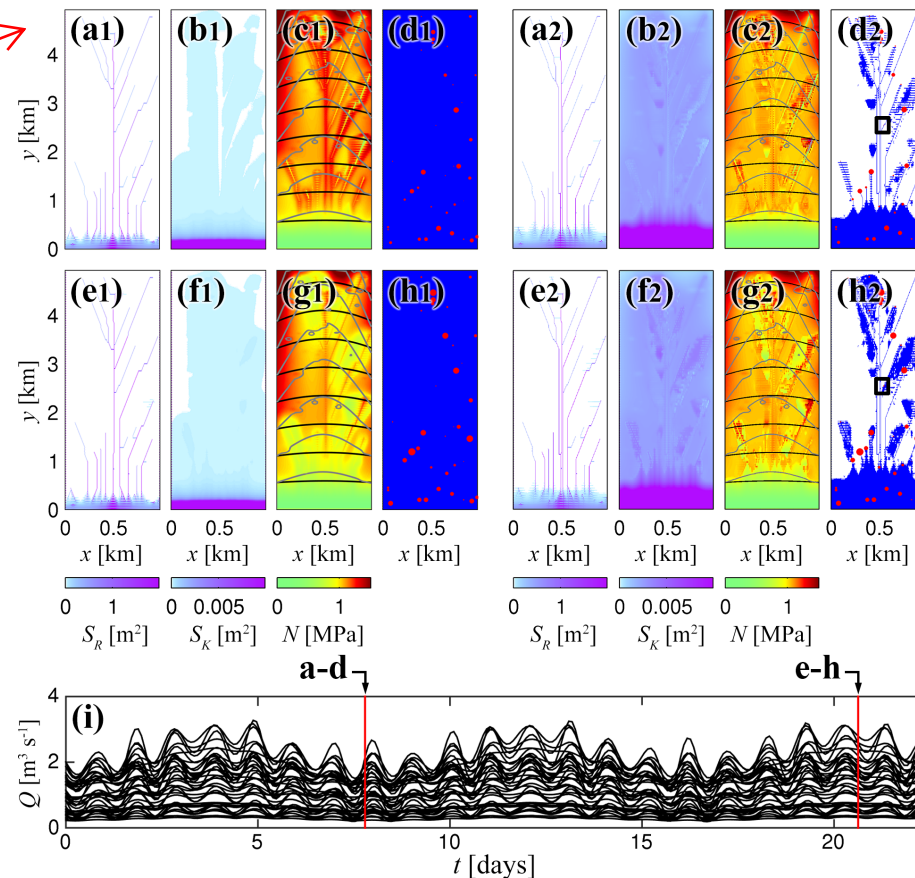


Figure 16. Snapshots of drainage system evolution – **Column 1** for the model without a percolation cut-off (left), and with it (right). **Panel a & e:** S_R conduit size. **Column 2** **Panel b & f:** S_K conduit size. **Column 3** **Panel c & g:** effective pressure, black lines are 100 m surface contours, grey lines 100 m bed contours. **Column 4** **Panel d & h:** connectedness of conduits, indicated in blue if $S_{R,ij} > S_{PR}$ or $S_{K,ij} > S_{PK}$ along a given edge, in white otherwise. Red dots indicate moulin locations, size of dot scaled with instantaneous water supply. **Row a and b** **Row a-d** show solutions at $t = 7.8$ days and **row e-h** at $t = 20.6$ days, respectively. **Panel e.** **Panel i:** water supply time series for all moulins in the domain.

Over time, water transport becomes concentrated in some areas, and probably becomes **channelized** ~~channelised~~: water flow ends up focused in R-channels surrounded by a distributed drainage system that carries relatively low water fluxes. Borehole water pressure data in most cases do not allow the direct identification of channels, ~~in~~. In fact, in most cases, our borehole array probably fails to intersect the narrow R-channels. However, in one instance we were able to confirm the existence of a channel from direct observation in a borehole in which the lowermost 50 cm were occupied by turbulent water flow.

The increase in effective pressure associated with **channelizations** ~~channelisation~~ leads to the progressive shut-down of drainage activity ~~of in~~ the surrounding distributed drainage system, possibly due to basal cavities becoming isolated from each other as they shrink under the effect of a larger effective pressure. ~~In~~ **During** long and hot enough **seasons** ~~summers~~, most of the bed can become disconnected, concentrating drainage in narrow pathways.

The **eventually eventual** complete shut-down of the entire drainage system at the end of the summer season is presumably the result of low water supply: high effective pressure and low dissipation rate in channels allow basal conduits to close. This appears to be strongly linked with the appearance of fresh snow cover, rather than the arrival of low temperatures alone (see section 4).

Most of ~~the our~~ observations are consistent with borehole data from other sites. However, the density of boreholes at South Glacier has allowed us to identify, in particular, the prevalence of **"switching events"** ~~"switching events"~~, through which the drainage system **focus** ~~focuses~~, and the **isolated disconnected** areas enlarge. Such **isolated disconnected** areas always exist, even during the spring event, ~~with isolation sometimes being reversed~~. **Isolated** ~~Disconnected~~ parts of the bed are necessary to account for many aspects of our data, including anti-correlation between **boreholes** ~~borehole~~ pressure time series, above-overburden **pressure** ~~water pressures~~, and the occurrence of strongly correlated high-frequency

New version of the figure comparing results from model runs with and without cavity-size cut-off

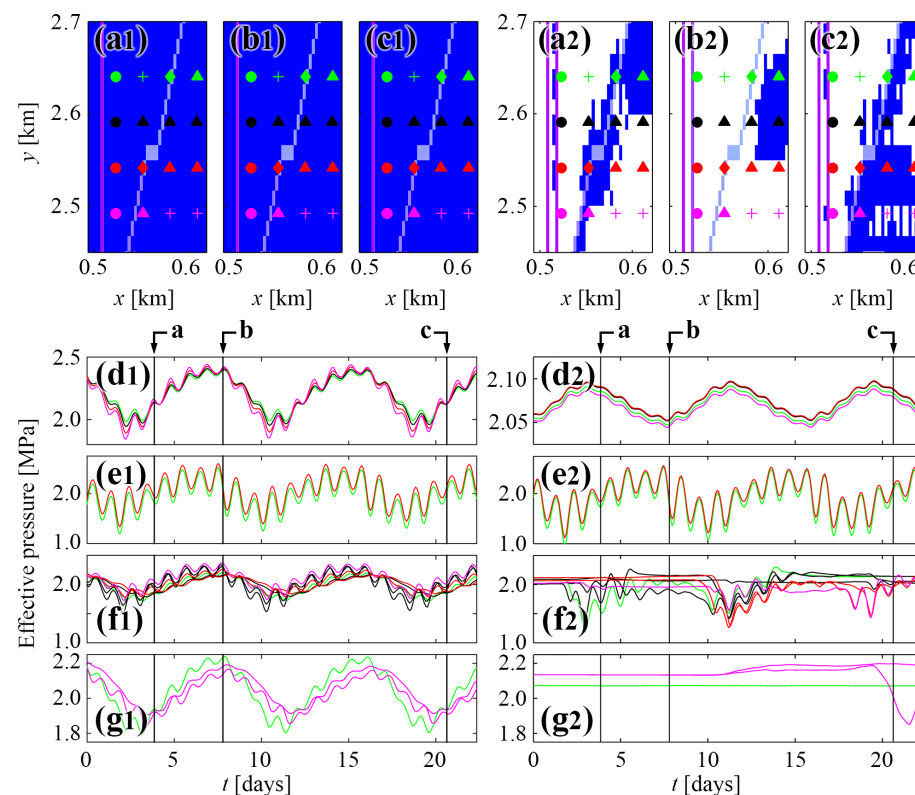


Figure 17. A synthetic borehole grid in the model with (right-hand column) and without a percolation cut-off (left-hand column), and with it (right). (a–c): enlargements of the inset box in Fig. 16(a4d2,h2) at times $t = 3.9$ (a), 7.8 (b) and 20.6 (c) days. Superimposed on the blue connectivity map is S_R conduit size, plotted using the same colour scheme as indicated by the colour bar in column 1 panels a & e in Fig. 16. Also shown are the locations of 16 synthetic boreholes, colour-coded by row. (d–g): Effective pressure time series from the boreholes, grouped according to borehole symbols: circles (d), diamonds (e), triangles (f), crosses (g). Each time series is colour-coded by row.

pressure variations in sets of widely spaced boreholes (see section 4.3). As in *Hoffman et al.* [2016], our data suggest that isolated-disconnected areas need not be completely isolated, but can experience slow leakage into the active ⁵ drainage system (see section 4.2).

In view of the above, perhaps the main shortcoming of most current drainage models is their inability to account for the evolution of an isolated-disconnected or weakly connected component [*Hoffman et al.*, 2016]. This ability can ¹⁰ however be incorporated in the current modelling framework as a percolation threshold, assuming that cavities only form a connected system once they reach a critical size. We have implemented this approach in a simple model, allowing us to reproduce qualitatively some of the main features of our ¹⁵ data-set: a dataset: sharply-defined drainage subsystems with insignificant diffusive pressure signal attenuation and the existence of isolated-disconnected areas (See section 5.1).

However, the ability of the system to fully shut-down requires the incorporation of other physical process that ²⁰ could allow the reactivation of the drainage system during the spring event, something that is probably accomplished by over-pressurization/overpressurisation. The model also requires a more careful treatment of normal stress redistribu-

tion, in particular in association with isolated and closely spaced cavities of very different water pressures. This is left ²⁵ for future work. In the future, we also hope that it will be possible to test models like the one presented here or more sophisticated versions of it, against detailed borehole data-sets datasets such as that from South Glacier.

Data availability. The presented dataset will be made publicly ³⁰ available in the future. Ongoing work is taking place to meet the format and create the ancillary data and documentation required for the release, that is expected to happen fully or partially by the end of 2018. In the meantime, it is available on request from the second author at cschoof@eoas.ubc.ca. The model code in Matlab and configuration parameters are included in the supplementary material. ³⁵

Competing interests. The authors declare that they have no competing interests

Acknowledgements. We thank Manar Al Asad, Faron Anslow, Ashley Bellas, Kyla Burrill, Emilie Delaroche, Jennifer Fohring, Tom-Pierre Frappé-Sénéclauze, Johan Gilchrist, Marianne Haseloff, Ian ⁴⁰

- Hewitt, Marc Jaffrey, Alex Jarosch, Conrad Koziol, Natalia Martinez, Arran Whiteford and Kevin Yeo for assistance in the field. Gwenn Flowers provided bed elevation and South Glacier AWS data ~~–additional as well as continuous help and advice without~~ which this project would not have succeeded. Additional AWS data were made available by Christian Zdanowicz and Luke Copland. We are indebted to Parks Canada and Kluane First Nation for their support and permission to operate at the field site, to Doug Makkonen, Dion Parker and Ian Pitchforth for expert flying, to Andy Williams, Sian Williams and Lance Goodwin for logistics support. This work was supported by the Natural Science and Engineering Research Council of Canada through Discovery Grants 357193-08 and 357193-13, Accelerator Supplement 446042-13, Northern Research Supplements 361960-06 and 361960-13 as well as Research Tools and Instruments Grant 376058-09; by the Polar Continental Shelf Project through grants 625-11, 638-12, 637-13, 663-14 and 667-15; and by the Canada Foundation for Innovation and British Columbia Knowledge Development Fund through Leaders Opportunity Fund project number 203786 and 227698.
- ## 20 References
- Alley, R., Blankenship, D., Bentley, C., and Rooney, S.: Deformation of till beneath ice stream B, West Antarctica, *Nature*, 322, 57–59, 1986.
- Andrews, L., Catania, G., Hoffman, M., Gulley, J., Lüthi, M., Ryser, C., Hawley, R., and Neumann, T.: Direct observations of evolving subglacial drainage beneath the Greenland Ice Sheet, *Nature*, 514, 80–83, 2014.
- Bartholomäus, T., Anderson, R., and Anderson, S.: Growth and collapse of the distributed subglacial hydrologic system of Kennicott Glacier, Alaska, USA, and its effects on basal motion, *journal of Glaciology*, 57, 985–1002, <https://doi.org/10.3189/002214311798843269>, 2011.
- Blake, E., Fischer, U., and Clarke, G.: Direct measurement of sliding at the glacier bed, *journal of Glaciology*, 40, 559–599, 1994.
- 35 Boulton, G. and Hindmarsh, R.: Sediment deformation beneath glaciers: rheology and geological consequences, *journal of Geophysical Research*, 92, 9059–9082, 1987.
- Boulton, G., Lunn, R., Vidstrand, P., and Zatsepin, S.: Subglacial drainage by groundwater–channel coupling, and the origin of esker systems: Part II – theory and simulation of a modern system., *Quat. Sci. Rev.*, 26, 1091–1105, 2007.
- Brinkerhoff, D., Meyer, C., Bueller, E., Truffer, M., and Bartholomäus, T.: Slow flow of granular aggregates: the deformation of sediments beneath glaciers, *Ann. Glaciol.*, 57, 1–12, <https://doi.org/10.1017/aog.2016.3>, 2016.
- 45 Bueller, E. and van Pelt, W.: Mass-conserving subglacial hydrology in the Parallel Ice Sheet Model version 0.6, *Geoscientific Model Development*, 8, 1613–1635, <https://doi.org/10.5194/gmd-8-1613-2015>, <https://www.geosci-model-dev.net/8/1613/2015/>, 2015.
- 50 Creyts, T. and Schoof, C.: Drainage through subglacial water sheets, 2009.
- Crompton, J., Flowers, G., Kirste, D., Hagedorn, B., and Sharp, M.: Clay mineral precipitation and low silica in glacier meltwaters explored through reaction path modelling, 2015.
- 55 de Fleurian, B., Gagliardini, O., Zwinger, T., Durand, G., Le Meur, E., Mair, D., and Råback, P.: A double continuum hydrological model for glacier applications, *The Cryosphere*, 8, 137–153, <https://doi.org/10.5194/tc-8-137-2014>, <https://www.the-cryosphere.net/8/137/2014/>, 2014.
- 60 Dodds, C. and Campbell, R.: Potassium-argon ages of mainly intrusive rocks in the Saint Elias Mountains, Yukon and British Columbia, Tech. rep., Energy, Mines and Resources Canada, 1988.
- Dow, C., Kulesa, B., Rutt, I., Tsai, V., Pimentel, S., Doyle, S., As, D., Lindbäck, K., Pettersson, R., Jones, G., and Hubbard, A.: Modeling of subglacial hydrological development following rapid supraglacial lake drainage, *journal of Geophysical Research: Earth Surface*, 120, 1127–1147, <https://doi.org/10.1002/2014JF003333>, 2015.
- 70 Efron, B. and Tibshirani, R.: *An Introduction to the Bootstrap*, Chapman & Hall/CRC, 1993.
- Engelhardt, H. and Kamb, B.: Basal sliding of Ice Stream B, West Antarctica, *journal of Glaciology*, 44, 223–230, 1998.
- Engelhardt, H., Harrison, W., and Kamb, B.: Basal sliding and conditions at the glacier bed as revealed by bore-hole photography, *journal of Glaciology*, 20, 469–508, 1978.
- 75 Flowers, G., Roux, N., Pimentel, S., and Schoof, C.: Present dynamics and future prognosis of a slowly surging glacier, *The Cryosphere*, 5, 299–313, 2011.
- 80 Flowers, G., Copland, L., and Schoof, C.: Contemporary glacier processes and global change: recent observations from the Kaskawulsh Glacier and Donjek Range, St. Elias Mountains, Arctic, *KLRS 50th Anniversary Issue*, 1–20, 2014.
- Flowers, G. E.: Modelling water flow under glaciers and ice sheets, *Proceedings of the Royal Society of London A*, 471, 2015.
- 85 Fountain, A. and Walder, J.: Water flow through temperate glaciers, *Rev. Geophys.*, 36, 299–328, 1998.
- Fountain, A., Schlichting, R., Jansson, P., and Jacobel, R.: Observations of englacial water passages: a fracture-dominated system, *Annals of Glaciology*, 40, 25–30, 2005.
- Fowler, A.: Sliding with cavity formation, *journal of Glaciology*, 33, 131–141, 1987.
- Fudge, T., Harper, J., Humphrey, N., and Pfeffer, W.: Diurnal water-pressure fluctuations: timing and pattern of termination below Bench Glacier, Alaska, USA, *Annals of Glaciology*, 40, 102–106, 2005.
- 95 Fudge, T., Humphrey, N., Harper, J., and Pfeffer, W.: Diurnal fluctuations in borehole water levels: configuration of the drainage system beneath Bench Glacier, Alaska, USA, *journal of Glaciology*, 54, 297–306, 2008.
- Gagliardini, O., Cohen, D., Råback, P., and Zwinger, T.: Finite-element modeling of subglacial cavities and related friction law, *J. Geophys. Res.*, 112, <https://doi.org/10.1029/2006JF000576>, 2007.
- 100 Gerrard, J., Perutz, M., and Roch, A.: Measurement of the velocity distribution along a vertical line through a glacier, *Proc. R. Soc. London*, 213, 546–558, 1952.
- Gordon, S., Sharp, M., Hubbard, B., Smart, C., Ketterling, B., and Willis, I.: Seasonal reorganization of subglacial drainage inferred from measurements in boreholes, *Hydrol. Process.*, 12, 105–133, 1998.
- 105 Harper, J., Humphrey, N., and Greenwood, M.: Basal conditions and glacier motion during the winter/spring transition, Worthington Glacier, Alaska, U.S.A., *J. Glaciol.*, 48, 42–50, 2002.
- 115

- Harper, J., Humphrey, N., Pfeffer, W., Fudge, T., and O'Neel, S.: Evolution of subglacial water pressure along a glacier's length, *Annals of Glaciology*, 40, 31–36, 2005.
- Harper, J., Bradford, J., and Humphrey, N.: Vertical extension of the subglacial drainage system into basal crevasses, *Nature*, 467, 579–82, 2010.
- Harper, J. T., Humphrey, N. F., and Pfeffer, W. T.: Three-Dimensional Deformation Measured in an Alaskan Glacier, *Science*, 281, 1340–1342, 1998.
- Hart, J., Rose, K., Clayton, A., and Martinez, K.: Englacial and subglacial water flow at Skálafellsjökull, Iceland derived from ground penetrating radar, in situ Glacsweb probe and borehole water level measurements, *Earth Surf. Process. Landforms*, 40, 2071–2083, 2015.
- Hewitt, I.: Modelling distributed and channelized subglacial drainage: the spacing of channels, *Journal of Glaciology*, 57, 302–314, 2011.
- Hewitt, I.: Seasonal changes in ice sheet motion due to melt water lubrication, *Earth Planet. Sci. Lett.*, 371, 16–25, 2013.
- Hewitt, I., Schoof, C., and Werder, M.: Flotation and free surface flow in a model for subglacial drainage. Part 2. Channel flow, *J. Fluid Mech.*, 702, 157–187, 2012.
- Hodge, S. M.: Direct Measurement of Basal Water Pressures: Progress and Problems, *Journal of Glaciology*, 23, 309–319, <https://doi.org/10.1017/S0022143000029920>, 1979.
- Hoffman, M. and Price, S.: Feedbacks between coupled subglacial hydrology and glacier dynamics, *Journal of Geophysical Research: Earth Surface*, 119, 414–436, <https://doi.org/10.1002/2013JF002943>, 2014.
- Hoffman, M., Andrews, L., Price, S., Catania, G., Neumann, T., Lüthi, M., Gulley, J., Ryser, C., Hawley, R., and Morriss, B.: Greenland subglacial drainage evolution regulated by weakly connected regions of the bed, *Nature Communications*, 7, 13903, <https://doi.org/10.1038/ncomms13903>, 2016.
- Hubbard, B., Sharp, M., Willis, I., Nielsen, M., and Smart, C.: Borehole water-level variations and the structure of the subglacial hydrological system of Haut Glacier d'Arolla, Valais, Switzerland, *Journal of Glaciology*, 41, 572–583, 1995.
- Huzurbazar, S. and Humphrey, N. F.: Functional clustering of time series: An insight into length scales in subglacial water flow, *Water Resources Research*, 44, 2008.
- Iken, A. and Bindschadler, R.: Combined measurements of subglacial water pressure and surface velocity of Findelengletscher, Switzerland: conclusions about drainage system and sliding mechanism, *Journal of Glaciology*, 32, 101–119, 1986.
- Iken, A. and Truffer, M.: The relationship between subglacial water pressure and velocity of Findelengletscher, Switzerland, during its advance and retreat, *Journal of Glaciology*, 43, 328–338, 1997.
- Iken, A., Röthlisberger, H., Flotron, A., and Haeberli, W.: The uplift of Unteraargletscher at the beginning of the melt season - a consequence of water storage at the bed?, *Journal of Glaciology*, 29, 28–47, 1983.
- Iverson, N. R., Baker, R. W., Hooke, R. L., Hanson, B., and Jansson, P.: Coupling between a glacier and a soft bed: I. A relation between effective pressure and local shear stress determined from till elasticity, *Journal of Glaciology*, 45, 31–40, <https://doi.org/10.1017/S0022143000003014>, 1999.
- Kamb, B.: Glacier surge mechanism based on linked cavity configuration of the basal water conduit system, *J. Geophys. Res.*, 92, 9083–9100, 1987.
- Kamb, B., Raymond, C., Harrison, W., Engelhardt, H., Echelmeyer, K., Humphrey, N., Brugman, M., and Pfeffer, T.: Glacier surge mechanism: 1982–1983 surge of Variegated Glacier, Alaska, *Science*, 227, 469–479, 1985.
- Kavanaugh, J. and Clarke, G.: Evidence for extreme pressure pulses in the subglacial water system, *Journal of Glaciology*, 46, 9083–9100, 2000.
- Lappégard, G., Kohler, J., Jackson, M., and Hagen, J.: Characteristics of subglacial drainage systems deduced from load-cell measurements, *Journal of Glaciology*, 52, 137–148, <https://doi.org/10.3189/172756506781828908>, 2006.
- Lefeuve, P., Jackson, M., Lappégard, G., and Hagen, J.: Interannual variability of glacier basal pressure from a 20 year record, *Annals of Glaciology*, 56, 33–44, 2015.
- Lefeuve, P., Zwinger, T., Jackson, M., Gagliardini, O., Lappégard, G., and Hagen, J.: Stress redistribution explains anti-correlated subglacial pressure variations, *Frontiers in Earth Science*, 5, 2018.
- Llibouty, L.: Contribution à la théorie du frottement du glacier sur son lit, *C. R. Hebd. Séances Acad. Sci.*, 247, 318–320, 1958.
- Llibouty, L.: General theory of subglacial cavitation and sliding of temperate glaciers, *Journal of Glaciology*, 7, 21–58, 1968.
- MacDougall, A. and Flowers, G.: Spatial and temporal transferability of a distributed energy-balance glacier melt model, *Journal of Climate*, 24, 1480–1498, 2011.
- Mair, D., Nienow, P., Willis, I., and Sharp, M.: Spatial patterns of glacier motion during a high-velocity event: Haut Glacier d'Arolla, Switzerland, *Journal of Glaciology*, 47, 9–20, 2001.
- Meierbachtol, T., Harper, J., Humphrey, N., and Wright, P.: Mechanical forcing of water pressure in a hydraulically isolated reach beneath Western Greenland's ablation zone, *Annals of Glaciology*, 57, 62–70, 2016.
- Murray, T. and Clarke, G.: Black-box modeling of the subglacial water system, *Journal of Geophysical Research*, 100, 10219–10230, 1995.
- Ng, F.: Canals under sediment-based ice sheets, *Ann. Glaciol.*, 30, 146–152, 2000.
- Nienow, P., Sharp, M., and Willis, I.: Ice sheet acceleration driven by melt supply variability, *Earth Surface Processes and Landforms*, 23, 825–843, 1998a.
- Nienow, P., Sharp, M., and Willis, I.: Seasonal changes in the morphology of the subglacial drainage system, Haut Glacier d'Arolla, Switzerland, *Earth Surf. Process. Landforms*, 23, 825–843, 1998b.
- Nienow, P. W.: Dye-tracer investigations of glacier hydrological systems, Ph.D. thesis, University of Cambridge, 1993.
- Nye, J.: Water flow in glaciers: jökulhlaups, tunnels and veins, *Journal of Glaciology*, 17, 181–207, 1976.
- Oldenborger, G. A., Clarke, G. K. C., and Hildes, D. H. D.: Hydrochemical coupling of a glacial borehole-aquifer system, *Journal of Glaciology*, 48, 357–368, <https://doi.org/10.3189/172756502781831232>, 2002.
- Paoli, L. and Flowers, G.: Dynamics of a small surge-type glacier using one-dimensional geophysical inversion, *Journal of Glaciology*, 55, 1101–1112, 2009.

- Röthlisberger, H.: Water pressure in intra- and subglacial channels, *journal of Glaciology*, 11, 177–203, 1972.
- Ryser, C., Lüthi, M., Andrews, L., Catania, G., Funk, M., Hawley, R., Hoffman, M., and Neumann, T.: Caterpillar-like ice motion in the ablation zone of the Greenland ice sheet, *J. Geophys. Res. Earth Surf.*, 119, 1–14, 2014a.
- Ryser, C., Lüthi, M., Andrews, L., Hoffman, M., Catania, G., Hawley, R., Neumann, T., and Kristensen, S.: Sustained high basal motion of the Greenland ice sheet revealed by borehole deformation, *journal of Glaciology*, 60, 2014b.
- Schoof, C.: The effect of cavitation on glacier sliding, *Proceedings of the Royal Society of London A: Mathematical, Physical and Engineering Sciences*, 461, 609–627, <https://doi.org/10.1098/rspa.2004.1350>, <http://rspa.royalsocietypublishing.org/content/461/2055/609>, 2005.
- Schoof, C.: Ice sheet acceleration driven by melt supply variability, *Nature*, 468, 803–806, 2010.
- Schoof, C., Hewitt, I., and Werder, M.: Flotation and free surface flow in a model for subglacial drainage. Part I. Distributed drainage, *J. Fluid Mech.*, 702, 126–156, 2012.
- Schoof, C., Rada, C., Wilson, N., Flowers, G., and Haseloff, M.: Oscillatory subglacial drainage in the absence of surface melt, *Cryosphere*, 8, 959–976, 2014.
- Sole, A., Mair, D., Nienow, P., Bartholomew, I., King, M., Burke, M., and Joughin, I.: Ice sheet acceleration driven by melt supply variability, *journal of Geophysical Research: Earth Surface*, 116, <https://doi.org/10.1029/2010JF001948>, 2011.
- Spring, U. and Hutter, K.: Conduit flow of a fluid through its solid phase and its application to intraglacial channel flow, *Int. J. Eng. Sci.*, 20, 327–363, 1982.
- Tarboton, D.: A new method for the determination of flow directions and upslope areas in grid digital elevation models, *Water Resources Research*, 33, 309–319, <https://doi.org/10.1029/96WR03137>, 1997.
- Truffer, M., Echelmeyer, K. A., and Harrison, W. D.: Implications of till deformation on glacier dynamics, *journal of Glaciology*, 47, 123–134, <https://doi.org/10.3189/172756501781832449>, 2001.
- Tsai, V. and Rice, J.: Modeling Turbulent Hydraulic Fracture Near a Free Surface, *journal of Applied Mechanics*, 79, <https://doi.org/10.1115/1.4005879>, 2012.
- Tulaczyk, S., Kamb, W., and Engelhardt, H.: Basal mechanics of Ice Stream B, west Antarctica: 1. Till mechanics, *journal of Geophysical Research: Solid Earth*, 105, 463–481, 2000.
- van der Wel, N., Christoffersen, P., and Bougamont, M.: The influence of subglacial hydrology on the flow of Kamb Ice Stream, West Antarctica, *J. Geophys. Res.*, 118, 97–110, 2013.
- Vivian, R.: The nature of the ice-rock interface: the results of investigation on 20 000 m² of the rock bed of temperate glaciers, *journal of Glaciology*, 25, 267–277, 1980.
- Walder, J.: Stability of sheet flow of water beneath temperate glaciers and implications for glacier surging, *journal of Glaciology*, 28, 273–293, 1982.
- Walder, J.: Hydraulics of subglacial cavities, *journal of Glaciology*, 32, 439–445, 1986.
- Walder, J. and Fowler, A.: Channelized subglacial drainage over a deformable bed, *journal of Glaciology*, 40, 3–15, 1994.
- Weertman, J.: General theory of water flow at the base of a glacier or ice sheet, *Reviews of Geophysics*, 10, 287–333, <https://doi.org/10.1029/RG010i001p00287>, 1972.
- Werder, M., Hewitt, I., Schoof, C., and Flowers, G.: Modeling channelized and distributed subglacial drainage in two dimensions, *J. Geophys. Res.*, 118, 2140–2158, 2013.
- Wheler, B. and Flowers, G.: Glacier subsurface heat-flux characterizations for energy-balance modelling in the Donjek Range, southwest Yukon, Canada, *journal of Glaciology*, 57, 121–133, 2011.
- Wheler, B., MacDougall, A., Flowers, G., Petersen, E., Whitfield, P., and Kohfeld, K.: Effects of temperature forcing provenance and lapse rate on the performance of an empirical glacier-melt model, *Arctic, Antarctic, and Alpine Research*, 42, 379–393, 2014.
- Wheler, B. A.: Glacier melt modelling in the Donjek Range, St Elias Mountains, Yukon Territory, Master's thesis, University of Alberta, 2009.
- Wilson, N., Flowers, G., and Mingo, L.: Comparison of thermal structure and evolution between neighboring subarctic glaciers, *journal of Geophysical Research*, 118, 1443–1459, 2013.
- Wright, P., Harper, J., Humphrey, N., and Meierbachtol, T.: Measured basal water pressure variability of the western Greenland Ice Sheet: Implications for hydraulic potential, *journal of Geophysical Research: Earth Surface*, 121, 1134–1147, <https://doi.org/10.1002/2016JF003819>, 2016.